

TECHNISCHE UNIVERSITÄT MÜNCHEN

Lehrstuhl für Entwicklungsgenetik

Functions of microRNAs in the developing midbrain-hindbrain of the mouse

Yen Kar Ng

Vollständiger Abdruck der von der Fakultät Wissenschaftszentrum Weihenstephan für Ernährung, Landnutzung und Umwelt der Technischen Universität München zur Erlangung des akademischen Grades eines

Doktors der Naturwissenschaften

genehmigten Dissertation.

Vorsitzender: Univ.-Prof. Dr. Erwin Grill

Prüfer der Dissertation: 1. Univ.-Prof. Dr. Wolfgang Wurst

2. Priv.-Doz. Dr. Johannes Beckers

Die Dissertation wurde am 21.06.2012 bei der Technischen Universität München eingereicht und durch die Fakultät für Wissenschaftszentrum Weihenstephan für Ernährung, Landnutzung und Umwelt am 30.07.2012 angenommen.

Content

1.0 Abstract	
1.1 Zusammenfassung.....	6
1.2 Abstract.....	8
2.0 Introduction	
2.1.1 Biogenesis of miRNAs and mechanism of action.....	11
2.1.2 miRNAs expressions and functions in the developing CNS.....	13
2.2 The development of CNS of the mouse.....	16
2.2.1 Development of the ventral mid-/hindbrain (vMH) neuronal populations of the mouse miRNAs expressions and functions in the developing CNS.....	16
2.2.2 Genetic mechanisms involved in differentiation of mdDA neuron.....	16
2.2.3 Genetic mechanisms involved in development of OM/TN and RN.....	20
2.3 Aims of the present work.....	22
3.0 Result	
3.1 miRNAs that might be involved in the regulation of the MHB GRN and mesDA neuron development as predicted by computational algorithms.....	23
3.1.1 Establishment of LNA-ISH detection method and the validation of miRNA expression patterns.....	28
3.1.1.1 miRNAs that are expressed in the developing mouse CNS.....	30
3.1.1.2 <i>miR-144</i> is specifically expressed in the liver during mouse embryonic development.....	35
3.1.2 Functional validation of predicted target genes for the miRNAs that showed expression in the CNS during development.....	36
3.1.2.1 <i>miR-709</i> but not <i>miR-705</i> targets <i>Wnt1 3'UTR</i>	37
3.1.2.2 <i>miR-712</i> targets <i>Wnt5b 3'UTR in vitro</i>	39
3.1.2.3 <i>miR-714</i> targets <i>Lef1 3'UTR</i> but not <i>Pitx3 3'UTR</i>	41
3.1.2.4 <i>miR-135b</i> does not target <i>Otx2-</i> and <i>Wnt6 3'UTR</i>	42
3.1.3 A new prediction approach to predict putative miRNAs that target <i>Wnt13'UTR</i>	43
3.1.4 Experimental validation of a putative novel 'miRNA recognition' motive/target enhancer signal.....	45
3.2 miRNAs that might be involved in vMH neuron development as determined by miRNA expression profiling of differentiating mESCs	
3.2.1 Directed differentiation of mouse ESC into mdDA and other types of ventral mid/hindbrain neurons.....	50
3.2.2 NGS profiling of miRNAs expressed during the directed differentiation of mouse ESCs into vMH neurons.....	52
3.2.3 Expression of <i>miR-125b</i> in the ventral anterior neural tube of the midgestational mouse embryo.....	55
3.2.4 Expression of <i>miR-125b</i> overlaps with the motoneuron markers <i>Phox2b</i> and <i>Sim1</i> in the basal plate of the murine mid- and hindbrain.....	59

3.2.5	<i>miR-125b</i> directly targets the <i>Phox2b</i> and <i>Sim1</i> 3'UTRs.....	62
3.2.6	<i>miR-125b</i> regulates the development of postmitotic <i>Phox2b</i> ⁺ / <i>Isl1</i> ⁺ OM/TN neurons and of <i>Nkx6-1</i> ⁺ BP progenitors <i>in vitro</i>	66
3.2.7	The numbers of proliferate cells in primary vMH cells including <i>Nkx6-1</i> ⁺ BP progenitors are decreased by <i>miR-125b</i> overexpression.....	75
3.2.8	Reduction of the <i>miR-125b</i> dosage in vMH primary cultures also increases their survival	77
3.3	Generation of <i>Shh-Cre-SBE1</i> transgenic mice for the fate-mapping and inactivation of conditional alleles in the rostral midbrain/caudal diencephalon.....	79
4.0	Discussion	
4.1	Prediction of miRNAs with bioinformatics tools is still not a very reliable method to detect novel miRNAs and their functional interactions with target mRNAs.....	84
4.2	A conserved primate “miRNA recognition motif” was not validated on a functional level for the mouse.....	88
4.3		
4.3.1	<i>MiR-125b</i> is expressed in a very specific spatiotemporal pattern in the developing murine MHR that correlates with the expression of its direct targets <i>Phox2b</i> and <i>Sim1</i>	94
4.3.2	Analyses of <i>miR-125b</i> function in mouse vMH neural development ...	96
4.4	Outlook: <i>miR-125b</i> function in vMH neuron development.....	104
5.0	Materials and Methods	
5.1	Materials	
5.1.1	General	
	equipments.....	105
5.1.2	Consumables.....	106
5.1.3	Chemicals.....	108
5.1.4	Commercial Kits.....	109
5.1.5	Enzymes.....	109
5.1.6	Antibodies.....	110
5.1.7	Buffers and solutions.....	110
5.1.8	LNA oligo probe to detect miRNA expression.....	113
5.1.9	Riboprobes to detect mRNA.....	114
5.1.10	Precursor miRNAs for luciferase assay.....	114
5.1.11	Vectors.....	114
5.1.12	Primers.....	115
5.1.12.1	Genotyping.....	115
5.1.12.2	luciferase sensor vectors.....	115
5.1.12.3	Site-directed mutagenesis on luciferase vector.....	116
5.1.12.4	Site-directed mutagenesis for <i>Wnt1</i> 3'UTR ‘miRNA recognition motive’.....	116
5.1.12.5	miRNA overexpressing (OE) construct.....	117
5.1.12.6	Lentivirus constructs.....	117
5.1.12.7	RT-qPCR Taqman primers.....	118
5.1.13	Cell culture medium.....	118

5.2	Methods	
5.2.1	Experimental animals	120
5.2.2	Genotyping	
5.2.2.1	Isolation of genomic DNA	120
5.2.2.2	PCR-genotyping	120
5.2.2.3	R26R reporter mice-genotyping	121
5.2.3	Histology	
5.2.3.1	Dissection of mouse embryos/brains	121
5.2.3.2	Paraffin embedding of mouse embryos	121
5.2.4	In Situ Hybridization (ISH) on paraffin sections	
5.2.4.1	Labelling of Locked Nucleic Acid (LNA) oligo detection probe	122
5.2.4.1.1	DIG-labeled LNA oligo detection probe	122
5.2.4.1.2	Radioactive-labeled LNA oligo detection probe	122
5.2.4.2	Riboprobes for RNA ISH	123
5.2.4.2.1	Cloning of riboprobes	123
5.2.4.2.2	Labelling of riboprobes	123
5.2.4.3	Processing of paraffin section for LNA ISH and RNA ISH	124
5.2.4.4	Detection of miRNA ISH with LNA probe on paraffin sections	124
5.2.4.4.1	DIG-labelled LNA detection probes	124
5.2.4.4.2	Radioactive-labelled LNA detection probes	125
5.2.4.5	Detection of mRNA ISH with riboprobe on paraffin sections	125
5.2.4.6	Exposure and developing of radioactively labelled sections	126
5.2.5	Immunohistochemistry	126
5.2.6	Vector Constructs	126
5.2.6.1	Luciferase sensor vectors	126
5.2.6.2	Site-directed Mutagenesis on luciferase vector	127
5.2.6.3	Site-directed mutagenesis for <i>Wnt1</i> 3'UTR "miRNA recognition motif" experiments	127
5.2.6.4	miRNA overexpression (OE) construct	127
5.2.6.5	Lentiviral vectors generation and lentivirus packaging	128
5.2.7	Restriction enzyme digestion/blunting/kinasing	128
5.2.8	Ligations	12
	8	
5.2.9	Transformation into competent bacteria	129
5.2.10	DNA mini- and maxi-preps	129
5.2.11	Sequencing of DNA	129
5.2.12	Luciferase sensor assay	129
5.2.13	Mouse ES cell differentiation	130
5.2.14	Primary cell culture	
5.2.14.1	Cover slip treatment and coating	130
5.2.14.2	Primary vMH culture	131
5.2.14.3	EdU treatment and staining	131
5.2.14.4	Immunocytochemistry	131
5.2.14.5	Cell counting	132
5.2.15	Isolation of total RNA	132
5.2.16	cDNA synthesis	132

5.2.17	Quantitative RT-PCR (qPCR).....	132
5.2.18	miRNA profiling with next generation sequencing (NGS).....	133
5.2.19	Statistical Analyses.....	134
5.2.20	X-Gal histochemistry.....	134
5.2.20.1	Whole mount X-gal staining.....	134
5.2.20.2	X-Gal staining on cryosection.....	134
5.2.21	Microscopy.....	134
6.0	References.....	136
7.0	Appendix	
7.1	Abbreviations.....	144
7.2	Index of figures and tables.....	147
7.3	Supplementary Figures	
7.3.1	MiRNAs predicted by five combined computational algorithms expression analyses.....	150
7.3.2	NGS miRNA profiling of differentiating mESCs into vMH neurons - validation of the profiling approach.....	154
7.3.3	Sequence of the <i>Shh-Cre-SBE1</i> construct used for production of <i>Shh-Cre- SBE1</i> transgenic mice (Clone A5).....	155
7.4	Acknowledgment.....	157
7.5	Curriculum Vitae.....	158

1.1 Zusammenfassung

MicroRNAs (miRNAs) sind kleine, 21-23 Nukleotide lange, nichtkodierende Ribonukleinsäuren (RNAs), die essentielle Funktionen im zentralen Nervensystem (ZNS) der Maus ausüben. MiRNAs spielen eine Schlüsselrolle in der posttranskriptionellen Regulierung der Genexpression, indem sie durch Basenpaarung mit komplementären Sequenzen in Boten-RNAs (mRNAs) die Translation dieser Ziel-mRNAs blockieren oder ihren Abbau induzieren. Seit der Entdeckung der ersten miRNA in *C. elegans*, *lin4*, im Jahre 1993, wurden bis heute mehr als Tausend verschiedene miRNAs in Tieren, Pflanzen und Viren identifiziert. Neuere Untersuchungen zeigten, dass miRNAs eine wichtige Rolle beim Übergang von proliferierenden neuronalen Vorläuferzellen zu postmitotischen, ausdifferenzierten Neuronen spielen. Im Rahmen meiner Doktorarbeit habe ich die Funktionen von miRNAs in der Entwicklung der Mittel- und Hinterhirn-Region (MHR) untersucht. Zunächst habe ich in Zusammenarbeit mit der Gruppe um Fabian Theis vom Institut für Bioinformatik und Systembiologie (IBIS) des Helmholtz-Zentrums München eine Kombination verschiedener Algorithmen zur Vorhersage von miRNAs angewandt, die bekannte und an der Entwicklung der MHR und ihrer neuronalen Zellpopulationen (inklusive der mesodiencephalen dopaminergen (mdDA) Neurone) beteiligte Gene regulieren sollen. Die vorhergesagten miRNAs wurden zunächst auf der Grundlage ihrer Expressionsmuster im sich entwickelnden ZNS und insbesondere in der MHR des Mausembryos validiert. Als nächstes wurden die miRNAs, deren Expression in der MHR detektiert wurde, mit Hilfe sogenannter „Sensor-Assays“ validiert, um festzustellen, ob sie die vorhergesagten Zielgene bzw. -mRNAs auch auf molekularer Ebene regulieren. Von den insgesamt 33 *in-silico* erfassten miRNAs konnten nur drei miRNAs auf Expressions- und molekularer Ebene validiert werden. Diese drei miRNAs regulieren die Expression der vorhergesagten Ziel-mRNAs. Eine Untersuchung ihrer biologischen Funktion *in vivo* war aber in diesem Fall sehr schwierig bis unmöglich, da zum einen keine der drei miRNAs eine regionenspezifische Expression zeigte und stattdessen alle drei miRNAs ubiquitär im gesamten Mausembryo einschließlich des sich entwickelnden Neuralrohrs transkribiert wurden, zum anderen weil zu viele Zielgene *in silico* vorhergesagt wurden, um sie gezielt untersuchen zu können. Diese Ergebnisse haben gezeigt, dass mathematische Algorithmen zur Vorhersage von

miRNAs und ihrer Zielgene eine immer noch zu hohe Rate an falsch-positiven Treffern aufweisen. Diese Programme und deren Resultate können deshalb nur sehr eingeschränkt zur Untersuchung der biologischen Funktion von miRNAs eingesetzt werden.

Aus diesen Gründen habe ich einen zweiten experimentellen Ansatz angewandt, indem ich unter Anwendung des sogenannten „Next Generation Sequencing (NGS)“ das Expressionsprofil der miRNAs erstellt habe, die während der gerichteten Differenzierung von Maus embryonalen Stammzellen (mESCs) in mdDA und andere VMH Neurone exprimiert werden. Unter den miRNAs mit der stärksten Expression in den ausdifferenzierten VMH Neuronen im Vergleich zu den pluripotenten, undifferenzierten mESCs befand sich *miR-125b*, die das Säuger-Ortholog von *C. elegans lin4* ist. Die nachfolgende Validierung dieses Ergebnisses zeigte, dass *miR-125b* in der Tat in der MHR und insbesondere in der Basalplatte (BP) des sich entwickelnden Mittel- und Hinterhirns der Maus exprimiert wird. Bemerkenswerterweise korreliert das Expressionsmuster von *miR-125b* in der ventralen MHR der Maus mit der Expression von *Phox2b* und *Sim1*, zwei der mittels TargetScan4.1 vorhergesagten Zielgene dieser miRNA. Die weitere molekulare Validierung dieser beiden *miR-125b* Zielgene mit Hilfe der zuvor erwähnten „Sensor Assays“ und der zielgerichteten Mutagenese ihrer vorhergesagten, konservierten Bindestellen innerhalb der 3'UTRs dieser mRNAs bestätigte diese zwei Kandidaten als direkte Zielgene von *miR-125b*. Um die biologische Funktion dieser miRNA eingehender zu untersuchen, habe ich unter Verwendung von primären VMH Zellkulturen *miR-125b* in diesen Zellen überexprimiert (sogenannte ‘*gain-of-function*’ Experimente) bzw. mittels sogenannter „Schwamm-Vektoren“ herunterreguliert (‘*loss-of-function*’ Experimente). Diese Experimente zeigten, dass die Zahl der *Phox2b*⁺ und *Isl1*⁺ Neurone des Nucleus oculomotorius (OM) und Nucleus trochlearis (TN) nach *miR-125b* Überexpression erniedrigt bzw. nach *miR-125b* Herunterregulierung erhöht ist. *Isl1* and *Phox2b* sind zwei Homöodomänen (HD) Transkriptionsfaktoren (TFs), die an der Entwicklung der OM/TN Neuronen in der MHR beteiligt sind. Eine mögliche Veränderung der *Sim1* Expression in neuralen Vorläuferzellen konnte in diesen Zellkulturen nicht untersucht werden, da die Expressionsstärke der *Sim1* mRNA nach Überexpression bzw. Herunterregulierung von *miR-125b* nicht verändert war und es

leider keinen funktionierenden Antikörper für dieses Protein gibt. Die Zahl der mes-/metencephalen BP-Vorläuferzellen, die den HD TF Nkx6-1 exprimieren, war nach Überexpression von *miR-125b* in diesen Kulturen jedoch deutlich reduziert. Außerdem war die Proliferation dieser Nkx6-1⁺ Vorläuferzellen im Speziellen als auch aller VMH Vorläuferzellen im Allgemeinen nach *miR-125b*-Überexpression reduziert, während die Herunterregulierung von *miR-125b* keinen Effekt auf die Proliferation dieser Zellen zeigte. Erstaunlicherweise war aber der apoptotische Zelltod nach Herunterregulierung der *miR-125b* Expression in den Primärkulturen signifikant reduziert, während die Überexpression von *miR-125b* keinen Effekt auf das Überleben der primären VMH Zellen zeigte. Insgesamt zeigen diese Ergebnisse, dass *miR-125b* die Differenzierung mes-/metencephaler BP Vorläuferzellen in postmitotische OM/TN Neurone kontrolliert, indem *miR-125b* die Expression von *Phox2b* und vermutlich auch von *Sim1* in diesen Zellen als auch deren Proliferation und Überleben reguliert.

1.2 Abstract

MicroRNAs (miRNAs) are 21-23 nucleotides, small non-coding RNAs which have essential functions in the mouse central nervous system. miRNAs are one of the key players to posttranscriptionally control gene expression by base-pairing with mRNAs containing a complementary sequence and either blocking translation or inducing the degradation of these target mRNAs. Since the discovery of *lin4*, the first miRNA found in *C. elegans* in 1993, more than a thousand miRNAs have been identified in animals, plants and viruses. Emerging findings suggested that miRNAs play a pivotal role in the transition from proliferating neural progenitors to postmitotic and differentiating neurons. Here I investigated the plausible functions of miRNAs in the development of the mid-/ hindbrain region (MHR). I first used combined computational algorithms, in collaboration with F. Theis's group at the Institute of Bioinformatics and Systems Biology (IBIS), Helmholtz Centre Munich, to predict miRNAs that might target known genes involved in the patterning of the MHR and in the development of ventral midbrain/hindbrain (VMH) neuronal populations, including the mesodiencephalic dopaminergic (mdDA) neurons. These predicted miRNAs were first validated based on their expression patterns in the developing CNS of the mouse embryo, particularly within the MHR. Next, miRNAs whose expression pattern was detected in this region were subsequently validated on a molecular level using 'sensor assays' to confirm their predicted target genes/mRNAs. Of a total of 33 *in silico* predicted miRNAs, only three miRNAs were correctly predicted to target three genes. However, since none of these miRNAs showed a mdDA-specific expression and were rather ubiquitously expressed throughout the mouse embryo including the developing neural tube, and since these three miRNAs were predicted *in silico* to target many candidate mRNAs, studying their *in vivo* function would have been very difficult or even impossible. These findings show that computational algorithms for the prediction of miRNAs and their targets are still giving a very high rate of false-positive hits, and that their output has only very limited use for subsequent biological validation.

I therefore used a different approach where miRNAs were profiled using next generation sequencing based on their expression during the directed differentiation of mouse embryonic stem cells (mESCs) into mdDA and other VMH neurons. Among the miRNAs that were most strongly upregulated in the differentiating neurons as compared

to the pluripotent, undifferentiated mESCs was *miR-125b*, a mammalian orthologue of *lin4*. Subsequent validation of these findings showed that *miR-125b* is indeed expressed within the MHR and strikingly within the basal plate (BP) of the developing murine mid-/ hindbrain. Notably, expression of *miR-125b* correlated with the expression of *Phox2b* and *Sim1*, two targets of this miRNA as predicted by TargetScan4.1, within the ventral MHR of the mouse. Subsequent validation confirmed that these two genes/mRNAs are direct targets of *miR-125b* using the previously mentioned sensor assays and site-directed mutagenesis of its predicted and conserved binding sites within the mRNA's 3'UTR. To investigate the biological function of this miRNA, I performed gain-of-function and loss-of-function experiments using VMH primary cell cultures. These experiments indeed showed that the numbers of *Phox2b*⁺ and *Isl1*⁺ oculomotor nucleus (OM) and trochlear nucleus (TN) neurons are decreased or increased upon *miR-125b* overexpression or knock-down, respectively. *Isl1* and *Phox2b* are two homeodomain (HD) transcription factors (TFs) involved in the proper development (OM/TN neurons are generated normally in *Phox2b* KO mice, and it has not been reported whether *Isl1* LOF (KO) leads to developmental defects of OM/TN neurons) of OM/TN neurons in the MHR. As the mRNA levels of *Sim1* were not regulated by *miR-125b* *in vitro* and due to the lack of a working antibody for *Sim1* protein, the impact of *miR-125b* overexpression or knock-down on *Sim1*-expressing BP progenitors could not be studied in these cultures. However, the numbers of mes-/metencephalic BP progenitors/precursors expressing the HD TF *Nkx6-1* were reduced upon *miR-125b* overexpression. Moreover, overexpression of *miR-125b* decreased the proliferation of these *Nkx6-1*⁺ BP progenitors as well as overall proliferation of VMH cells, whereas the knockdown of *miR-125b* did not affect cell proliferation in these cultures. Surprisingly, apoptotic cell death was decreased upon *miR-125b* knock-down, albeit an opposing effect was not observed after *miR-125b* overexpression. Altogether, these results indicate that *miR-125b* controls the differentiation of mes-/metencephalic BP progenitors into postmitotic OM/TN neurons by regulating the expression of *Phox2b* and possibly also of *Sim1* in these cells, as well as their proliferation and survival.

2.0 Introduction

microRNAs (miRNAs) are small (~22 nucleotide), noncoding RNAs that act to control the expression of sets of genes and are thus thought of as master regulators of gene expression. It binds to a complementary sequence in the 3'-primed untranslated region (3'-UTR) of its target mRNA and thus the expression of this mRNA is silenced; although the binding of miRNAs within the coding sequence (CDS) or 5'-UTR has now been reported in several cases. A seven nucleotide 'seed sequence' (at position 2-8 from the 5' end) in miRNAs seems to be crucial for miRNA action in animal cells, and other nucleotide positions may contribute small but important effects to miRNA action. Since the discovery of the founding microRNAs (miRNA) family members *lin4* and *let7* in *C.elegans* (Lee et al., 1993; Reinhart et al., 2000), hundreds of miRNAs have been identified across species (Lagos-Quintana et al., 2002). Experimental studies have established crucial functions of miRNAs in regulating many developmental events including proliferation, differentiation, apoptosis during embryogenesis (Yang and Wu, 2006); (O'Rourke et al., 2006) and in neurodegenerative diseases.

2.1.1 Biogenesis of miRNAs and mechanism of action

The biogenesis of miRNAs has been extensively reviewed by many researchers (Bartel, 2004; Tomari and Zamore, 2005; Ketting, 2011). Firstly, a primary-miRNA (pri-miRNA) which contains a 7-methyl guanosine cap and a poly(A) tail is produced by RNA polymerase II in the nucleus. Next, the pri-miRNA forms a specific hairpin-shaped stem-loop structure, followed by the recognition and cleavage by Drosha (a RNase III endonuclease) and a cofactor DGCR8 (Pasha) which functions as a molecular anchor necessary for the recognition of pri-miRNA (Denli et al., 2004), to become a pre-miRNA which consists of ~60-75 nucleotides. The hairpin RNA is then exported to the cytoplasm by the Exportin-5 (Exp5), a member of the Ran transport receptor family (Hutvagner et al., 2001; Bohnsack et al., 2004) (Figure 4). In the cytoplasm, the pre-miRNA is further processed by the enzyme *Dicer1*, resulting in a duplex of 19-24 nucleotides with 5' phosphates and a 2-nucleotide 3' overhang (Gregory and Shiekhattar, 2005). Helicase then unwinds the duplex into a separate mature miRNA and an opposite strand (miRNA*). The mature miRNA, on one hand, incorporates into

the miRNA-induced silencing complex (miRISC) that includes the Argonoute (Ago) proteins. On another hand, the opposite strand (miRNA*) is eliminated (Khvorova et al., 2003). The mature miRNA-RISC complex regulates their targets by either inducing the degradation of the target mRNA (high degree of complementarity) or suppressing mRNA translation (low degree of complementarity) which leads to the repression of protein production.

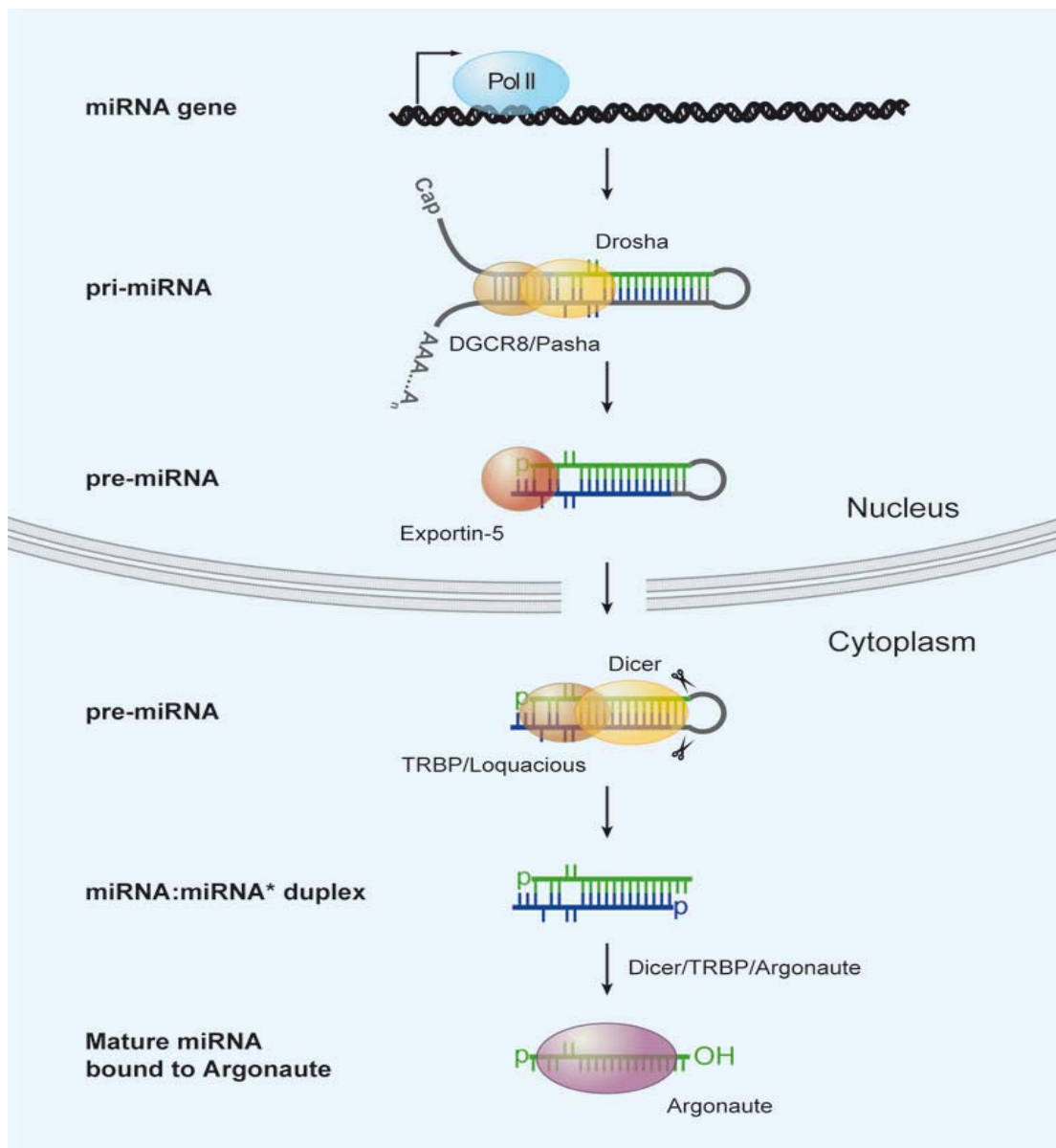


Figure 1. Biogenesis of miRNA. Pri-miRNA is firstly transcribed by RNA Pol II in the nucleus, followed by the subsequent processing of the pri-miRNA by Drosha and its partner to produce ~70 nt pre-miR that is exported into cytoplasm by Exportin 5. In the cytoplasm, pre-miR is processed by *Dicer1* RNase into the mature duplex miRNA. The mature miRNA is loaded into the miRNA-associated multi-protein RNA-induced silencing complex (miRISC) that includes the Argonoute proteins.

2.1.2 miRNAs expressions and functions in the developing CNS

Several studies have examined the expression profiles of miRNAs in developing and adult mouse central nervous system (CNS) (Bak et al., 2008; Dogini et al., 2008). Technological advancements have allowed for high-throughput and higher resolution analysis to be done in various regions including in the brain. For instance, *miR-218* is a brain-enriched miRNA (Sempere et al., 2004; Lau et al., 2008; Lugli et al., 2008) while *miR-222* is expressed in the telencephalon (Kapsimali et al., 2007); *miR-9* is expressed in both neural progenitors and their differentiated neurons while *miR-124* (Mishima et al., 2007) is expressed in neural precursors and maintained in mature neurons. Moreover, studies revealed that apart from tissue-specific miRNAs distribution in the CNS, miRNAs can also exhibit species-specific expression. For instance, while *miR-125b* expression is enriched in the zebrafish CNS, its expression is confined to the mid-hindbrain boundary in the mouse at early development (Ason et al., 2006). These studies suggest that miRNAs transcriptional regulations are highly divergent. Recent evidence suggest that miRNAs have emerged as important players in controlling cell differentiation and pattern formation processes, including neuronal patterning in *C. elegans* (Johnston and Hobert, 2003) and control of cell proliferation (Brennecke et al., 2003) as well as cell death (Xu et al., 2003). Interestingly, the first discovered miRNA, *lin4* (*miR-125b* in mammals), was found to be involved in regulating stage-specific processes during *C. elegans* larval development. In this regard, little is known about the role of miRNAs in the development of CNS of the mouse in general and in midbrain-hindbrain region (MHR) in particular.

2.2 The development of CNS of the mouse

During the development of the embryonic central nervous system (CNS), the mechanisms that specify regional identity and subsequently generate distinct neuronal subtypes are acquired through progressive restriction of developmental potential under the influence of local environment signals. Early on, neural signals from anterior visceral endoderm (AVE) (Ang et al., 1994; Beddington and Robertson, 1998) and mesendoderm (Ang and Rossant, 1993; Ang et al., 1994) induce the formation of neural plate. The neural plate then folds in upon itself, fuses at the dorsal apex forming the neural tube, which will later be subdivided into brain and spinal cord. The neural tube is subsequently patterned along the antero-posterior (AP), dorso-ventral (DV) (Shimamura et al., 1995) and left-right (medio-lateral) axes (Altmann and Brivanlou, 2001). Along the AP axis, from rostral to caudal, three major brain vesicles are first formed: forebrain, midbrain and hindbrain. Later on and as development progresses, these domains are subsequently specified into segments or neuromeres. The forebrain gives rise to the prosencephalon which comprises of telencephalon and diencephalon; midbrain or mesencephalon remains a unique and single mesomere whereas the hindbrain or rhombencephalon is subdivided into metencephalon and myelencephalon (Fig.1a) (Cambroner and Puelles, 2000).

Evidence for the localization of morphogenetic signals at specific locations directing the AP and DV patterning events has suggested the concept of "secondary organizer regions" (Martinez, 2001). These organizers are a group of cells located in key regions of the embryonic brain that emit signals capable of both inducing and patterning the surrounding tissue (Puelles and Rubenstein, 2003). Several successfully identified signals are morphogens Sonic hedgehog (Shh) (Echelard et al., 1993), wingless-type MMTV integration site family, member 1 (Wnt1) (McMahon and Moon, 1989) and Fibroblast growth factor 8 (Fgf8) (Fig. 2a) (Crossley and Martin, 1995). Three centers/organizers have been identified to date: the isthmus organizer (IsO) at the mid-hindbrain boundary; the zona limitans intrathalamica (zli) at the prethalamus-thalamus (p2/p3) boundary and the anterior neural ridge (ANR) at the rostral end of the secondary prosencephalon (Echevarria et al., 2003). The IsO possesses midbrain- and cerebellum –inducing properties and its positioning at the MHB is a crucial event that controls midbrain and cerebellum development. The IsO is characterized by the

localized expression of several secreting molecules such as Fgf8 and Wnt1 (Partanen, 2007) and transcription factors such as En, Pax, Otx and Gbx families (Rhinn and Brand, 2001)

Complementary to these transversal segmentation and AP patterning, longitudinal domains are also present along the DV axis (Fig. 2a,b). From ventral to dorsal, these are the floor plate (FP), basal plate (BP), alar plate (AP) and roof plate (RP) (Fig. 2b) (Shimamura et al., 1995). These are the result of two opposed signaling which confer to DV axis: Shh secreted ventrally from the notochord (Chiang et al., 1996) while bone morphogenetic proteins (BMPs) are secreted dorsally from the boundary of neural and non-neural ectoderm and roof plate (Lee and Jessell, 1999). In the midbrain, the adult mesencephalon has a clear DV organization. Dorsally, the tectum comprises the layered structure of superior colliculi and the globular structure of inferior colliculi. Ventrally, the tegmentum contains several distinct neuronal populations which are mostly organized in nuclei.

Gain and loss of function experiments indicate that Shh is both necessary and sufficient to induce ventral cell types (Chiang et al., 1996) (Briscoe et al., 2000; Joksimovic et al., 2009). Interestingly, recent data have shown that the generation of DA and OM but not of RN neurons depends on early Shh signaling from the midbrain FP (Perez-Balaguer et al., 2009).

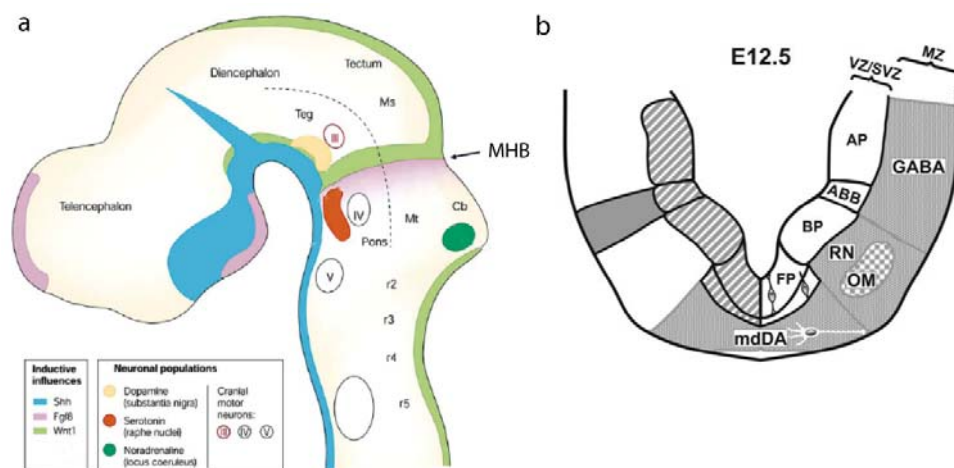


Figure 2. Schematic sections showing sagittal (a) and coronal (b) view of a murine embryo neural tube during midgestation, expression of the secreted factors Fgf8,

Wnt1, Shh and expression domains of some ventral midbrain- hindbrain neuronal populations. (a) The anterior neural tube is subdivided in the A/P axis into forebrain (telencephalon and diencephalon), midbrain (mesencephalon) and hindbrain (metencephalon and myelencephalon) (Modified picture from (Prakash and Wurst, 2004) (b) and in the D/V axis into floor plate, basal plate and alar plate. In the midbrain, mdDA neuron is located in FP, OM and red nucleus neurons are located in the BP; serotonergic neuron and trochlear nuclear are locate in the hindbrain. Abbreviations: AP, alar plate; ABB, alar basal boundary; BP, basal plate; Cb, cerebellum; FP, floor plate; H, hindbrain; M, midbrain; Ms, mesencephalon, Mt, metencephalon; mdDA, meso-dien Dopaminergic neuron; MZ, mantle zone; OM, oculomotor; RN, red nucleus; r(1-5), rhombomere; SVZ, subventricular zone; Teg, tegmentum; VZ, ventricular zone.

2.2.1 Development of the ventral mid-/hindbrain (vMH) neuronal populations of the mouse

During the mouse embryonic development, the vMH is organised into several distinct nuclei. Some of them are well-defined, for instance meso-diencephalic dopaminergic (mdDA) neuronal population which is located in the ventral midline of the midbrain FP. Lateral to the FP is the BP oculomotor (OM) nucleus (Fig. 2a-b). Another midbrain BP neuronal population, the red nucleus (RN), is located ventral to the OM, dorsal to the substantia nigra and lateral to the ventral tegmental area (VTA).

2.2.2 Genetic mechanisms involved in differentiation of mdDA neuron

Among the ventral midbrain tegmentum neuronal populations, mdDA populations of the substantia nigra (SN) and ventral tegmental area (VTA) have received the most attention as the result of its implication in diverse psychiatric and neurological disorders such as schizophrenia and Parkinson's disease (PD) (Hornykiewicz, 1978). Moreover, mdDA neurons are essential in the generation of reward and in the development of addictive behaviors such as drug addiction (Chao and Nestler, 2004). Notably, Parkinson's disease is the most common neurodegenerative movement disorder which onsets around at the age of 50-60. Degeneration of mdDA

neuron in the substantia nigra pars compacta (SNc) causes the depletion of dopamine in the striatum, which is the main target of the axonal projections originating from the SNc. Despite the availability of effective symptomatic drugs and treatments, there is presently no cure for PD. One possible treatment would be replacing the degenerating mdDA neurons in the human SNc with healthy mdDA neurons which were generated from directed differentiation of stem cells (Winkler et al., 2005). Therefore, further investigation to understand both the genetic and epigenetic cues controlling the development of mdDA neuron is essential for successful cell replacement therapy in PD.

The genetic cascade responsible for the developmental program of mdDA neurons has been extensively reviewed (Table 1, Fig. 3) (Prakash and Wurst, 2006) (Simeone, 2005) (Smits et al., 2006). In brief, there are three major groups of factors involved in the development of mdDA neurons. One group is formed by extracellular signals involved in the induction of the dopaminergic phenotype. Those secreted factors are for example Shh, Fgf8, TGFs, and Wnt1. It has been demonstrated that Shh alone is capable of inducing mdDA neuron in the ventral mesencephalon (Hynes et al., 1995) but an addition of Fgf8 is required to generate DA neurons in other neural territories (Ye et al., 1998). The Second group is composed of transcription factors such as Otx2, En1/2, Lmx1a/b, Nr4a2 (Nurr1) and Pitx3 (Table1), among others, that are involved in the intrinsic cell specification and differentiation program of this pre-specified cell type. Expressions of some of these early factors (first and second groups) are required to activate Th expression in mdDA precursors. Table 1 summarized these transcription factors and their roles in mdDA neuron development. Lastly, there is a group of genes related to expression of all the enzymes, transporters, and receptors (Slc6A3, D1-like family, D2-like family and etc) are required for the proper synthesis, storage, release, and reuptake of dopamine by these neurons (Puelles, 2007).

Furthermore, Wnt1 has been shown to be needed for both induction of the progenitor and terminal differentiation of the mdDA neurons (Prakash et al., 2006). Expression of Wnt1 starts at embryonic day 8.0 (E8.0) in a broad domain within the presumptive midbrain and later at E9.5 appears as a ring encircling the neural tube at the mid-hindbrain boundary (MHB). At this stage, Wnt1 is also expressed in the dorsal midline (roof plate) of the midbrain and caudal diencephalon and ventrally, it is restricted to two stripes along the lateral midbrain FP within the cephalic flexure. It

should be noted that Wnt1 expression domain overlaps with the mdDA progenitor domain at E9.5 and of later mdDA neuron at E10.5-12.5. For these reasons, Wnt1 appeared to be a candidate conferring the development of mdDA neuron (Prakash et al., 2006). Interestingly, only a few tyrosine hydroxylase (Th), which is the rate-limiting enzyme in DA biosynthesis, expressing mdDA neurons were found in the Wnt1^{-/-} mice. However, these few Th⁺ cells fail to initiate Pitx3 expression. Conversely, ectopic Wnt1 expression in the En domain (*En1^{+Wnt1}*) mice did not result in ectopic mdDA neurons in the rostral, suggesting a causal relationship between Wnt1 expression and mdDA neuron development (Prakash et al., 2006).

Table 1. A summary of the role of transcription factors in mdDA neuron development.

Transcription factor	Expression localization	Function in mdDA cells	References
Otx2	Progenitors	Required for regional and neuronal specification of mdDA progenitors	Puelles et al., 2003; Puelles et al., 2004; Vernay et al., 2005
Msx1	Progenitors	Required for neuronal differentiation	Andersson et al., 2005
Mash1	Progenitors	Not required for neuronal differentiation but can compensate for Ngn2 function	Kele et al., 2006
Lmx1b	Progenitors	Required for maintenance of mature mdDA neuron	Smidt et al., 2000
En1/2	Progenitor, immature and mature neurons	Required for the generation and survival of mature mdDA neurons	Simon et al., 2001; Alberi et al., 2004;
Nurr1	Immature and mature neurons	Required for the maintenance of mature mdDA neurons and their expression of late differentiation markers	Zetterstrom et al., 1997; Saucedo-Cardenas et al., 1998; Wallen et al., 1999; Wallen et al., 2001; Smits et al., 2003
Pitx3	Mature neurons	Required for Th-expression in a subset of mature mdDA neurons	Hwang et al., 2003; Nunes et al., 2003; van den Munchhof et al., 2003; Smidt et al., 2004; Maxwell et al., 2005

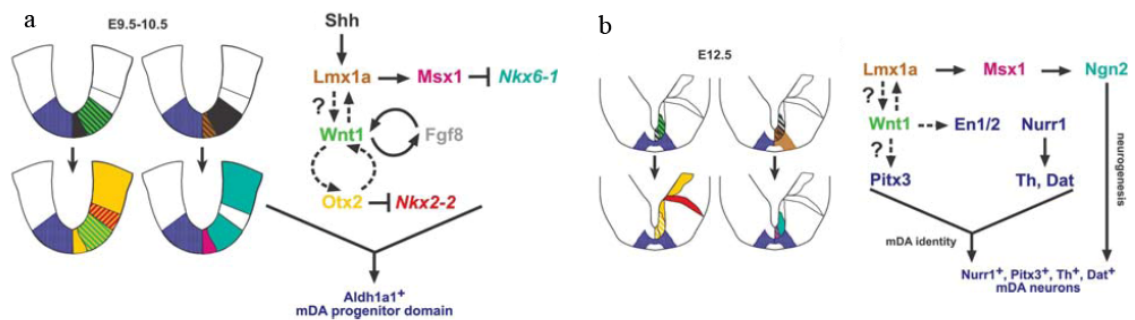


Figure 3. Schematic illustrations show (a) establishment of the mdDA progenitor domain during early stages of the mouse neural development and (b) determination of the mdDA neuron cell fate in mdDA precursors at intermediate stages of mouse neural development. Picture taken from (Prakash and Wurst, 2006).

2.2.3 Genetic mechanisms involved in development of OM/TN and RN

Compared to mdDA neurons, less is known about the cues controlling the development of other ventral midbrain neuronal populations such as OM, trochlear nucleus (TN) and RN (Fig. 4). Both OM/TN and RN nuclei belong to part of the motor systems, however their functions and connections are distinct from each other. The OM nucleus appears very early in development. This was evidenced by experimental enlargement of the Shh expression domain in the ventral midbrain at approx. E9.5, which alters other ventral nuclei but not the OM nucleus, suggesting that the OM nucleus had already been determined at that time (Puelles et al., 2004). The OM gives rise to the third (nIII) cranial nerve, controlling four out of six eye muscles, allowing eye movement and parasympathetic regulation of eye accommodation and pupil contraction (Evinger, 1988). Meanwhile, another motoneuron (MN) population, the TN, located in the rostral hindbrain close to the MHB, gives rise to the fourth (nIV) cranial nerve which regulates the movements of the contralateral superior oblique muscle of the eye.

The LIM homeodomain (HD) TF *islet1* (*Isl1*), a generic MN markers, is expressed in the OM/TN (Ericson et al., 1992; Agarwala and Ragsdale, 2002). However, its function in the developing OM/TN remains unknown. Expression studies conducted on mouse have identified the paired-like homeobox gene *Phox2a* and its paralogue *Phox2b* as HD TF expressed in the motor nuclei of the hindbrain and also in OM/TN. In the developing OM/TN motor nuclei, *Phox2a* expression preceded that of *Phox2b* where *Phox2a* mRNA was detected at E9 and the protein was found a day later at E10. *Phox2a* expression was found in OM/TN progenitors and is required for the proper development of OM/TN, as loss-of-function of *Phox2a* leads to the agenesis of the OM/TN in the mice (Pattyn et al., 1997), zebrafish (Guo et al., 1999) and human (Nakano et al., 2001). More recent findings have shown some shared competency between the *phox2a/b* genes in the development of MNs. Expression studies showed that *Phox2b* is also expressed in midbrain OM neurons and is essential for the production of branchio-visceral MN precursor (Pattyn et al., 2000). While *Phox2a* is mostly expressed in the progenitors, *Phox2b* is expressed in the postmitotic neurons and not essential alone for their generation of the OM/TN nuclei. Gain-of-function experiments in the chicken spinal cord showed *Phox2b* regulates neuronal cell cycle

exit, driving progenitors out of the cell cycle and consequently emigrate out of the VZ into the MZ (Dubreuil et al., 2000).

The RN, by contrast, contains no MNs but is a cerebellar-related nucleus mediating motor cortex and cerebellar outflow to spinal cord in the control of limb movements (Holstege and Tan, 1988; Keifer and Houk, 1994). The RN is organized in two subpopulations, the anterior parvocellular part located in the posterior diencephalon and the posterior magnocellular part located in the mesencephalon (Massion, 1967), and contains both excitatory glutamate and inhibitory gamma-aminobutyric acid (GABA)-synthesizing neurons. This neuron population arises laterally to the mdDA domain, from BP progenitors expressing *Shh* and *Nkx6-1*⁺. Therefore, both the OM and RN neurons most likely share the same progenitor pool in the ventricular epithelium (Agarwala and Ragsdale, 2002). Two homeobox genes, *Pou4f1* (*Brn3a*) and *Emx2*, identify the RN territory and both genes are required for the proper development and/or survival of the RN (McEvelly et al., 1996; Agarwala and Ragsdale, 2002). In *Emx2*^{-/-} mice, *Brn3a*⁺ RN neurons are generated but are not detected beyond E16.5. In *Brn3a*^{-/-} mice, RN are lost by E18.5 (McEvelly et al., 1996; Xiang et al., 1996; Agarwala and Ragsdale, 2002).

While it is not yet fully comprehended the functions of *Nkx6-1* homeobox transcription factor in the OM/TN and RN of the developing midbrain, several studies revealed that it is required for the development of hindbrain and spinal somatic MNs and interneurons (INs) (Broihier et al., 2004; Hutchinson et al., 2007). Paralogues *Nkx6-1* and *Nkx6-2* are transcriptional repressors induced by *Shh* signaling in the ventral midbrain, hindbrain and spinal cord (Briscoe et al., 2000), and are required for the proper migration and axon pathfinding of hindbrain visceral MNs but not the initial specification (Muller et al., 2003). In mice, *Nkx6-1* is expressed in ventral midbrain FP and BP progenitors and also in post-mitotic *Islet1* positive (*Isl1*⁺) OM/TN (Prakash et al., 2009).

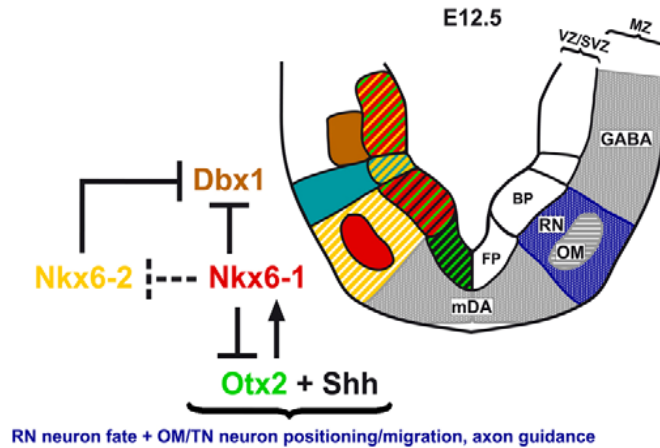


Figure 4. Schematic coronal section of the ventrolateral midbrain at E12.5 which gives rise to OM and RN. The left half of the schematic illustrates the different expression and progenitor domains at this stage, giving rise to the neuronal populations depicted on the right. Picture taken from (Prakash et al., 2009).

2.3 Aims of the present work

In this work, I have experimentally validated five miRNAs predicted by computational algorithms to be involved in the regulation of the IsO GRN and mdDA neuron development. In addition, using miRNA profiling based on directed differentiation of mouse embryonic stem cells (mESCs) into mdDA and other VMH neurons; I uncovered a novel function of *miR-125b* in the CNS. *MiR-125b* is expressed highly within the BP of the midbrain and rostral hindbrain. I showed that *Sim1*, which is speculated to be a BP progenitor RN marker, and *Phox2b*, a postmitotic marker of OM/TN, are direct targets of *miR-125b*. Lentivirus transduced primary cultures by either overexpression or knockdown of *miR-125b* revealed that *miR-125b* controls the differentiation of mes-/metencephalic BP progenitors into postmitotic OM/TN and/or RN neurons by regulating the expression of *Phox2b*, *Nkx6-1* and possibly also of *Sim1* in these cells, as well as their proliferation and survival.

3.0 Results

Enormous efforts have been made to elucidate the developmental genetic cues of various neuronal populations, particularly vMH neurons such as mdDA, OM and RN neurons. In this regard, many secreted factors and transcription factors have been unravelled and were shown essential in giving rise to these vMH neuronal populations. However, little is known about the roles of miRNAs in this regard. To answer this question, two distinct strategies were employed. Firstly, a combination of five distinct computational algorithms was used to mine putative miRNAs that might be involved in the regulation of the MHB genetic regulatory network (GRN) and mdDA neuron development. The subsequent experimental validation showed that many candidate miRNAs were incorrectly predicted. Therefore, a second, experimental approach was chosen by profiling miRNAs expressed during the differentiation of mouse ES cells into vMH neurons *in vitro*. This method proved to be more successful to single out functionally relevant and context-specific miRNAs.

3.1. miRNAs that might be involved in the regulation of the MHB GRN and mdDA neuron development as predicted by computational algorithms

The searches for miRNAs with the computational prediction strategy was initiated with a gene list comprising genes involved in the development of the MHB GRN and mdDA neurons (1st priority) or of other vMH neurons (2nd priority), and in Parkinson's disease (last priority), respectively (Table 2). The computational predictions were done in collaboration with Dr. D. Trümbach (IDG) and the group of Prof. Dr. F. Theis (IBIS). Firstly, using miRBase, Dr. D. Trümbach generated a list of miRNAs predicted to target known mRNAs from the list of genes of interest as mentioned above (Fig. 5). Next, together with Dr. D. Lutter from IBIS, a refinement criteria were introduced where five different mining tools (miRBase (Griffiths-Jones et al., 2006; Kozomara and Griffiths-Jones, 2011), PicTar (Krek et al., 2005; Griffiths-Jones et al., 2006), TargetScan (Friedman et al., 2009), miRNAMAP2.0 (Hsu et al., 2006; Hsu et al., 2008), TargetSpy (self-made)) were used to filter the pre-selected miRNAs. Under these refinement criteria, a miRNA is considered a candidate if the same miRNA has appeared in three out of five bioinformatics mining tools. This has resulted in 155

miRNAs. Then, a logical state of ON/OFF table from the genes of interest (Table 2) was defined for three mouse embryonic stages, namely E8.5, E10.5 and E12.5. An ‘OFF’ means miRNA is ‘ON’/expressed; an ‘ON’ means that the miRNA is ‘OFF’/ not expressed at the corresponding stage. miRNAs that target at minimum of two ‘OFF’ genes and no ‘ON’ gene for each developmental stage were subsequently selected. This resulted in a final list of 33 candidate miRNAs (Fig. 6, Table 3).

Table 2. Candidate genes involved in the development of the MHB GRN, mdDA and other vMH neuronal populations, and in PD.

Genes of interest involved in MHB GRN/mdDA neuron development (1 st priority)					
<i>Otx2</i>	<i>Fgf8</i>	<i>Nr4a2</i>	<i>Foxa1/2</i>	<i>Msx1</i>	<i>Vmat2</i>
<i>Wnt1</i>	<i>Wnt5a</i>	<i>Pitx3</i>	<i>Nkx2-2</i>	<i>Ngn2</i>	<i>Fzd3/6/9</i>
<i>Shh</i>	<i>Aldh1a1</i>	<i>Th</i>	<i>Lmx1a/b</i>	<i>Slc6a3</i>	<i>Lef1</i>
Genes of interest involved in the development of other vMH neuron populations (2 nd priority)					
<i>Phox2a/b</i>	<i>Nkx6-1/2</i>	<i>Pou4f1</i>	<i>Isl1</i>	<i>Ascl1</i>	<i>Dbx1</i>
<i>Ngn1</i>	<i>Pax6</i>	<i>Helt</i>			
Genes of interest involved in Parkinson’s Disease (Last priority)					
<i>Sncα</i>	<i>Pink1</i>	<i>Lrrk2</i>	<i>Park7</i>	<i>Park2 (Parkin)</i>	

Table 3. Final selection of 33 miRNAs predicted from a combination of computational algorithms with their predicted target genes.

miRNA	Target gene	miRNA	Target gene	miRNA	Target gene
<i>miR-7b</i>	<i>Sncα</i>	<i>miR-212</i>	<i>Fzd3</i>	<i>miR-452</i>	<i>Nkx2-2</i>
<i>miR-17-3p</i>	<i>Adh1a1</i>	<i>miR-224</i>	<i>Adh1a1</i>	<i>miR-469</i>	<i>Pitx3</i>
<i>miR-22</i>	<i>Nkx2-2</i>	<i>miR-300</i>	<i>Isl1</i>	<i>miR-674</i>	<i>Phox2b</i>
<i>miR-30a-3p</i>	<i>Pou4f1</i>	<i>miR-320</i>	<i>Phox2b</i>	<i>miR-679</i>	<i>Pou4f1</i>
<i>miR-34a</i>	<i>Lef1</i>	<i>miR-328</i>	<i>Shh</i>	<i>miR-684</i>	<i>Helt</i>
<i>miR-132</i>	<i>Wnt1</i>	<i>miR-350</i>	<i>Foxa2</i>	<i>miR-689</i>	<i>Foxa2</i>

<i>miR-133a</i>	<i>Pitx3</i>	<i>miR-365</i>	<i>Pax6</i>	<i>miR-693-3p</i>	<i>Nr4a2</i>
<i>miR-133b</i>	<i>Pitx3</i>	<i>miR-378</i>	<i>Foxa1</i>	<i>miR-705</i>	<i>Wnt1</i>
<i>miR-138</i>	<i>Phox2b</i>	<i>miR-449a</i>	<i>Lef1</i>	<i>miR-709</i>	<i>Wnt1</i>
<i>miR-144</i>	<i>Fzd6</i>	<i>miR-449b</i>	<i>Lef1</i>	<i>miR-712</i>	<i>Wnt5a</i>
<i>miR-210</i>	<i>Foxa1</i>	<i>miR-449c</i>	<i>Lef1</i>	<i>miR-714</i>	<i>Lef1</i>

I validated these predictions by three criteria: (1) the expression of the miRNA must be detectable in MHB tissues and/or in mdDA or other vMH neurons of the developing mouse embryo; (2) the miRNA must downregulate the mRNA/protein expression of its predicted target as assessed in luciferase sensor assays; and (3) site-directed mutagenesis of the predicted binding sites (seed sequence) of the miRNA in its target 3'UTR must abolish the miRNA-mediated downregulation of this target. To establish the first criterium, Locked Nucleic Acid-based *in situ* hybridization (LNA-ISH) was first performed to establish the spatiotemporal expression pattern of the 33 candidate miRNAs during mouse embryonic development. The analyses were conducted on mouse embryos at embryonic day (E) 10.5, when the MHB/IsO is fully established and mdDA neurons proliferate, at E12.5, the stages when the mdDA neurons differentiate and the expression of mdDA marker genes mentioned earlier are detectable in the ventral midbrain of the mouse neural tube (reviewed in Prakash and Wurst, 2006), and at E17.5, when mdDA neurons are almost fully mature and express several marker genes, including genes involved in PD.

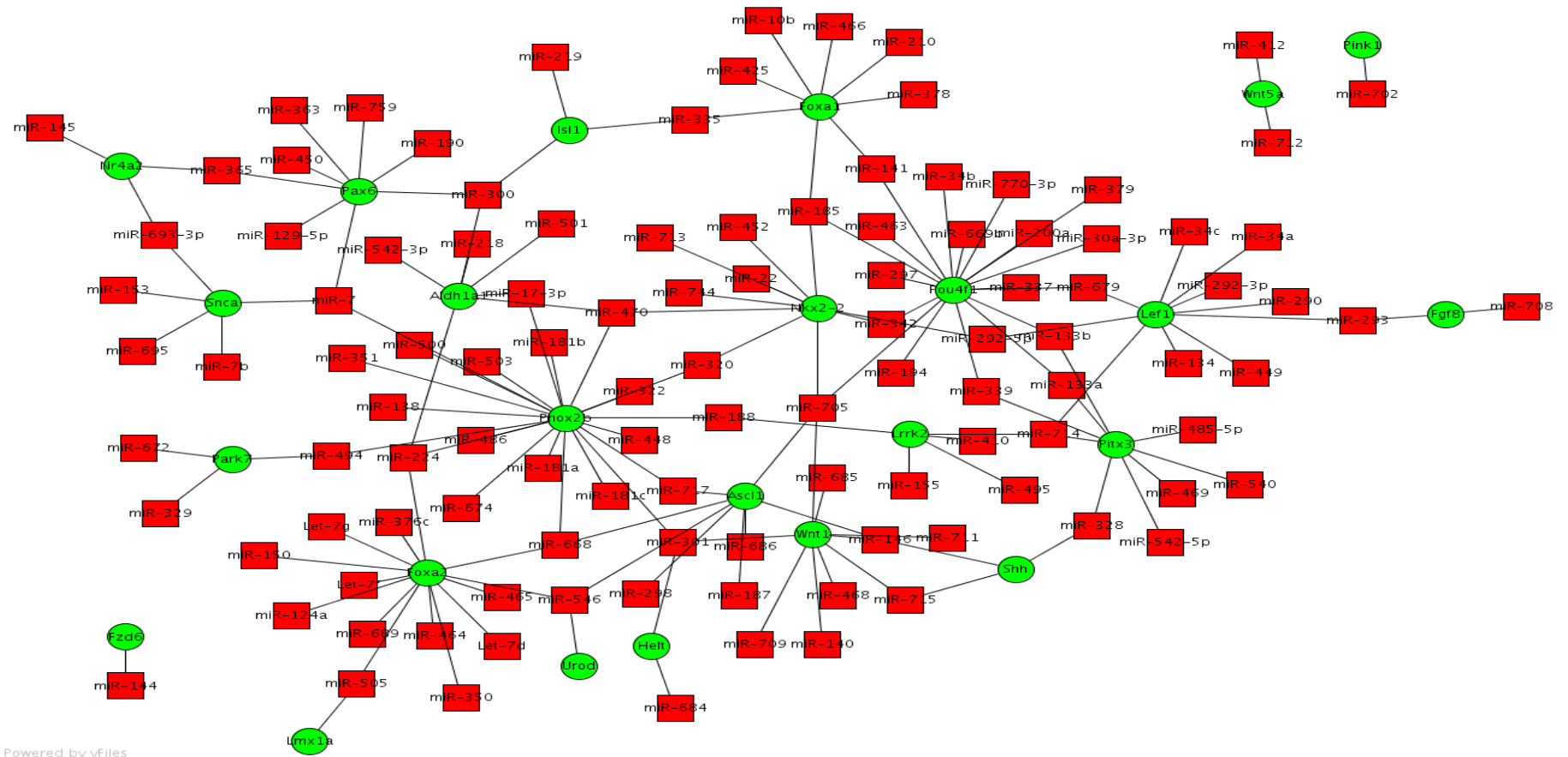


Figure. 5 155 candidate miRNAs predicted to target genes involved in the development of the MHB GRN, of mDDA and of other vMH neuronal populations, and in PD (courtesy of D. Trümbach)

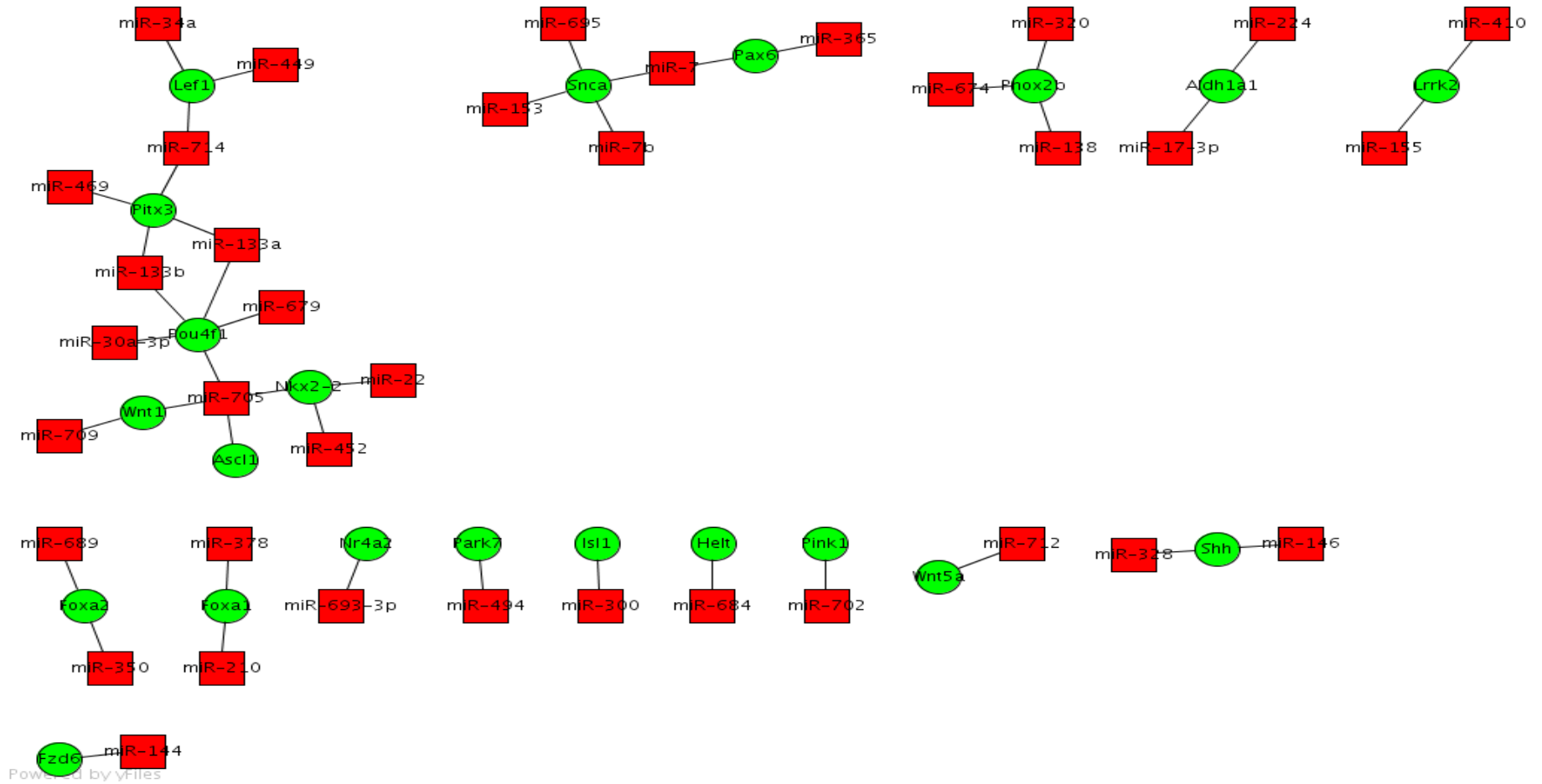


Figure 6. 33 candidate miRNAs after logical filtering for “ON/OFF” states of miRNAs from the previous list (see Fig. 5) were predicted to target genes involved in the development of the MHB GRN, of mdDA and of other vMH neuronal populations, and in PD - there are still PD genes included in this list! (courtesy of D. Trümbach).

3.1.1. Establishment of the LNA-ISH detection method and the validation of miRNA expression patterns

The LNA-ISH method had to be first established in our lab. To control for my results, I used three miRNAs with a known expression pattern in the murine CNS as positive controls. These miRNAs comprised *miR-9* (Kapsimali et al., 2007), *miR-135a* and *miR-135b* (Lagos-Quintana et al., 2002; Kim et al., 2004) (Fig. 7). My results using LNA-ISH of consecutive midsagittal sections revealed that *miR-9* is exclusively expressed in the CNS, only sparing the mid-hindbrain boundary (MHB) as reported by (Leucht et al., 2008) in the zebrafish (Fig. 7b,d). *miR-135a* and *miR-135b*, which differ only by one nucleotide in the mature miRNA sequence (outside the seed region), have very similar expression patterns where specific expression at E10.5 is detected in the forebrain, midbrain (Fig. 7f,h) and spinal cord (data not shown). At E12.5, *miR-135a/b* expression is found in the entire brain and spinal cord (Fig. 7j,l). Interestingly, a distinct expression of *miR-135a/b* is observed also in the mouse liver at E12.5 (Fig. 7h,l, white arrows). As negative control, I used *Scramble-miR* (Exiqon, Denmark), which has a similar length and LNA content as other LNA-oligos but whose sequence bears no homology to any known microRNA or mRNA sequence in human, mouse and rat. (Morton et al., 2008) and has therefore been shown to be unable to hybridize to other single-stranded nucleic acids and to give any signal. As expected, ISH with the *Scramble-miR* probe consistently showed no signal in any sections in all experiments performed with this probe (Fig. 7n,p).

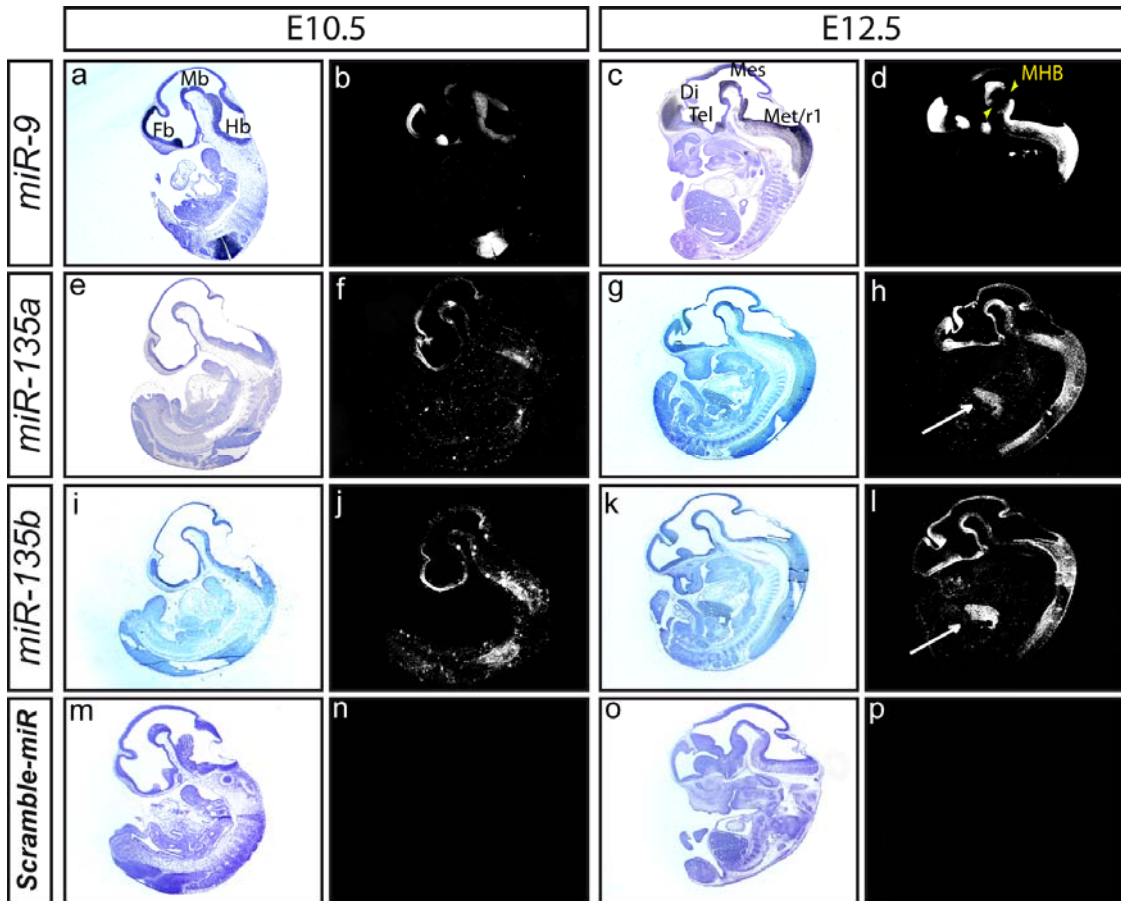


Figure 7 Positive and negative controls used for radioactive *in situ* hybridization detection of miRNAs on paraffin sections of whole mouse embryos. a-p: Representative entire embryo view in midsagittal sections from E10.5 (a-b, e-f, i-j, m-n) and E12.5 (c-d, g-h, k-l, o-p) CD-1 mouse embryos hybridized with LNA-based ISH probes for *miR-9* (a-d), *miR-135a* (e-h), *miR-135b* (i-l) and scrambled-miR (m-p). Dorsal is at the top, anterior to the left. Three miRNAs (*miR-9*, *miR-135a* and *miR-135b*) are chosen as positive control due to their CNS-specific expression pattern. Notably, *miR-135a/b* expression was also detected in the liver at E12.5 (h,l, white arrows). *Scramble-miR* (Exiqon probe) served as a negative control that should not give any signal as it cannot hybridize to single-stranded nucleic acids (mRNA, miRNA). Bright field pictures are counter-stained with Cresyl Violet. Dark field pictures in b,d showed that *miR-9* is expressed in the entire CNS including Fb and Hb but sparing the MHB (*miR-9* expression in the entire Mb and spinal cord is not shown in these pictures due to the sectioning level). Dark field pictures in f, j showed that *miR-135a/b* is expressed within the neural tube including Fb, Mb and Hb. At E12.5, dark field pictures in h,l showed that *miR-135a/b* is expressed in Tel, Di, Mes, Met, spinal cord and liver (white arrow). Abbreviations: Di, diencephalon; Fb, forebrain; Hb, hindbrain; Mb, midbrain; Mes, mesencephalon; Met metencephalon; MHB, mid-hindbrain boundary; r1, rhombomere 1; Tel, telencephalon.

3.1.1.1. miRNAs that are expressed in the developing mouse CNS

From the expression profiling of the 33 predicted miRNAs, the expression pattern of 29 candidate miRNAs could not be determined because of either the expression of the miRNAs were not detectable in MHR or ubiquitously widespread throughout the embryo, thus making those miRNA candidates expression profile difficult to be interpreted (Dark field pictures shown in supplementary in Fig. S1). Table 4 summarises the ISH results of the 29 candidate miRNAs expression pattern. However, four candidate miRNAs (*miR-705*, *miR-709*, *miR-712* and *miR-714*) showed a distinctive expression pattern in the mouse embryo during midgestational stages (Fig. 8). The expression of these four miRNAs fulfilled the first criterion where expressions were detectable in the MHR. Notably, apart from the CNS, all of the four miRNAs are also expressed in the peripheral nervous system (PNS) including the dorsal root ganglia (DRG). All except *miR-705* appear to be most strongly expressed in the CNS and DRG (Fig. 8).

Table 4: Summary of *in silico* predicted miRNAs expression patterns during midgestational (E10.5, E12.5) of the mouse.

miRNA	Expression pattern	miRNA	Expression pattern	miRNA	Expression pattern
<i>miR-133a</i>	Nil	<i>miR-328</i>	Nil	<i>miR-378</i>	Nil
<i>miR-133b</i>	Nil	<i>miR-7b</i>	Nil	<i>miR-689</i>	Ubi.Exp
<i>miR-210</i>	Ubi.Exp	<i>miR-350</i>	Nil	<i>miR-679</i>	Ubi.Exp
<i>miR-34a</i>	Nil	<i>miR-320</i>	Ubi.Exp	<i>miR-212</i>	Nil
<i>miR-449a</i>	Nil	<i>miR-300</i>	Nil	<i>miR-132</i>	Nil
<i>miR-449b</i>	Nil	<i>miR-365</i>	Nil	<i>miR-693-3p</i>	Ubi.Exp
<i>miR-449c</i>	Nil	<i>miR-17</i>	Nil	<i>miR-469</i>	Nil
<i>miR-138</i>	Nil	<i>miR-22</i>	Nil	<i>miR-224</i>	Nil
<i>miR-452</i>	Ubi.Exp	<i>miR-30a</i>	Nil	<i>miR-674</i>	Nil
<i>miR-684</i>	Nil				

N.B.: Nil = Expression could not be determined. Silver grains could be detected in the dark field pictures. Ubi.Exp = Ubiquitous expression. An even distribution of signals (silver grains) was observed throughout the embryo as observed in the dark field. In some instances, the signals could be observed in the bright field pictures, where the blue-ish cresyl violet stained tissue was seen as 'black'.

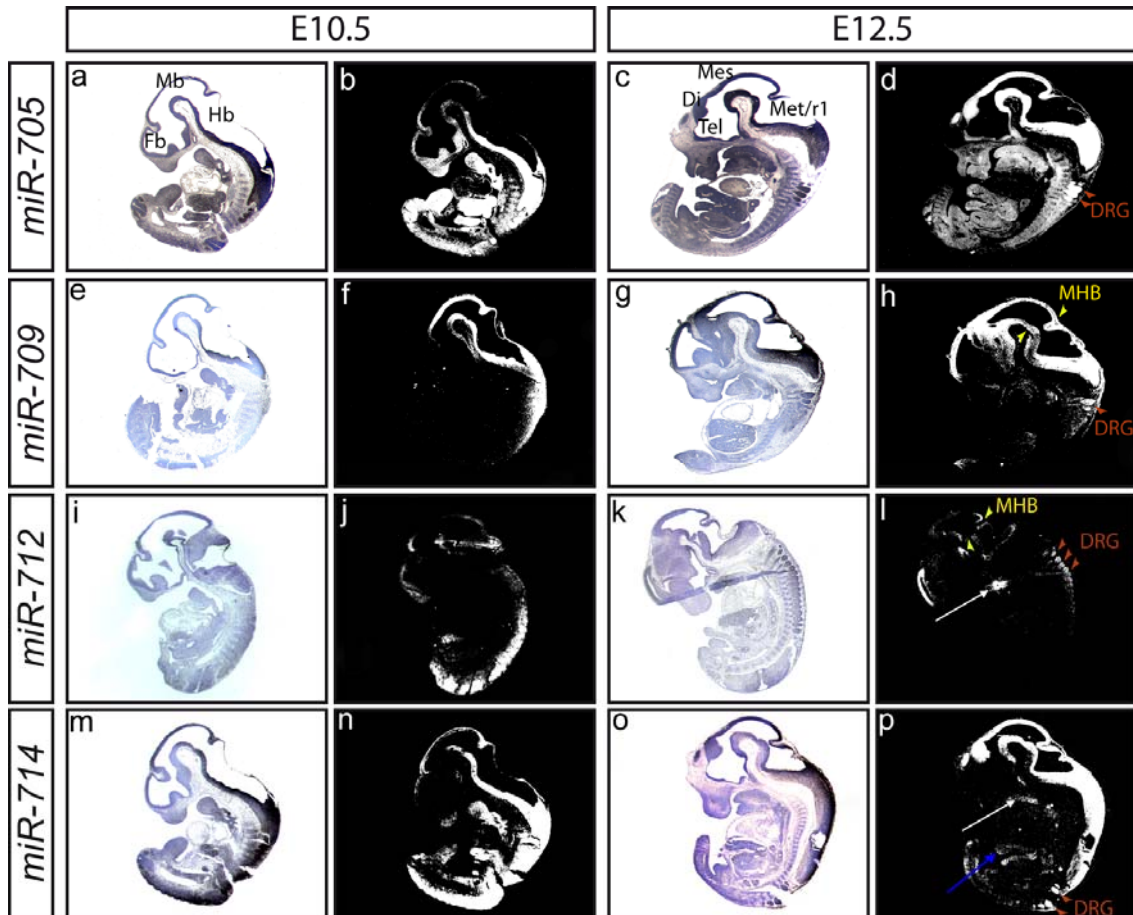


Figure 8. Expression patterns of the four miRNAs found to be expressed in the CNS/MHR/MHB of the midgestational mouse embryo. a-p: Representative entire embryo view in midsagittal sections from E10.5 (a-b, e-f, i-j, m-n) and E12.5 (c-d, g-h, k-l, o-p) CD-1 mouse embryos hybridized with LNA-based ISH probes for *miR-705* (a-d), *miR-709* (e-h), *miR-712* (i-l) and *miR-714* (m-p). Dorsal is at the top, anterior to the left. Bright field pictures were counter-stained with Cresyl Violet. Yellow arrow head: MHB; red arrow head: DRG; white arrow: tongue; blue arrow: liver. Abbreviations: Di, diencephalon; DRG, dorsal root ganglia; Fb, forebrain; Hb, hindbrain; Mb, midbrain; Mes, mesencephalon; Met metencephalon; r1, rhombomere 1; Tel, telencephalon.

At E10.5, lower expression of *miR-705* is observed in the dorsal midbrain (tectum) and mesencephalic flexure (Fig.8b). Two days later at E12.5, higher expression of *miR-705* appeared in the MHR/CNS including the entire brain and spinal cord. Higher expression in the DRG is observed at this stage (Fig. 8d, red arrow head).

MiR-709 is expressed at E10.5 in the anterior neural tube including hindbrain, midbrain and part of the forebrain (diencephalon) but sparing the majority of the forebrain (Fig. 8e,f). At E12.5, a relatively strong expression of *miR-709* is observed in the dorsal forebrain (cortex and dorsal thalamus), dorsal midbrain (tectum), hindbrain

(caudal rhombomere 1) and DRG (red arrow head) (Fig. 8g,h) while lower expression level is observed in the ventral midbrain and rostral rhombomere 1 at both sides of the ventral MHB (yellow arrow head) (Fig. 8g,h). Noteworthy, *miR-709* is still not expressed in the ventral forebrain at this stage (Fig. 8g,h).

Expression of another tested miRNA, *miR-712*, at E10.5 is observed in the dorsal telencephalon, dorsal diencephalon, at both sides of the MHB and in the spinal cord while a weaker expression is observed in the dorsal and ventral midbrain (Fig. 8i,j). Two days later at E12.5, a very similar expression of *miR-712* is observed. For instance, expression of *miR-712* is observed in cortex (dorsal telencephalon), tectum (dorsal midbrain), tegmentum (ventral midbrain) and both sides of the MHB (yellow arrow head). However, expression is also observed in the DRGs at this stage (red arrow head) (Fig. 8k,l).

MiR-714 has a wide-spread expression in the E10.5 mouse embryo, however lower expression of *miR-714* is observed in the dorsal midbrain and rostral ventral midbrain but sparing the majority of the dorsal forebrain and the entire ventral forebrain (Fig. 8m,n). At E12.5, *miR-714* expression appeared high in the dorsal and ventral diencephalon, mesencephalon, MHB, metencephalon and spinal cord. However, *miR-714* expression was not observed in the telencephalon at this stage. A weaker expression of *miR-714* is also observed in the liver (blue arrow) and tongue (white arrow) (Fig. 8p).

To further elucidate the expression of these four miRNAs at a later developmental stage, ISH was performed in the E18.5 embryonic brain, which is shortly before birth of the mouse embryo. At this stage, although the MHB does not exist at this stage anymore, the mdDA and vMH, do however still exist. Noteworthy, all four tested miRNAs were expressed in the olfactory bulb, upper layers of the cortex, outer layers (EGL and/or PC/BG layer) of the cerebellum, and in the brainstem (Fig. 9). Apart from these common expression sites of the four miRNAs, *miR-705* and *miR-714* are also expressed in the striatum, dorsal thalamus, pontine nuclei and brainstem (the pontine nuclei are only a very small part of the rostral brainstem), and together with *miR-709* in the dorsal tectum (superior and inferior colliculi) (Fig. 9b,d,h). *miR-705* is additionally expressed in the mammillary body (mb, white arrow in Fig. 9a), whereas *miR-712* is only expressed in the inferior colliculi (Fig. 9e,f).

Altogether, given by the expression patterns of all four miRNAs (*miR-705*, *miR709*, *miR-712*, *miR-714*) appeared in and overlapping with the expression domain of the targets of interest (mdDA/vMH neurons), these four miRNAs therefore fulfilled the first criterion. Among them, both *miR-705* and *miR-709* are potentially more interesting candidates given that *Wnt1* is the predicted target gene. Furthermore, expression of *miR-705* in the striatum at E18.5 makes it an interesting candidate as this region is a target of and involved in PD. miRNAs that were expressed in other regions (for instance: *miR-144* expresses in the liver) but not in the developing MHR, or miRNAs which expression patterns could not be determined/ ubiquitous in the embryonic tissues, are not considered for further analyses.

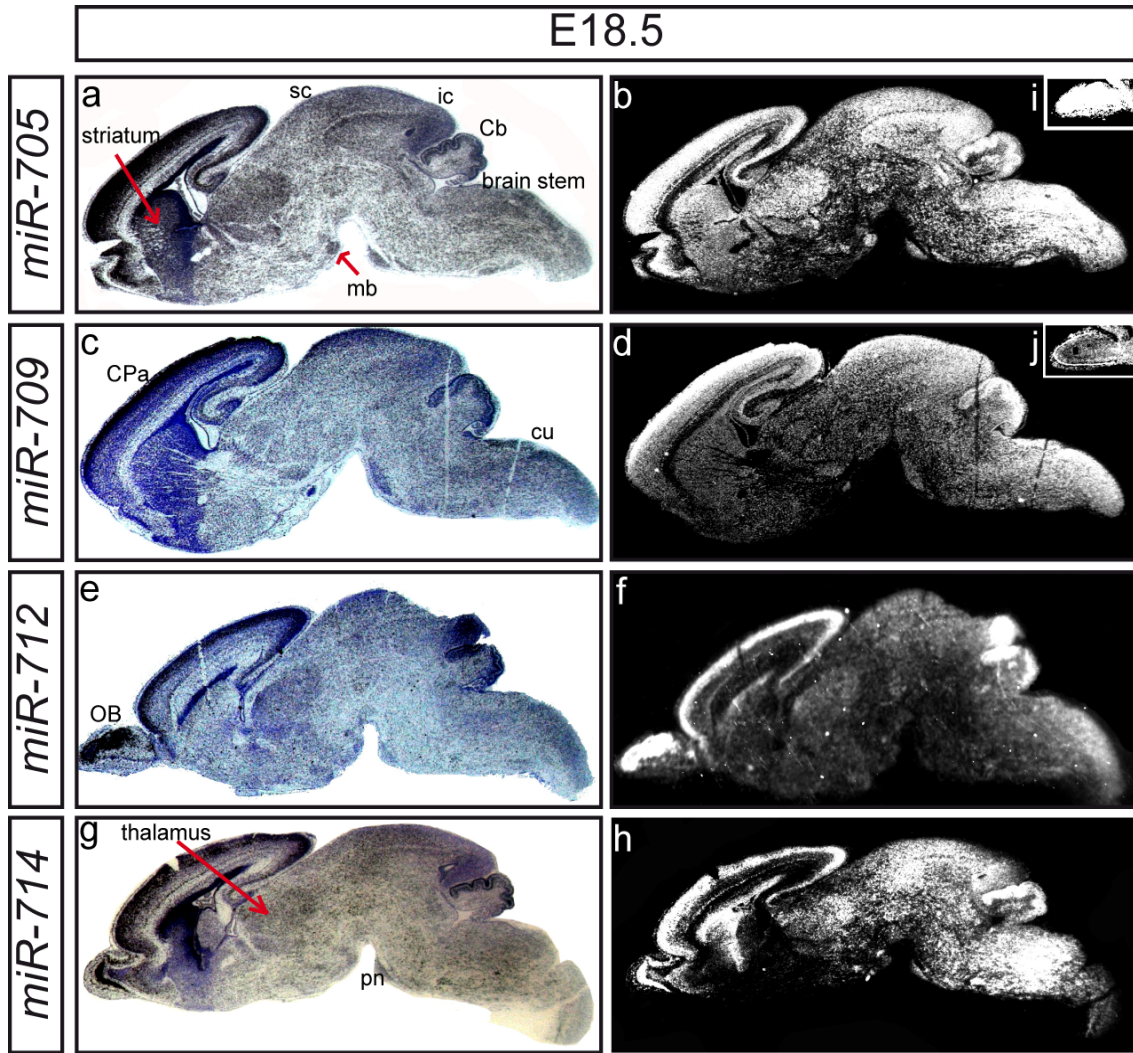


Figure 9. Expression patterns of *miR-705*, *miR-709*, *miR-712* and *miR-714* using LNA-ISH on sagittal brain sections of E18.5 embryos. a-h: Representative sagittal sections from E18.5 CD-1 mouse brain hybridized with LNA-based ISH probes for *miR-705* (a,b,i), *miR-709* (c,d,j), *miR-712* (e,f) and *miR-714* (g,h). Insets in (i,j) showed expression observed in the OB. Dorsal is at the top, anterior to the left. Bright field pictures (a,c,e,g) were counter-stained with Cresyl Violet. All four tested miRNAs showed common expression in the olfactory bulb, dorsal layers of the cortex, outer layer of the cerebellum and in brainstem. Abbreviations: cmt, centromedian thalamic nucleus; cu, cuneate nucleus; CPa, Parietal cortex; EGL,Cb, external granular layer of cerebellum; ic, inferior colliculus; mb, mamillary body; OB, olfactory bulb; pn, pontine nuclei; sc, superior colliculus; vmh, ventromedial hypothalamic nucleus.

3.1.1.2. *miR-144* is specifically expressed in the liver during mouse embryonic development

Interestingly, in the course of my expression screenings I noted that one of the tested miRNAs, *miR-144*, is not expressed in the E10.5 mouse embryo (Fig. 10b) but at E12.5, it is exclusively expressed in the embryonic liver (Fig. 10d). It is noted that the liver does not yet exist at E10.5 as an organ although the liver primordium is specified at this stage and therefore implies that *miR-144* is essential for liver development. This was in the fact the only miRNA from all tested whose expression was restricted to a single organ of the developing mouse embryo, whereas all others showed a far more wide-spread expression pattern.



Figure 10. *miR-144* is specifically expressed in the liver of the midgestational mouse embryo. a-d: Representative entire embryo view in sagittal sections from E10.5 (a,b) and E12.5 (c,d) CD-1 mouse embryos hybridized with LNA-based ISH probe for *miR-144* (a-d). Dorsal is at the top, anterior to the left. Bright field pictures were counter-stained with Cresyl Violet. Specific expression pattern was observed in the liver revealed from dark field picture of E12.5 embryo (d). Abbreviations: Di, diencephalon; Fb, forebrain; Hb, hindbrain; Mb, midbrain; Mes, mesencephalon; Met metencephalon; r1, rhombomere 1; Tel, telencephalon.

3.1.2. Functional validation of predicted target genes for the miRNAs that showed expression in the CNS during development

As a second criterion for the selection of relevant miRNAs, I had established the functional validation of those miRNAs whose expression pattern is consistent with a possible function in MHB and mdDA and/or vMH neuron development. To confirm that the four miRNAs previously validated by their expression patterns could regulate their predicted target genes/mRNAs, I next performed luciferase sensor assays with the 3'UTRs of the predicted targets and the four previously validated miRNAs (*miR-705*, *miR-709*, *miR-712* and *miR-714*) which showed a specific but dynamic expression in the CNS. In addition, another miRNA, *miR-135b*, which I showed was exclusively expressed in the CNS were included in these assays given its predicted target genes involving in the development of mdDA and/or other vMH neuron. Summary of the candidate miRNAs with their predicted target mRNAs is shown in Table 5.

These assays consist in the cloning of the 3'UTR of the target genes downstream to the Luciferase CDS, which is expressed under the control of a strong, ubiquitous promoter (Fig. 11). The cloned 3'UTR sequence contains the predicted miRNA binding sites (seed sequences) for the miRNA of interest. Transfection of the miRNA together with the luciferase sensor vector into cultured cells should result in a measurable (by chemiluminescence) down-regulation of luciferase expression if this miRNA recognizes its predicted target sequences within the cloned 3'UTR. These vectors are also called "sensor vectors" as co-transfection of a miRNA together with its sensor vector will lead to a down-regulation of luciferase expression if the interaction (binding) of the miRNA to its predicted binding sites is functional i.e. will lead to the degradation and/or translational repression of the corresponding mRNA. Noteworthy, I observed a down-regulation of luciferase activity after co-transfection of the precursor miRNA and the pGL3 Promoter vector (without any 3' UTR cloned into it) in some instances, which I considered to be "off-target" effects of the corresponding miRNA. Furthermore, the "off-target" effect caused by the miRNA on the "empty" pGL3 Promoter vector is usually greater than the negative (Scramble miR) control precursor miRNA from Ambion (U.S.A.), which consists of a scrambled sequence that should not bind to any known mRNAs. I therefore decided to use the co-transfections of pGL3 Promoter vector without 3'UTR ("empty vector") and the corresponding miRNA as control in my

experiments, in order to elucidate the specific interaction of the miRNA regulation and its target mRNA's 3'UTR but not other unspecific interactions with other parts of the sensor vector.



Figure 11. A schematic diagram showing the luciferase sensor vector used for the *in vitro* luciferase sensor assays. The 3'UTR of the predicted target gene is cloned downstream of the firefly luciferase coding sequence (CDS) that is expressed under the control of the SV40 promoter.

Table 5. Selected candidate miRNAs (based on their CNS expression pattern) with their predicted target mRNAs.

miRNA	Target mRNAs
<i>miR-705</i>	<i>Wnt1</i>
<i>miR-709</i>	<i>Wnt1</i>
<i>miR-712</i>	<i>Wnt5a, Wnt5b</i>
<i>miR-714</i>	<i>Pitx3, Lef1</i>
<i>miR-135b</i>	<i>Wnt6, Otx2</i>

3.1.2.1. *miR-709* but not *miR-705* targets *Wnt1* 3'UTR

Transfections of *pre-miR-705* together with its predicted target gene *Wnt1* 3'UTR construct did not have an effect on *Wnt1* 3'UTR-controlled luciferase expression, albeit a greater reduction of luciferase activity is observed when a higher dosage (30 nM) *pre-miR-705* was used in the sensor assay which however did not reach statistical significance (Fig. 12a). However, with a similar concentration tested on another miRNA, 30 nM *pre-miR-709* exerted a repressive effect on *Wnt1* 3'UTR-mediated luciferase expression in the sensor assay, where approximately 23 % reduction of luciferase activity is observed (Fig. 12d). To confirm that the repressive effect of *miR-709* on

Wnt1 3'UTR-controlled luciferase expression was due to a direct binding of *miR-709* to the predicted target (seed) sequences in this 3'UTR and not due to other unknown binding sites, I performed subsequently mutational analyses of these seed sequences. Two *miR-709* binding sites were predicted by miRBase (microCosm), a bioinformatics prediction software, in the *Wnt1* 3'UTR (Fig. 12c), the approximate position of the two *miR-709* seed sequence (binding sites) is shown in Fig. 12b. Site-directed mutagenesis of these two predicted *miR-709* binding sites (seed sequences) in the *Wnt1* 3'UTR did indeed rescue the luciferase expression back to normal levels (pGL Promoter vector without 3'UTR) (Fig. 12d), suggesting the specificity of the two *miR-709* binding sites/'seed sequence' are confirmed by the site-directed mutagenesis.

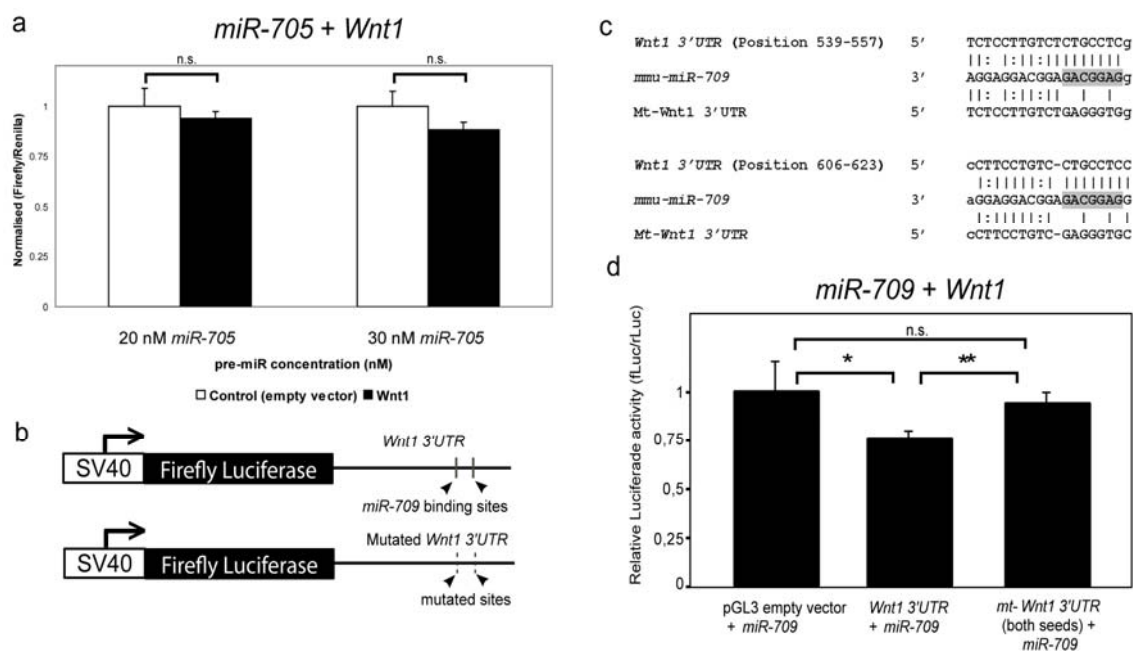


Figure 12. *MiR-709* targets the *Wnt1* 3'UTR *in vitro*. (a) Luciferase sensor assays after co-transfection of *mmu-miR-705* precursor miRNA and a sensor vector that a) does not contain any 3'UTR ('empty vector') or b) a sensor vector containing the *Wnt1* 3'UTR at the 3' end of the Luciferase CDS ('*Wnt1*'), show that *miR-705* did not significantly down-regulate *Wnt1* 3'UTR-mediated Luciferase expression ($p > 0.05$ in the Student's T-test). (b) Schematic drawing of the *Wnt1* 3'UTR sensor vector showing the approximate position of the two *miR-709* seed sequences (binding sites) predicted by miRBase (microCosm) within the *Wnt1* 3'UTR and its mutated counterpart (mutant, Mt). (c) Sequence of the two *mmu-miR-709* binding sites in the *Wnt1* 3'UTR, with the conserved 7 nt seed sequence highlighted in gray background letters. Site-directed mutagenesis of these two seed sequences was done by exchanging

the nucleotides within the *Wnt1* 3'UTR sensor vector ("*Mt-Wnt1*3'UTR") as indicated earlier. (d) Luciferase sensor assays after cotransfection of 30 nM *mmu-miR-709* precursor miRNA and a sensor vector that a) does not contain any 3'UTR ("empty vector") or b) a sensor vector containing the *Wnt1* 3'UTR at the 3' end of the Luciferase CDS show that *miR-709* down-regulates *Wnt1* 3'UTR mediated Luciferase expression by approx. 23% (*Wnt1* 3'UTR + *miR-709*: 0.771±0.037, mean±sd). Site-directed mutagenesis of both seed sequences within the *Wnt1* 3'UTR sensor vector (*Mt-Wnt1* 3'UTR) abolished this negative regulation of *Wnt1* 3'UTR by *mmu-miR-709* (*Mt-Wnt1* 3'UTR + *miR-709*: 0.93±0.067, mean±sd), indicating that this effect was specific for the predicted *miR-709* binding sites (single asterisk, $p < 0.05$; double asterisk, $p < 0.01$; Students' T-test). Values for the "empty vector" control was set as "1", and all other values were normalized to this control.

3.1.2.2. *miR-712* targets *Wnt5b* 3'UTR *in vitro*

It was also predicted that *mir-712* targets *Wnt5a* and *Wnt5b*. To validate the bioinformatics prediction, I transfected *pre-miR-712* with its predicted target gene *Wnt5a/Wnt5b* luciferase sensor construct into HEK293T cells. The luciferase sensor assay revealed that *Wnt5a* 3'UTR-controlled luciferase expression was not significantly down-regulated despite increasing dosages of *pre-miR-712* used in the sensor assays (Fig. 13). However, *pre-miR-712* exerted a repressive effect on the *Wnt5b* 3'UTR with all tested concentration of *pre-miR-712* in the sensor assays. Luciferase activity was down-regulated by approximately 25 %, 22 % and 31 % relative to the control (pGL3 Promoter vector + *pre-miR-712*) when 10 nM, 30 nM and 50 nM, respectively, of *pre-miR-712* were added into the culture. This was, however, not validated by site-directed mutagenesis.

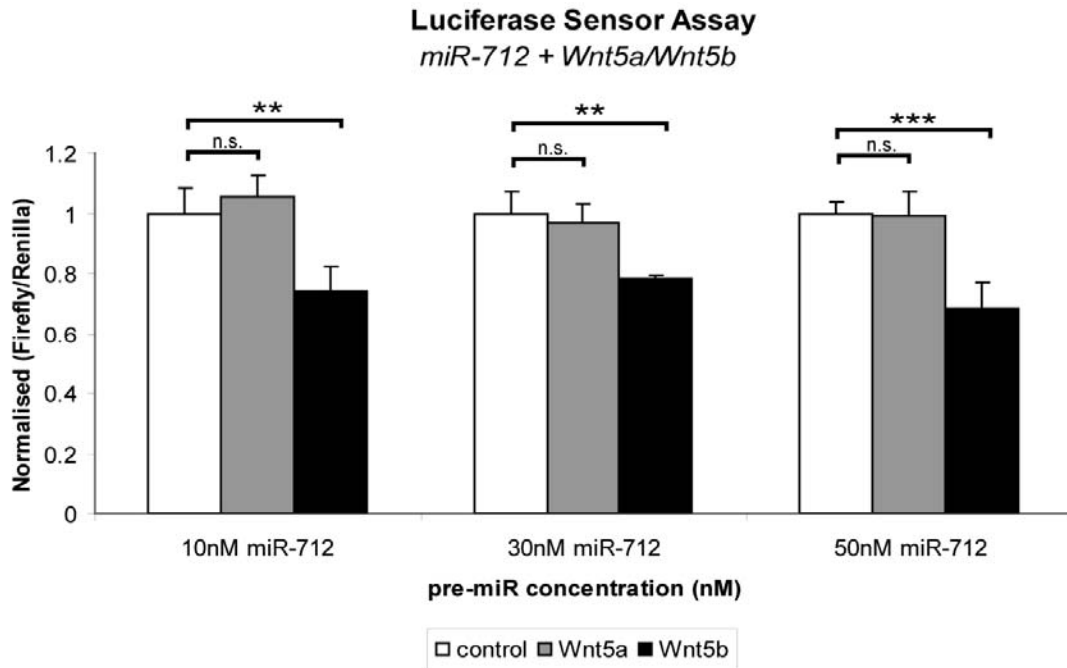


Figure 13. *MiR-712* targets *Wnt5b* 3'UTR *in vitro*. Luciferase sensor assays after co-transfection of *mmu-miR-712* precursor miRNA and a sensor vector that a) does not contain any 3'UTR ('empty vector') or b) a sensor vector containing the *Wnt5a/Wnt5b* 3'UTR at the 3' end of the Luciferase CDS ('*Wnt5a/Wnt5b*'). Luciferase sensor assay show that *miR-712* did not significantly down-regulate *Wnt5a* 3'UTR-mediated luciferase expression ($p > 0.05$ in the Student's T-test). However, co-transfections of *pre-miR-712* and *Wnt5b* down-regulates *Wnt5b* 3'UTR-mediated luciferase expression by 25 % (*Wnt5b* 3'UTR + 10 nM *miR-712*: 0.745 ± 0.078 , mean \pm sd), 22 % (*Wnt5b* 3'UTR + 30 nM *miR-712*: 0.78 ± 0.012 , mean \pm sd) and 31 % (*Wnt5b* 3'UTR + 50 nM *miR-712*: 0.686 ± 0.086 , mean \pm sd) when 10 nM, 30 nM and 50 nM, respectively, of *pre-miR-712* were added. (single asterisk, $p < 0.05$; double asterisk, $p < 0.01$; double asterisk, triple asterisk, $p < 0.005$; Student's T-test). Values for the "empty vector" control was set as "1", and all other values were normalized to this control.

3.1.2.3. *MiR-714* targets the *Lef1* 3'UTR but not *Pitx3* 3'UTR

Another tested miRNA, *miR-714*, did not show significant down-regulation of *Pitx3* 3'UTR-controlled luciferase expression with both tested *pre-miR-714* concentrations, namely 20 nM and 30 nM. However, *Lef1* 3'UTR-controlled luciferase activity was significantly reduced by 31 % and 22 % as compared to the control (pGL3 Promoter vector + *pre-miR-714*) when 20 nM and 30 nM, respectively, of *pre-miR-714* used, indicating that the *Lef1* 3'UTR is a direct target of *miR-714* (Fig. 14). This was, however, not validated by site-directed mutagenesis.

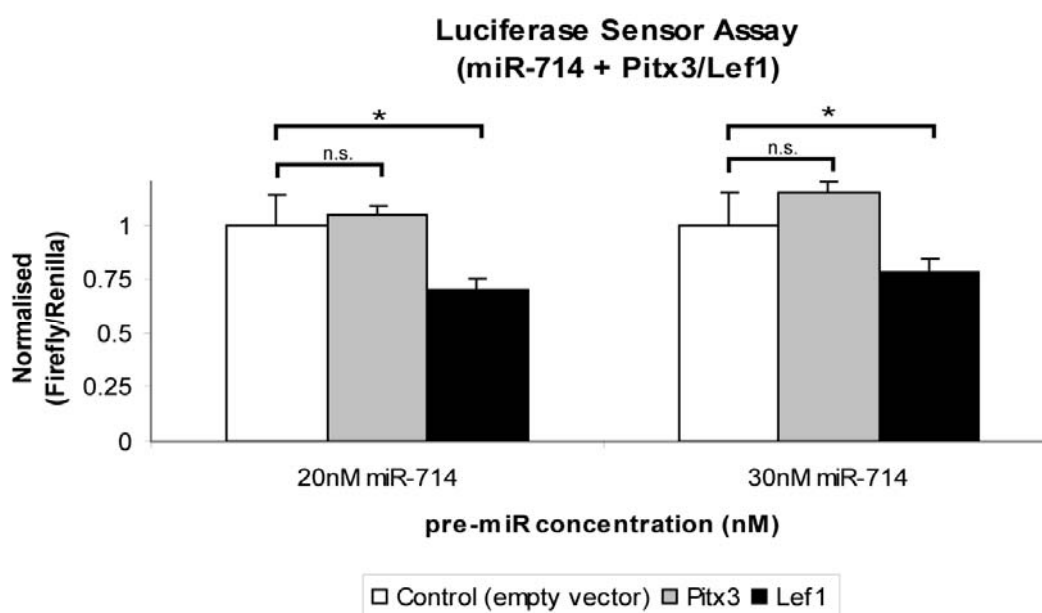


Figure 14. *MiR-714* targets *Lef1* 3'UTR *in vitro*. Luciferase sensor assays after co-transfection of 20 nM or 30 nM *mmu-miR-714* precursor miRNA and a sensor vector that a) does not contain any 3'UTR ("empty vector") or b) a sensor vector containing the *Pitx3/Lef1* 3'UTR at the 3' end of the luciferase CDS (*Pitx3/Lef1*). Luciferase sensor assay show that *miR-714* fails to reduce the *Pitx3* 3'UTR-controlled luciferase activity significantly. *Lef1* 3'UTR-controlled (*Lef1* 3'UTR + 20 nM *miR-714*: 0.70±0.049; *Lef1* 3'UTR + 30 nM *miR-714*: 0.78±0.063; mean±sd) luciferase activity was reduced significantly compared to controls. (single asterisk, $p < 0.005$; Students' T-test). Values for the "empty vector" control was set as "1", and all other values were normalized to this control.

3.1.2.4. *MiR-135b* does not target *Otx2*- and *Wnt6* 3'UTR

Co-transfections of *pre-miR-135b* and its predicted target genes *Otx2* 3'UTR or *Wnt6* 3'UTR luciferase sensor constructs did not down-regulate significantly the expression of luciferase from the sensor constructs, even though the concentration of *pre-miR-135b* was step-wise increased in these assays. However, some but non-significant reduction of both *Otx2*/*Wnt6* 3'-UTR mediated luciferase activity was observed when a higher concentration of *pre-miR-135b* was added (Fig. 15).

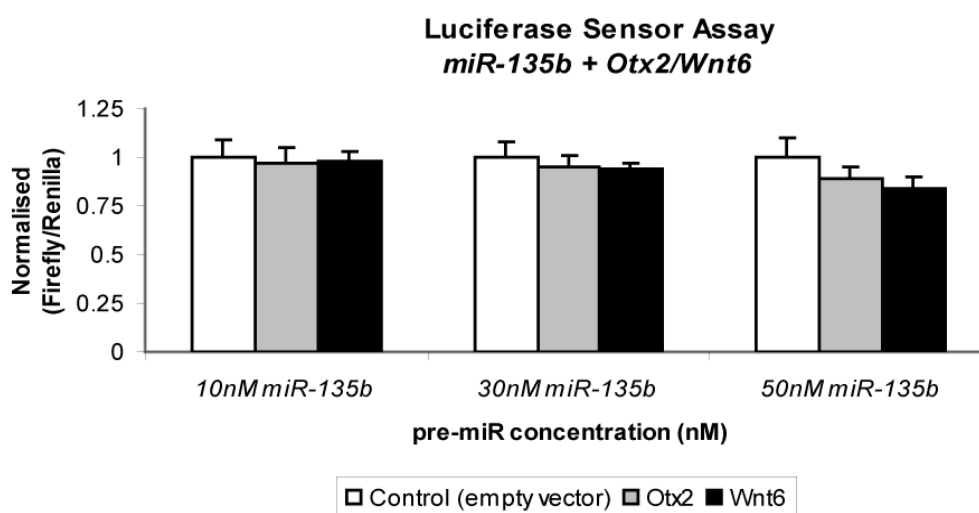


Figure 15. Luciferase sensor assay revealed that *miR-135b* does not target *Otx2*- and *Wnt6* 3'UTR. Luciferase sensor assays after co-transfections of 10, 30 or 50 nM of *pre-miR-135b* and a sensor vector that a) does not contain any 3'UTR ("empty vector") or b) a sensor vector containing the *Otx2*/*Wnt6* 3'UTR at the 3' end of the Luciferase CDS show that *miR-135b* fails to reduce the *Otx2* 3'UTR-controlled and *Wnt6* 3'UTR-controlled luciferase activity compared to controls. ($p > 0.05$ in the Student's T-test). Values for the "empty vector" control was set as "1", and all other values were normalized to this control.

Taken together, the predicted binding sites (seed sequences) of three of the four miRNAs previously validated in the expression profiling, namely *miR-709*, *miR-712* and *miR-714* in selected indeed showed repressive effect on *Wnt1* 3'UTR, *Wnt5b* 3'UTR and *Lef1* 3'UTR, respectively. In summary, from a total of 33 candidates miRNAs predicted from a combination of five different computational algorithms, only three miRNAs showed expression patterns in the developing CNS of the murine and their targets were successfully validated through *in vitro* functional analyses (luciferase sensor assay).

3.1.3. A new prediction approach to predict putative miRNAs that target the *Wnt13'UTR*

Another prediction tool named RNA22 (Miranda et al., 2006), that is not based on cross-species conservation and is resilient to noise as compared to the previously used prediction tools (miRBase, PicTar, TargetScan, miRNAMAP2.0 and TargetSpy) was used to harbor miRNAs which could target *Wnt1 3'UTR*. RNA22 first finds putative miRNA binding sites in the sequence of interest then identifies the targeting miRNA. Based on my previous experience, I decided to validate these miRNAs on the molecular level (correct target site prediction tested in luciferase sensor assays) before I would analyse their expression patterns in the developing mouse embryo using LNA-based ISH. Using the RNA22 prediction tool, four new miRNAs were predicted to target the *Wnt1 3'UTR* (Table 6), which is very GC-rich.

Table 6. Four miRNAs predicted to target *Wnt1 3'UTR* using RNA22 bioinformatics tool.

miRNAs predicted to target murine <i>Wnt1</i> <i>3'UTR</i>
<i>mmu-miR-877</i>
<i>mmu-miR-7b</i>
<i>mmu-miR-342-5p</i>
<i>mmu-miR-221</i>

Luciferase sensor assays revealed that co-transfection of increasing amount of *pre-miR-877* or *miR-7b* with the *Wnt1 3'UTR* sensor construct does not result in a significant down-regulation of luciferase expression compared to control (pGL3 Promoter vector + *pre-miR877/pre-miR-7b*), (Fig. 16a,b). Conversely, both *miR-342-5p* and *miR-221* showed a significant reduction of *Wnt1 3'UTR*-mediated luciferase activity with all tested concentrations. Luciferase activity was reduced by 32 %, 44 % and 29 % when 10 nM, 30 nM and 50 nM, respectively, of *pre-miR-221* were used (Fig. 16d). Co-transfection of 5 nM, 20 nM and 50 nM, respectively, of *pre-miR-342-5p* resulted in a 48 %, 51 % and 55 % reduced luciferase expression from the *Wnt1 3'UTR* sensor construct (Fig. 16c).

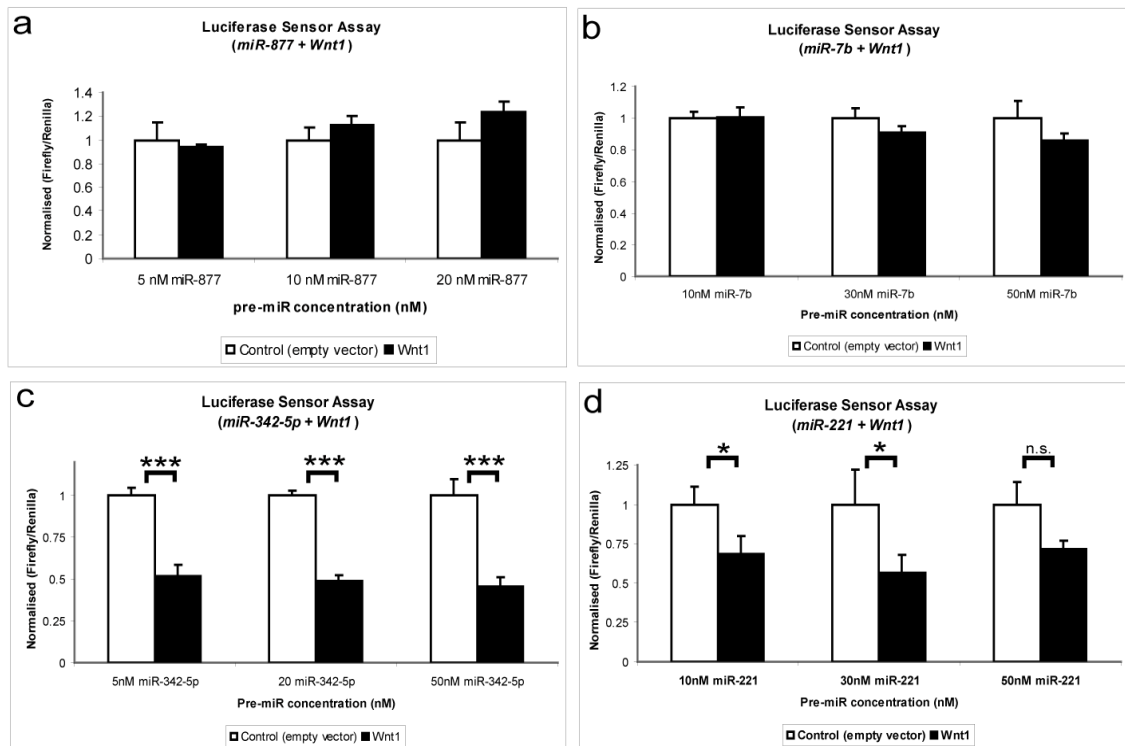


Figure 16. Both *miR342-5p* and *miR-221* target the murine *Wnt1* 3'UTR *in vitro*. (a-d) Luciferase sensor assays after co-transfection with precursor miRNA and sensor construct that a) does not contain any 3'UTR ("empty vector") or b) a sensor vector containing the *Wnt1* 3'UTR at the 3' end of the luciferase CDS. (a, b) Co-transfections of *miR-877* or *miR-7b* with *Wnt1* 3'UTR luciferase reporter appeared to have no repressive effect on the luciferase expression in all tested concentrations. (c) Co-transfections of *miR-342-5p* with *Wnt1* 3'UTR luciferase reporter reduced the luciferase activity in all tested concentrations (*Wnt1* 3'UTR + 5 nM *miR-342-5p*: 0.52 ± 0.069 ; *Wnt1* 3'UTR + 20 nM *miR-342-5p*: 0.49 ± 0.036 ; *Wnt1* 3'UTR + 50 nM *miR-342-5p*: 0.45 ± 0.059 ; mean \pm sd) compared to control. (d) Co-transfections of *miR-221* and *Wnt1* 3'UTR-mediated sensor vector down-regulates *Wnt1* 3'UTR-mediated luciferase expression by 32 %, 44 % and 29 % compared to control when 10 nM, 30 nM and 50 nM, respectively, of *pre-miR-221* was used (*Wnt1* 3'UTR + 10 nM *miR-221*: 0.683 ± 0.117 ; *Wnt1* 3'UTR + 30 nM *miR-221*: 0.566 ± 0.116 ; *Wnt1* 3'UTR + 50 nM *miR-221*: 0.715 ± 0.052 ; mean \pm sd). (single asterisk, $p < 0.05$; double asterisk, $p < 0.05$; triple asterisk, $p < 0.0005$; Students' T-test). Values for the "empty vector" control was set as "1", and all other values were normalized to this control.

3.1.4. Experimental validation of a putative novel ‘miRNA recognition’ motive/target enhancer signal

miRNAs are generally perceived to exert their post-transcriptional effects via direct binding in the 3'UTR of their target mRNAs, although several reports indicate that miRNA:mRNA post-transcriptional regulation can also occur in other regions such as the 5'UTR (Jopling et al., 2005; Lytle et al., 2007; Orom et al., 2008) or in the 3'UTR together with the CDS (Wightman et al., 1993) or in the CDS alone (Duursma et al., 2008; Tay et al., 2008). A detailed sequence analysis of the 3'UTRs of all known cDNAs from human, chimpanzee and orang-utan (both are primates), mouse, chicken, and fruitfly performed with bioinformatics tools by my collaboration partner, Dr. V. Stümpflen at the IBIS, revealed the presence of a highly conserved sequence motif in approx. 10% of the primate cDNAs, but only in 0.2% (mouse), 0.02% (chicken) and 0.018% (fruitfly) of the cDNAs of other vertebrate and invertebrate species (Schmidt et al., 2009). This finding suggested that this sequence motif (Fig. 17) is only conserved in primate species during evolution. One hypothesis of the Dr. V. Stümpflen group was that this motif is highly conserved because it might be implicated in the posttranscriptional control of gene expression by miRNAs in primates but not in other vertebrates and invertebrates. Interestingly however, this motif is also present in the 3'UTR of the murine *Wnt1* gene. To obtain a first hint towards a putative/possible functional implication of this motif in miRNA-mediated posttranscriptional regulation of gene expression, and having two previously characterised miRNAs that target the *Wnt1* 3'UTR (*miR-709* (confirmed by site-directed mutagenesis) and *miR-221*, I therefore tested whether site-directed mutagenesis of this motif in the *Wnt1* 3'UTR sensor construct used in the previous experiments would affect the specific miRNA-mediated down-regulation of luciferase activity in the sensor assays. Figure 18a shows the approximate location of the conserved putative motive in the *Wnt1* 3'UTR and the approximate position of the binding sites for *miR-709* and *miR-221*).

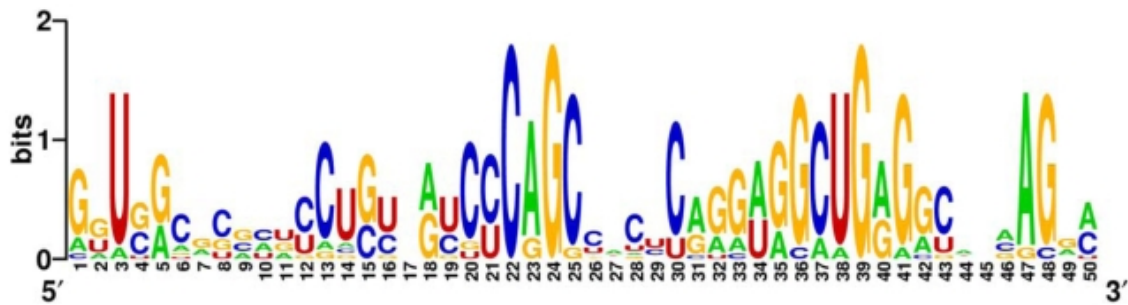


Figure 17. The putative conserved RNA motive. Sequence logo plot of a putative novel miRNA target context sequence motif downstream of experimentally supported human miRNA target sites. The overall height of the stack indicates the sequence conservation at that position, while the height of symbols within the stack indicates the relative frequency of each nucleic acid at that position. The motif shown here was calculated from the non-redundant sequence set with maximum 65% allowed homology. Noteworthy are the overall high GC content, the strong increase of cytosine nucleotides around the motif position 22 and a peak of guanine residues around motif positions 39 (excerpt from (Schmidt et al., 2009) of this motif).

To this end, three mutagenised *Wnt1* 3'UTR luciferase sensor vectors (named Motive1.5, Motive 2.1 and Motive 3.1) were constructed using either the entire or a bipartite motif sequence and based on the degree of conservation of these sequences (Fig. 18b,c). Motive 1.5 was generated by site-directed mutagenesis in total seven nucleotides within both ('upstream' and 'downstream') regions of the motive (Fig. 18b). Motive 2.1 and Motive 3.1 were generated by site-directed mutagenesis of the nucleotides in either region ('upstream' and 'downstream', respectively) (Fig. 18b,c). Importantly, site-directed mutagenesis of these motif sequences did not affect the predicted binding sites (seed sequences) of the tested miRNAs, *miR-709* and *miR-221*.

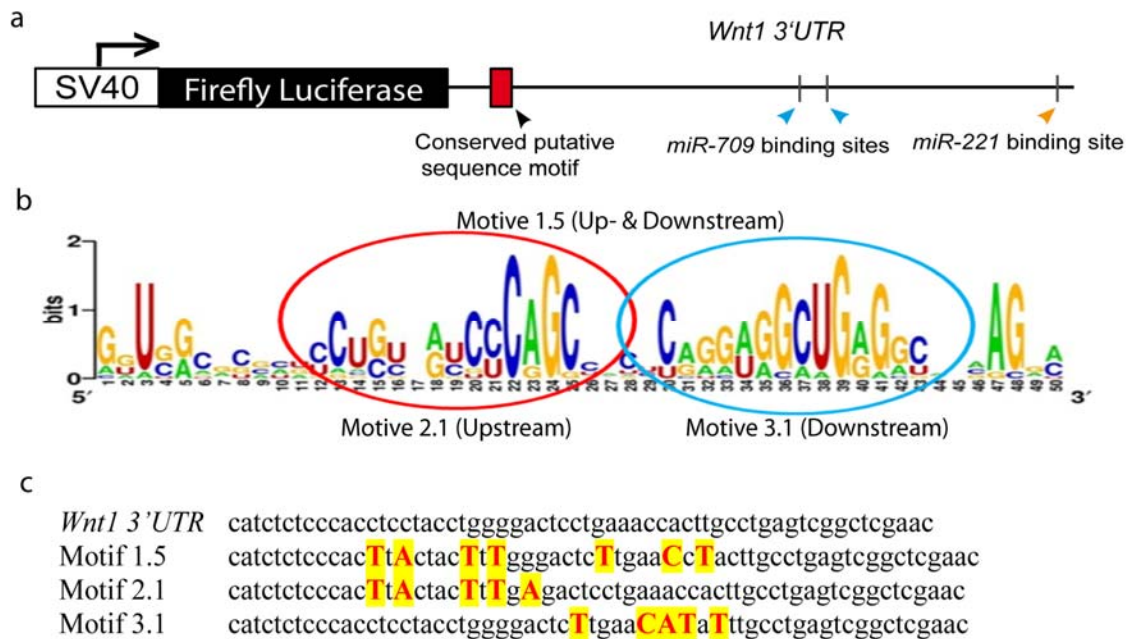


Figure 18. Strategy to generate three different mutagenic *Wnt1 3'UTR* luciferase constructs for the putative “miRNA recognition” motif in vertebrates. (a) A schematic diagram showing the approximate location of the putative ‘miRNA recognition’ motif/ miRNA target enhancer signal, of the two *miR-709* binding sites and of the *miR-221* binding site within the *Wnt1 3'UTR* of the *Wnt1 3'UTR* sensor construct used in previous experiments. (b) A schematic diagram showing the three sequences within the “miRNA recognition” motif (Motif 1.5, Motif 2.1 and Motif 3.1) that were defined for construction of the corresponding mutagenized sensor vectors. (c) Sequence of the three mutagenized motifs within the “miRNA recognition” motif (as indicated above) after site-directed mutagenesis of the corresponding *Wnt1 3'UTR* sensor vector.

Transfection of the wild-type (unmodified *Wnt1 3'UTR*) and mutant *Wnt1 3'UTR* luciferase sensor constructs together with 30nM *pre-miR-709* (most effective concentration as used previously) reduced the luciferase activity to 65% in the case of the wild-type, as expected, but also in the case of all three mutant constructs, indicating that site-directed mutagenesis of this conserved sequence motif did not affect *miR-709*-mediated down-regulation of luciferase activity controlled by the *Wnt1 3'UTR* (Fig. 19). A similar result was obtained with 30nM *miR-221* using the same constructs (Fig. 19). Therefore, I can conclude that site-directed mutagenesis of the sequence of this putative novel ‘miRNA recognition’ motif does not affect miRNA-mediated down-regulation of luciferase expression controlled by the mouse *Wnt1 3'UTR* harbouring this motif, and I can therefore also exclude a putative function of this motif in this context.

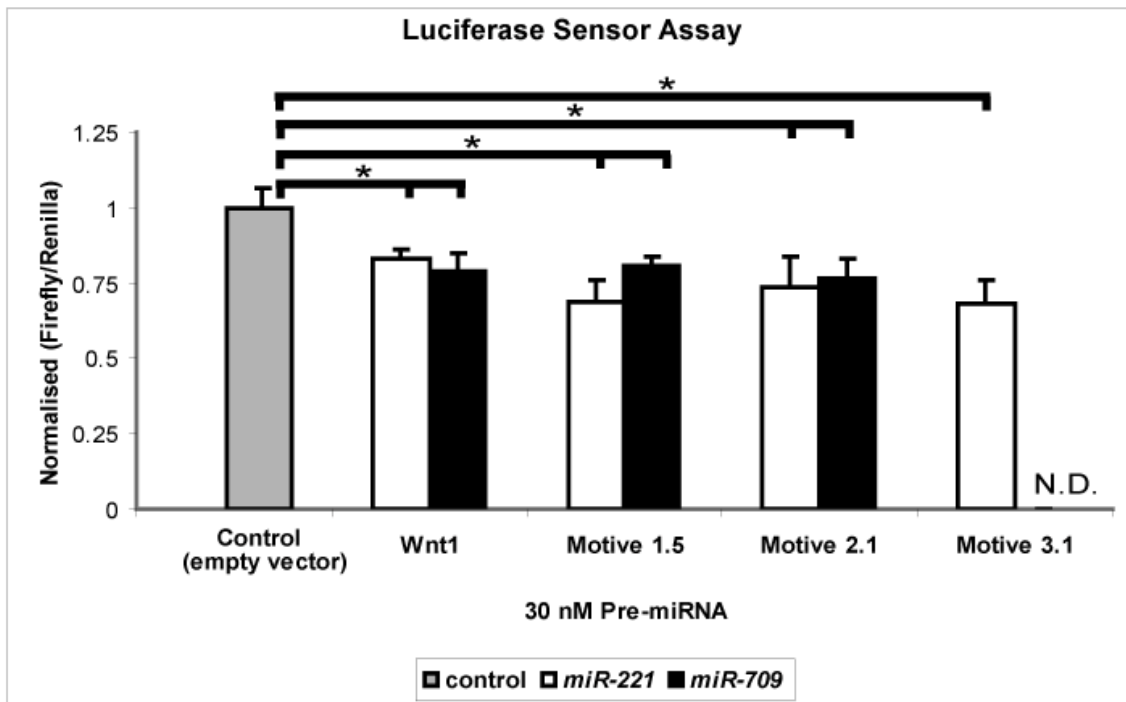


Figure 19. Relative luciferase activity of the *Wnt1* 3'UTR sensor vector (wild-type) and the three *Wnt1* 3'UTR sensor vectors in which three sequence motifs/part of the “XY” motif were mutated, after co-transfection of 30nM *pre-miR-221* or *pre-miR-709* in HEK293T cells. Luciferase sensor assays after co-transfection of 30 nM *miR-221/miR-709* precursor miRNA and a sensor vector that a) does not contain any 3'UTR ("empty vector") or b) a sensor vector containing the *Wnt1* 3'UTR at the 3' end of the Luciferase CDS show that *miR-221* down-regulates *Wnt1* 3'UTR-mediated luciferase expression by 17 % (*Wnt1* 3'UTR + 30 nM *miR-221*: 0.829±0.035; mean±sd) compared to controls. Co-transfection of all three 'Motive Vectors' with 30 nM *pre-miR-221* failed to abolish the luciferase repression (Motive 1.5 + 30 nM *miR-221*: 0.69±0.069; Motive 2.1 + 30 nM *miR-221*: 0.737241±0.101; Motive 3.1 + 30 nM *miR-221*: 0.682±0.078). Similarly, co-transfection of 30 nM *miR-709* and sensor vector containing *Wnt1* 3'UTR down-regulates luciferase expression by 21 % (*Wnt1* 3'UTR + 30 nM *miR-709*: 0.79±0.057) compared to control. Co-transfection of all three 'Motive Vectors' with 30 nM *pre-miR-709* failed to abolish the repression on luciferase activity (Motive 1.5 + 30 nM *miR-709*:0.81±0.03; Motive 2.1 + 30 nM *miR-709*: 0.76±0.064). * $p < 0.05$ in Students' T-test. N.A.= not analysed. Values for the “empty vector” control was set as “1”, and all other values were normalized to this control.

Taken together, the experimental “validation” of miRNAs predicted by computational algorithms show that these bioinformatics prediction tools are still not specific/perfect enough to fully rely on their prediction outcomes, at least to date. In fact, my experimental results show that the bioinformatics predictions led to many false-positive (predicted but not experimentally validated) candidate miRNAs. In this regard,

I showed that experimental validations combining miRNA expression patterns and functional studies with sensor assays (including site-directed mutagenesis) confirmed only one miRNA (*miR-709*) from a total of 33 initial candidate miRNAs, was correctly predicted.

The next step in an experimental validation of *miR-709* would be *in utero* electroporation of *miR-709* at the MHR to study the gain/loss-of-function phenotype in the developing MHB of the murine embryo. However, it is technically challenging to electroporate at the MHB of the murine embryo earlier than E12.5 (as the formation of MHB occurs much earlier approximately at E9.5). Creation of *miR-709* knock-out mice is however, time-consuming and therefore I sought for an alternative method for miRNA profiling.

3.2. miRNAs that might be involved in vMH neuron development as determined by miRNA expression profiling of differentiating mESCs

I next sought to profile miRNAs from biological-derived samples to obtain more reliable biological-derived information compared to previously bioinformatics prediction method, to search for miRNAs that are involved in the developing MH neurons and mdDA neurons, as it was my initial goal from the beginning. *In vitro* cell cultures, particularly directed-differentiation of ESC into vMH neurons offers the unique possibilities to recapitulate/resemble *in vivo* embryonic development, as different developmental stages (such as progenitors, precursors, differentiating and mature neurons) could be isolated and harvested from each development stage and it is also less time-consuming. Next generation sequencing (NGS) was employed to profile miRNAs due to its superiority over microarray. In principle, NGS could correctly determine what is measured, avoiding false signal from a cross-hybridizing target molecule (happens in microarray) and allowing a quantitative measurement of each sequence that is present in the sample.

3.2.1. Directed differentiation of mouse ESC into mdDA and other types of ventral mid-/hindbrain neurons

A mESC differentiation protocol developed by (Lee et al., 2000) that efficiently generates vMH neurons and MNs was employed. The ESC differentiation protocol (Lee et al., 2000) is named ‘5-Stage Protocol’ because of the five distinct stages which the mESC go through during their differentiation into neurons, of which involves propagation of ESCs (Stage 1), formation of embryoid bodies (EBs) (Stage 2), selection of neural stem cells (NSCs) (Stage 3), expansion of NSCs (Stage 4) and further maturation of NSCs to vMH neurons (Stage 5). A sketch of ESC differentiation to midbrain and hindbrain neuronal populations (5-stage protocol) is shown in (Fig. 20a). Successful differentiation of the mESCs into one of the desired neuronal cell types (mdDA neurons) was routinely monitored, where a subset of these cells was plated onto cover slips and immunostaining for a mdDA-specific marker, such as Th, was performed at the end of the differentiation procedure (after 6 days in culture), as shown in Fig 20b. The total RNA was isolated from the cells at three different stages, namely

from undifferentiated ESCs (Stage 1), NSCs/ Nestin⁺ cells (Stage 3) and differentiated mdDA/vMH neurons (Stage 5) to determine the identity of the miRNAs which are expressed at these stages in a subsequent miRNA expression profiling experiment.

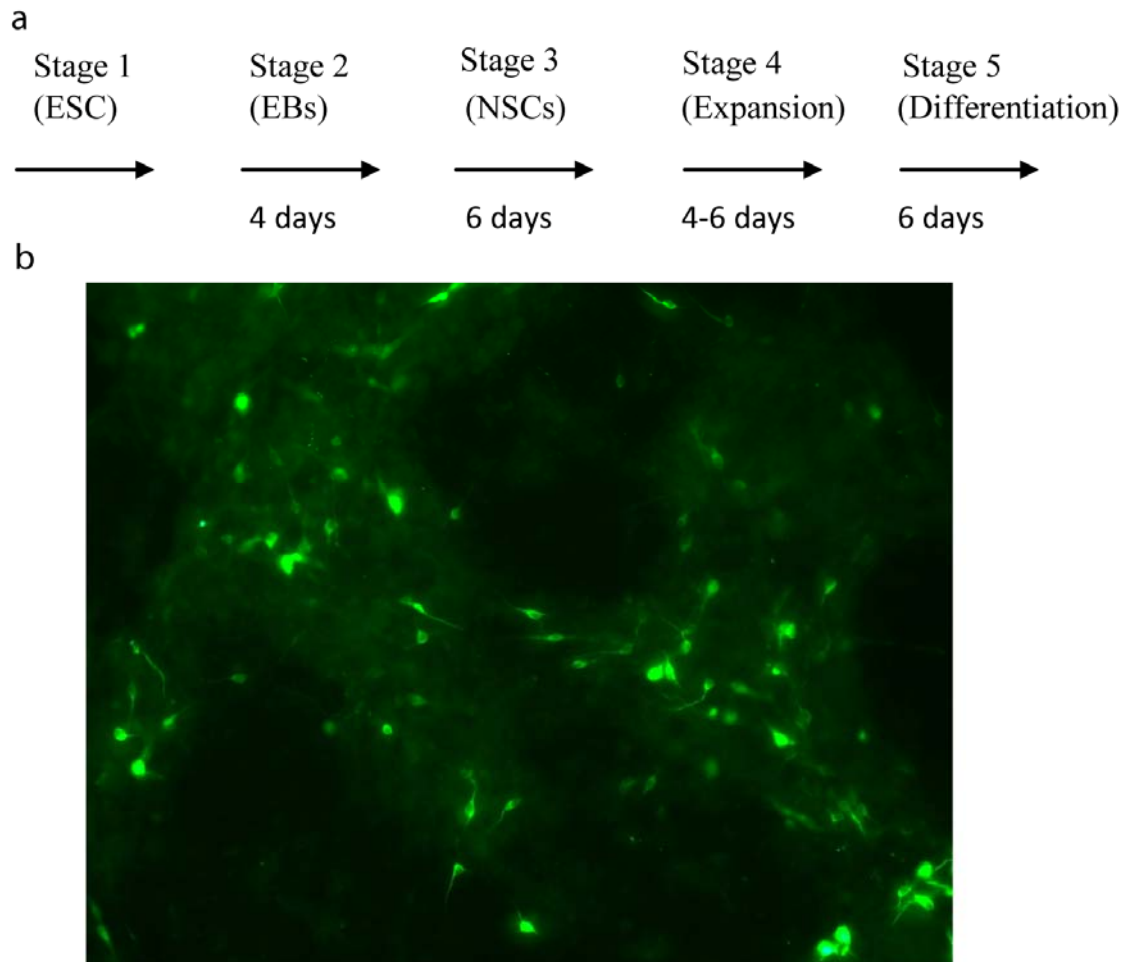


Figure 20. (a,b) Time-line of the 5-stage protocol for mESC differentiation into vMH neurons and confirmation of successful differentiation into Th⁺ neurons. (a) Sketch showing the timeline for the differentiation procedure (5-Stage Protocol) to generate vMH neuronal populations from mouse ESCs. Approximately 25 days were required to obtain differentiated vMH neurons. (b) Th⁺ Immunostaining showed a successful differentiation of mESC into Th⁺ mdDA neurons.

3.2.2. NGS profiling of miRNAs expressed during the directed differentiation of mouse ESCs into vMH neurons

Profiling of the miRNAs expressed at the three previously mentioned stages (undifferentiated mouse ESCs (Stage1), neural precursors NSCs (Stage 3) and differentiated vMH neurons (including mdDA and motor neurons) (Stage 5) using the differentiation protocol according to Lee et al. (2000) was done by NGS technology. This approach revealed the presence of over 400 distinct miRNAs expressed during the 5-stage differentiation procedure, indicating miRNAs are crucial and involved in the differentiation processes.

To identify those miRNAs that are enriched either in the undifferentiated ESC stage (Stage 1) or in the differentiated vMH neurons (Stage 5), I then compared the quantitative reads. The reads are quantitative and uniquely mapped miRNAs, which are generated by filtering RNA samples to retain 17-30 nt small molecules, then mapped to known mouse pre-miRNA sequences deposited in miRBase and summarised in terms of gene expression counts. By comparing the quantitative reads of differentiated neuron (stage 5) over the undifferentiated mESCs (stage 1), I obtained a fold change of all miRNAs which showed the changes of the miRNA levels during the course of differentiation. Importantly, published miRNAs that are induced upon differentiation of neural precursors/progenitors into neurons, such as all the *let-7* family members (having/comprising seven members: *let-7a*, *let-7b*, *let-7c*, *let-7d*, *let-7e*, *let-7f* and *let-7g*)(Reinhart et al., 2000) was particularly highly expressed in the differentiated vMH neuron stage as compared to the undifferentiated ESC stage, in which they were expressed only in low levels (Supplementary Fig. S2). Conversely, ESC-specific miRNAs, such as all the *miR-290* family members (five members: *miR-291*, *miR-292*, *miR-293*, *miR-294*, *miR-295*) (Wang et al., 2008), were enriched in the ESCs as compared to the differentiated vMH neuron stage (Supplementary Fig. S2). Noteworthy, *miR-295* was abundantly expressed in the undifferentiated ESCs (Stage 1) and its expression level dropped sharply when their differentiation was induced (stage 3) and further dropped at the terminally differentiated neurons (stage 5). Conversely, *let-7a* and *miR-9* were the most highly enriched miRNAs in the differentiated vMH neurons. These data indicated the validity of my approach and the selective enrichment of ESC- or neuron-specific miRNAs at the expected stages of the differentiation procedure according to (Lee et al., 2000).

Next, selected miRNAs were ranked according to their fold change which was obtained from reads of terminally differentiated neuron (stage 5)/ undifferentiated ESCs (stage 1) generated from NGS. By doing so, I determined the most abundant miRNAs which were enriched in the differentiated vMH neurons. Figure 21 shows the read number of the controls (*miR-295* (enriched in ESCs) and *let-7a* and *miR-9* (enriched in differentiated vMH neurons) and of the top ten up-regulated miRNAs in the differentiated vMH neurons (stage 5 of the differentiation procedure) in each of the 3 differentiation stages. These data show that *miR-125b* was the second most strongly up-regulated miRNA in the differentiated vMH neurons (final differentiation stage). The other 9 miRNAs were (in decreasing read number order): *miR-181a*, *miR-206*, *miR-99a*, *miR-135a*, *miR-181b*, *miR-100*, *miR-137*, *miR-383* and *miR-153* (Fig. 21).

The mESC differentiation into vMH neurons according to the protocol by (Lee et al., 2000) generates a heterogeneous cell population (including neurons but also glial and other non-neural cell types such as fibroblasts, neural crest cells, etc) in the culture dish (unpublished data). Another protocol established by (Bibel et al., 2004) (hereafter named “Bibel differentiation protocol”) renders a more homogeneous population of (glutamatergic) neurons, with very few “contaminant” progenitor and glial cells as compared to the 5-stage protocol. We therefore also profiled the miRNAs expressed during the differentiation of mESCs into glutamatergic neurons according to (Bibel et al., 2004) (work done by C. Peng). To confirm that the selected miRNAs from the 5-stage differentiation protocol are neuron-associated miRNAs, I compared them to the NGS data generated from the Bibel differentiation protocol. Interestingly, the selective up-regulation of *miR-9*, *miR-125b*, *miR-181a*, *miR-181b* and *miR-383* in differentiated neurons as compared to undifferentiated mESCs was also confirmed with the Bibel differentiation protocol (data not shown). I therefore focussed my further experimental analyses on these top candidate miRNAs which might play a role in vMH neuron development. Two most upregulated miRNAs (*miR-125b* and *miR-181a*) *in vivo* expression pattern was screened. Nevertheless, *miR-181a* did not show any detectable signal during mouse embryo development (E10.5 and E12.5) and therefore was discarded from further analysis (data not shown).

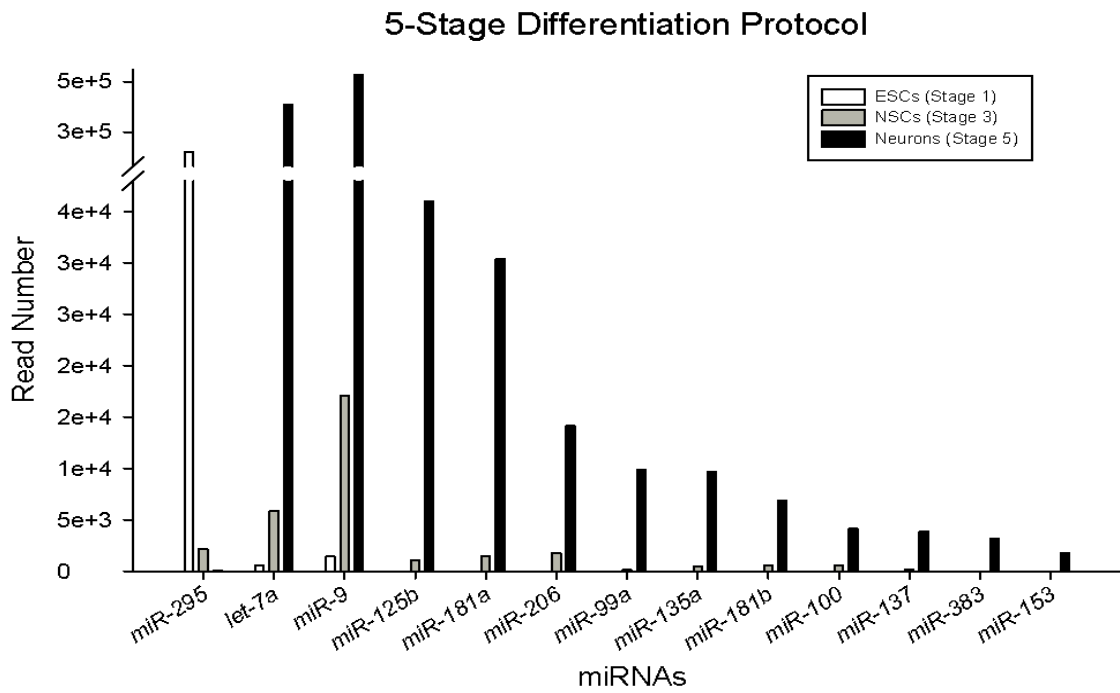


Figure 21. Enriched miRNAs in differentiated neurons using the ESC differentiation protocol by Lee et al. (2000). *MiR-295* is enriched in undifferentiated mESCs (Stage 1) while *let-7a* and *miR-9* are abundantly expressed/enriched in the terminally differentiated neurons (Stage 5). *MiR-125b* was the second most abundant miRNA among the top 10 miRNAs that were enriched in differentiated neurons. The reads (read number) are quantitative and uniquely mapped miRNAs which showed the abundance of the miRNAs.

3.2.3. Expression of *miR-125b* in the ventral anterior neural tube of the midgestational mouse embryo

As *miR-125b* was one of the most strongly upregulated miRNAs in differentiated vMH neurons as compared to undifferentiated mESCs, I decided to first analyze its *in vivo* expression pattern in the developing mouse embryo, focussing on the MHR, as the directed-differentiation ESCs protocol generated relatively high vMH neurons. Using a DIG-labelled LNA *miR-125b* detection probe (LNA-ISH probe), expression of *miR-125b* was detected on sagittal sections in the cephalic flexure of the E10.5 mouse embryo and also dorsally in midbrain (Fig. 22a). Notably, expression of *miR-125b* in this region was restricted to the outer layer of the neuroepithelium corresponding to the mantle zone (that harbours the postmitotic and differentiating neurons at this stage) and spared the ventricular/subventricular zone containing the proliferating and undifferentiated neural precursors. On coronal sections of the E12.5 ventral midbrain, *miR-125b* was most strongly expressed in the SVZ/IZ of the basal plate, alar-basal boundary and ventral alar plate, with few cells expressing *miR-125b* also found in the VZ of the BP, ABB and ventral AP, and in the SVZ/IZ of the floor plate (Fig. 22b).

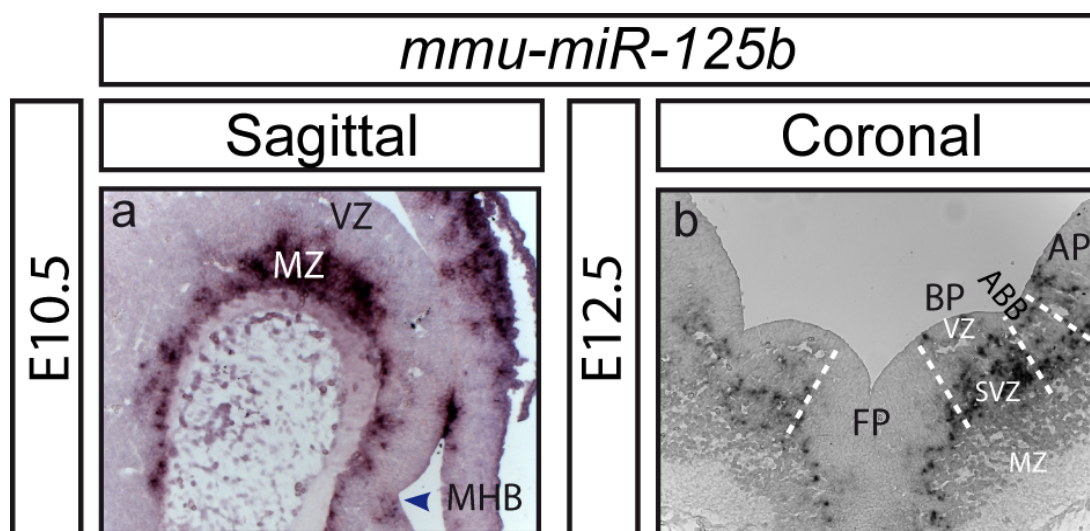


Figure 22. Expression of *miR-125b* in the midgestational mouse embryo. (a,b) Representative bright-field sagittal (a) and coronal midbrain (b) sections. Anterior left, dorsal top of wild-type (CD-1) mouse embryos at E10.5 (a) and E12.5 (b). (a) At E10.5, *miR-125b* expression was detected in the MZ of the cephalic flexure and in the MZ of the dorsal midbrain. (b) At E12.5, *miR-125b* is most strongly expressed in the SVZ/IZ of the BP, ABB and AP, with few cells expressing *miR-125b* also found in the VZ of BP,

ABB, ventral AP and in the SVZ of the FP. Abbreviations: AP, alar plate; BP, basal plate; FP, floor plate; MHB, Mid-hindbrain boundary; MZ, mantle zone; SVZ, subventricular zone; VZ, ventricular zone.

As the DIG-labelled LNA-ISH probe for detection of *miR-125b* may not be as sensitive as a radioactive detection method, I therefore also performed LNA-ISH on midgestational mouse embryos using radioactively labelled LNA probes. The radioactive LNA-ISH revealed that between E10.5 and E12.5, *miR-125b* is expressed along the rostral-caudal (A/P) axis of the anterior neural tube including fore-, mid- and hindbrain as assessed on sagittal sections (Fig. 23a,e,i) with a particular enrichment around the MHB and in the cephalic flexure. On coronal sections, *miR-125b* exhibited a weak expression along the D/V axis of the neural tube, including the FP, of the E10.5 mouse embryo (Fig. 23b-d). At later stages (E11.5 and E12.5), *miR-125b* expression was mostly confined to the BP (Fig. 23f-h,j-l). Examination of serial coronal sections along the A/P axis of the embryo revealed that a particularly strong expression of *miR-125b* was detected in the BP of the caudal midbrain/rostral hindbrain including the MHB

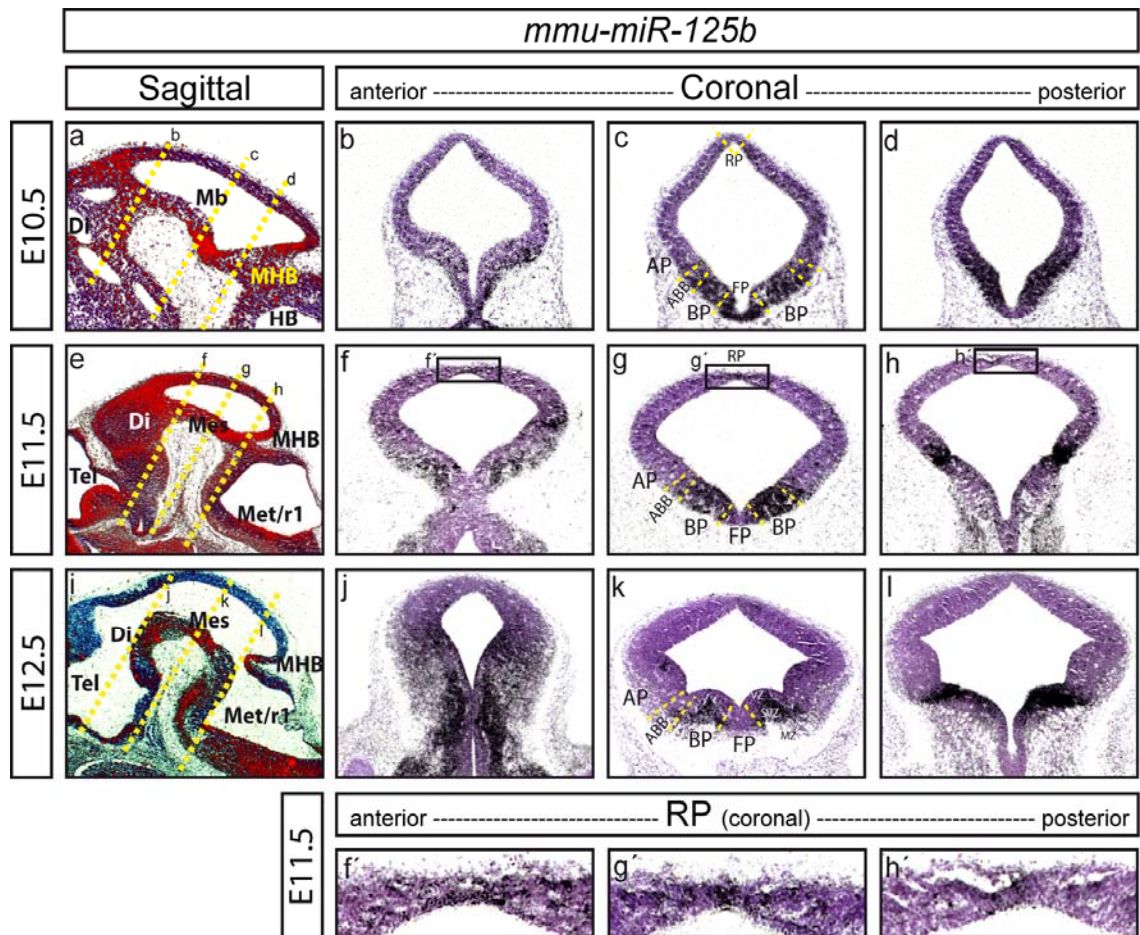


Figure 23. Expression of *miR-125b* in the midgestational mouse embryo. (a-l) Representative bright-field sagittal (a,e,i) and coronal midbrain (b-d, f-h, j-l) sections (anterior left, dorsal top; coronal level indicated by broken lines in a, e, i) of wild-type (CD-1) mouse embryos at E10.5 (a-d), E11.5 (e-h) and E12.5 (i-l). Sagittal sections in (a, e, i) were pseudo-colored for better visualization of the *miR-125b* ISH signal (red). The most anterior coronal section corresponds to the diencephalic/rostral midbrain, the middle section to the midbrain proper, and the posterior section to the MHB/rostral hindbrain. *miR-125b* was expressed predominantly in ventral regions of the anterior neural tube. At E10.5, *miR-125b* is expressed in the FP, BP and extends dorsally into the AP and RP. At E11.5, *miR-125b* was expressed strongest in the midbrain BP (g) and ABB (h), and appears to retract from the midbrain lateral FP (g). A distinctive roof plate signal was observed at this stage throughout the dorsal midbrain (f'-h'). At E12.5, *miR-125b* exhibited a distinct expression pattern in different brain regions: in the ventrolateral rostral midbrain/caudal diencephalon (j), it was widely expressed in the SVZ and MZ; in the midbrain, strongest *miR-125b* expression was observed in the SVZ/MZ of the BP; and in the caudal midbrain/rostral hindbrain, a very strong expression of *miR-125b* was detected throughout the VZ, SVZ and MZ of the BP and ABB. Abbreviations: AP, alar plate; ABB, alar basal boundary; BP, basal late; Di, diencephalon; Fb, forebrain; FP, floor plate; Hb, hindbrain; Mb, midbrain; Mes, mesencephalon; Met, metencephalon; MHB, mid-hindbrain boundary; MZ, mantle zone; r1, rhombomere 1; RP, roof plate; SVZ, subventricular zone; Tel, telencephalon; VZ, ventricular zone.

Notably, ISH of E10.5 sagittal and coronal sections revealed that although *miR-125b* appeared to be expressed weakly throughout the MH neuroepithelium, an apparent stronger expression was observed in the ventral neural tube including the FP and BP (Fig. 23a-d), as evidenced on serial coronal midbrain sections (data not shown). The most anterior coronal section corresponds to the diencephalic/rostral midbrain, the middle section to the midbrain proper, and the posterior section to the MHB/rostral hindbrain. Noteworthy, E10.5 was the only stage where *miR-125b* was expressed within the entire midbrain floor plate. In the MHB region/rostral hindbrain, *miR-125b* was expressed strongly in the basal plate but sparing the floor plate, and exhibited a decreasing expression gradient towards the RP.

One day later at E11.5, dorsal expression of *miR-125b* became weaker to undetectable, except a distinctive signal for *miR-125b* was observed in the RP at this stage extending from the diencephalon into the rostral hindbrain (Fig. 23f'-h'). A strong expression of *miR-125b* was detected in the VZ, SVZ and MZ of the midbrain basal plate (Fig. 23e-h). At this time-point, *miR-125b* appeared to retract from the medial floor plate of the diencephalon, mesencephalon and metencephalon, but scattered *miR-125b* expression was observed in the lateral floor plate of the mesencephalon (Fig. 23g).

At E12.5, *miR-125b* expression was almost completely excluded from the dorsal di-, mes and metencephalon and appeared to be exclusively confined to the ventral neural tube (Fig. 23j-l). Notably, a small *miR-125b* expression domain was detected in the dorsal MHB on sagittal sections (Fig. 23i). In the ventral diencephalon, *miR-125b* expression extended throughout the SVZ/MZ of the neuroepithelium but sparing the VZ of the FP (Fig. 23j). Similarly in the mesencephalon, strong *miR-125b* expression extended throughout the SVZ and MZ of the BP/ABB, with a few scattered *miR-125b* positive cells found in the VZ (Fig. 23k), whereas in the metencephalon (Fig. 23l), *miR-125b* was strongly expressed in the VZ and SVZ and appeared to spare the MZ. Interestingly, a weaker *miR-125b* expression was noted in the alar-basal-boundary (ABB) of the E12.5 mesencephalon, with mostly confined to the SVZ/MZ (Fig. 23k), which is contrary to the high expression of *miR-125b* in the ABB of the metencephalon (Fig. 23l).

The prominent expression of *miR-125b* in the ventral mes- and rostral metencephalon prompted me to analyse this in more detail. Firstly, a web-based open access software - TargetScan 4.1 (<http://www.targetscan.org/>) was used to predict mRNA targets of *miR-125b*. Secondly, a selection of candidate mRNAs was obtained from the list of all putative *miR-125b* targets predicted by the TargetScan software using the following three criteria: conservation across species, a known involvement in the development of ventral mesencephalic/rostral metencephalic neurons (such as OM/TN, RN and GABAergic neurons), and most importantly, a correlation between the expression of *miR-125b* and of the candidate mRNA within the mes-/metencephalic BP. Two of the predicted mRNA targets, namely *Phox2b* and *Sim1*, fulfilled these criteria and were therefore selected as potential *miR-125b* target candidates. *Phox2b* is a postmitotic marker for somatic MNs arising from the BP in the midbrain and hindbrain (Pattyn et al., 2000b), and *Sim1* is a marker for BP neural progenitors (Fan et al., 1996). I therefore focused my subsequent *miR-125b* expression pattern analyses in relation to these two markers, as any interaction of *miR-125b* and its putative targets might result in either a mutually exclusive or in a partially overlapping expression pattern (Liu and Kohane, 2009).

3.2.4. Expression of *miR-125b* overlaps with the motoneuron markers *Phox2b* and *Sim1* in the basal plate of the murine mid- and hindbrain

The distinctive expression of *miR-125b* within the BP of the mesencephalon and rostral metencephalon (MHB region) (Fig. 23) suggested that *miR-125b* might be co-expressed with known markers for MNs populations arising from the mesencephalic/metencephalic BP, such as *Phox2b*⁺ and *Isl1*⁺ postmitotic oculomotor (OM) and trochlear nucleus (TN) MNs, or *Nkx6-1*⁺/*Sim1*⁺ neural progenitors in the mesencephalic BP, that generate both OM and red nucleus (RN) neurons. Co-expression of *Phox2b/Sim1* and *miR-125b* suggest a possible mRNA-miRNA interaction. I therefore performed an ISH with a *miR-125b* LNA probe and riboprobes for *Phox2b* and *Sim1* on consecutive serial coronal sections from midgestational mouse embryos to co-localize the corresponding signals in ventral MH tissues.

At E10.5, *miR-125b* overlaps to a large extent with *Phox2b* (Fig. 24c) and *Sim1* (Fig. 24e) in the midbrain BP. Indeed, as reported earlier, *miR-125b* expression was observed throughout the MH neuroepithelium including VZ, SVZ and MZ (Fig. 23a-d), and overlapped with postmitotic *Phox2b*⁺ OM neurons that have already been generated at this time-point (Pattyn et al., 1997) and are located in the MZ and with *Sim1*⁺ neural progenitors/precursors in the VZ and SVZ of the midbrain BP. A similar overlapping expression of *miR-125b* with *Phox2b* (Fig. 24h) and *Sim1* (Fig. 24j) in the midbrain BP was observed at E11.5. Notably, *miR-125b* expression at E12.5 had refined to a distinct domain comprising mostly the *Sim1*⁺ VZ/SVZ (progenitor) domain in the midbrain BP (Fig.24o) and the MZ of the lateral FP, overlapping only to a minor extent with the *Phox2b*⁺ domain in the MZ of the midbrain BP (Fig.24m).

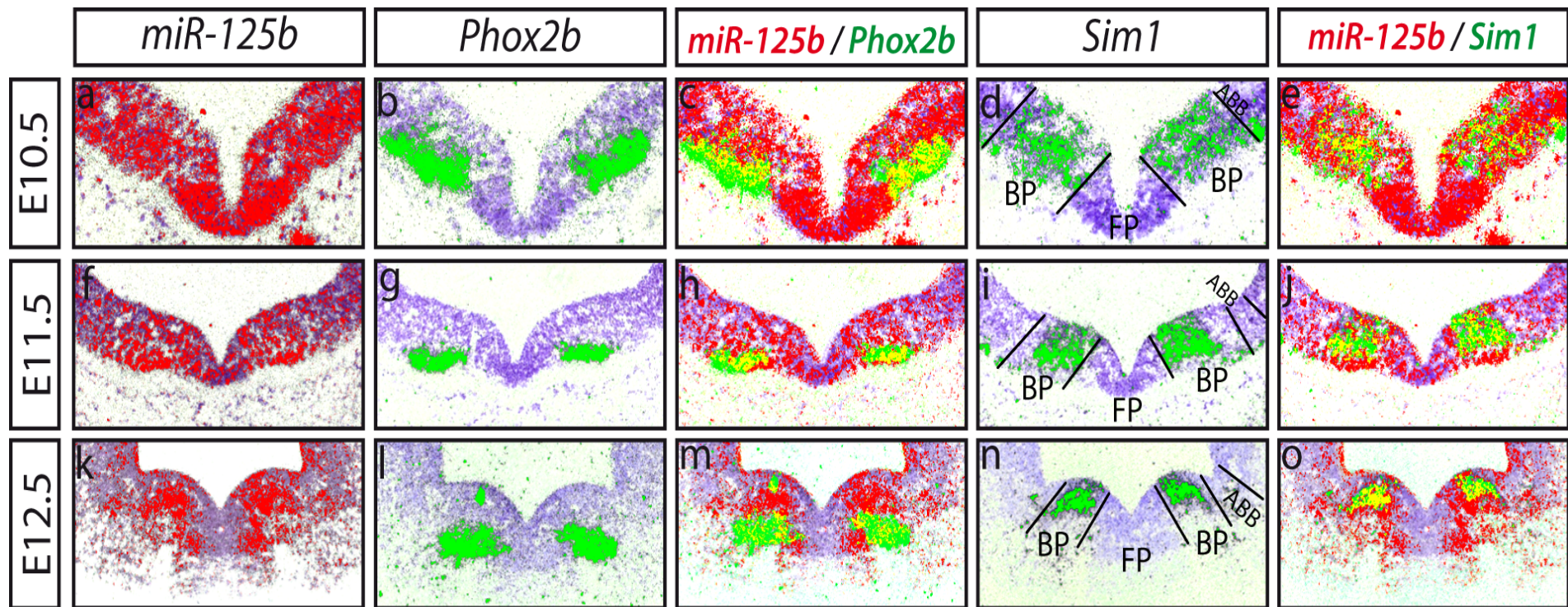


Figure 24. Overlapping expression of *miR-125b* with *Sim1*⁺ mes-/metencephalic BP progenitors/precursors and partial overlap of *miR-125b* expression with postmitotic *Phox2b*⁺ OM/TN MNs in the midgestational mouse embryo. a-o: Representative close-up views of the ventral midbrain/rostral hindbrain on pseudo-colored overlays of consecutive coronal sections from E10.5 (a-e), E11.5 (f-j), and E12.5 (k-o) CD-1 mouse embryos hybridized with a *miR-125b* LNA probe (red in a,f,k) or riboprobes for *Phox2b* (green in b,g,l) and *Sim1* (green in d,i,n); overlapping expression domains appear in yellow. Dorsal is at the top.

3.2.5. *miR-125b* directly targets the *Phox2b* and *Sim1* 3'UTRs

Given the distinctive and partly overlapping expression pattern of *miR-125b* and *Phox2b/Sim1* in the midgestational mouse mesencephalon/rostral metencephalon and in particular in the midbrain BP, I next assessed whether *Phox2b* and *Sim1* mRNAs are directly targeted by *miR-125b*. To this end, I used a web-based open access software - TargetScan 4.1 (<http://www.targetscan.org/>) to search for *miR-125b* binding sites (seed sequences) within the *Phox2b* and *Sim1* 3'UTRs. Notably, the *miR-125b* seed sequence in both predicted target mRNAs is conserved in broad variety of mammals (Fig. 25).



Figure 25. Alignment of the seed sequences/bindings sites for *miR-125b* within the *Phox2b* 3'UTR (a) and *Sim1* 3'UTR (b) of five mammalian species with the *miR-125b* sequence as predicted by TargetScan 4.1. The *miR-125b* seed sequence (highlighted in cyan) is conserved across 5 mammalian species, ranging from mouse, rat to primates including human.

To test whether the *Phox2b* and *Sim1* 3'UTRs are indeed directly targeted/bound by *miR-125b* on the molecular level, I performed luciferase sensor assays with the mouse *Phox2b* and *Sim1* 3'-UTRs after co-transfection of a *pre-miR-125b* precursor miRNA in HEK293T cells, as already described in section 2.2.12. Co-transfection of a

luciferase sensor construct containing the 3'UTR of the corresponding predicted target mRNA and the precursor *miR-125b* revealed that the luciferase activity of the *Phox2b* 3'UTR- and *Sim1* 3'UTR sensor vectors was significantly reduced by 18 % and 37 %, respectively, relative to the control (empty pGL3 Promoter Vector + *pre-miR-125b*) (Fig. 26c).

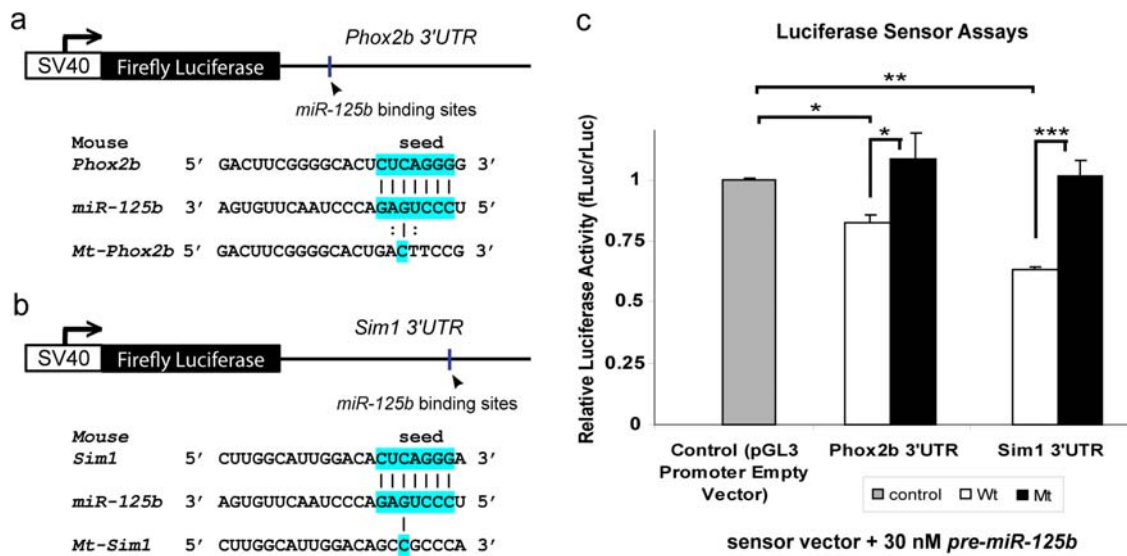


Figure 26. Murine *Phox2b* and *Sim1* 3'UTRs are regulated by *miR-125b*. (a and b) Schematic diagrams showing the approximate location of the *miR-125b* seed sequence/binding site within the *Phox2b* 3'UTR (a) or *Sim1* 3'UTR (b). The *miR-125b* seed sequence in the corresponding 3'UTR is shown in the top row, the mature *miR-125b* sequence is shown in the middle row, and the mutated seed sequence within the corresponding 3'UTR is shown in the bottom row. (c) Luciferase sensor assays after co-transfection of *mmu-miR-125b* precursor miRNA and a sensor vector that a) does not contain any 3' UTR ("empty vector") or b) a sensor vector containing the 3' UTR of the predicted target genes at the 3' end of the Luciferase CDS showed a reduction of luciferase activity of both *Phox2b* 3'UTR- and *Sim1* 3'UTR-mediated luciferase expression (*Phox2b* 3'UTR + *miR-125b*: 0.82±0.03, mean±SEM; *Sim1* 3'UTR + *miR-125b*: 0.63±0.01, mean±SEM) compared to control. Site-directed mutagenesis of the seed sequences within the *Phox2b* 3'UTR (*Mt-Phox2b* 3'UTR) and *Sim1* 3'UTR (*Mt-Sim1* 3'UTR) abolished this negative regulation by *pre-miR-125b* (*Mt-Phox2b* 3'UTR + 30 nM *pre-miR-125b*: 1.08±0.105; *Mt-Sim1* 3'UTR + 30 nM *pre-miR-125b*: 1.01±0.065; mean±sd), indicating that this effect was specific for the predicted *miR-125b* binding sites. (n = 3, *p < 0.05; ** p < 0.01; *** p < 0.001; Student's-T-test). Value for the "empty vector" control was set as "1", and all other values were normalized to this control.

To confirm that the *pre-miR-125b*-induced downregulation of the corresponding sensor activity was indeed mediated by the predicted *miR-125b* binding sites/seed sequences within the *Phox2b*- and *Sim1* 3'UTR, I performed site-directed mutagenesis of these predicted *miR-125b* seed sequences (binding sites), as shown in Fig. 26a,b. Co-transfection of the mutated *Mt-Phox2b* 3'UTR sensor vector and *pre-miR-125b* abolished the repression of the wild-type *Phox2b* 3'UTR-mediated luciferase activity by *miR-125b*. Similarly, co-transfection of *Mt-Sim1* 3'UTR sensor vector and *pre-miR-125b* rescued the *Sim1* 3'UTR-mediated luciferase activity to control levels. These results indicated that the negative regulation of the *Phox2b* and *Sim1* 3'UTR by *miR-125b* is in fact mediated by the predicted *miR-125b* seed sequences within these 3'UTRs.

To confirm these results, I repeated these experiments using a vector for the constitutive overexpression (OE) of *miR-125b* driven by the chicken β actin promoter/CMV enhancer (CAG) promoter (Fig. 27a). Co-transfection of 900 ng *miR-125b* overexpression vector and 300 ng luciferase sensor vector with the 3'UTR of the predicted target mRNA resulted in an even stronger (as compared to the experiments using a *pre-miR-125b*) reduction of luciferase activity by 40 % (*Phox2b*) and 50 % (*Sim1*) relative to the control (Fig. 27b). These data confirmed my previous results showing that *Phox2b*- and *Sim1* 3'UTR-mediated luciferase expression is also down-regulated after constitutive overexpression of *miR-125b*, and suggested that constitutive OE of *miR-125b* might lead to higher *miR-125b* levels in the transfected cells and might thus be more effective for the regulation of 3'UTR-mediated luciferase expression in the sensor assays as compared to the lower levels/transient activity (lower uptake/transfection; faster decay) of the transfected *pre-miR-125b*.

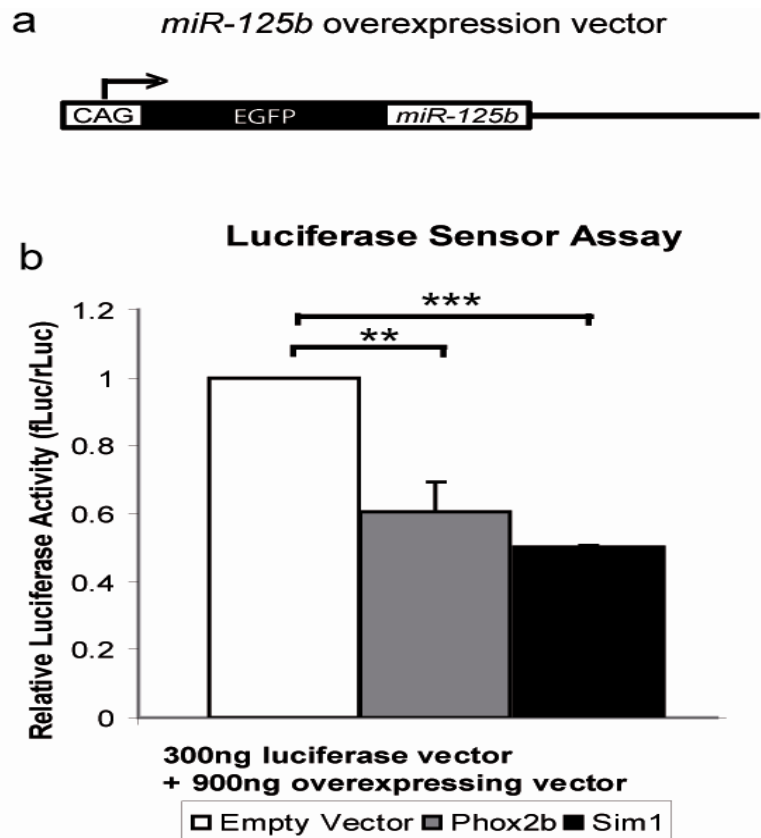


Figure 27. Constitutive overexpression of *miR-125b* results in a strong downregulation of mouse *Phox2b*- and *Sim1* 3'UTR-mediated luciferase expression. **a)** A schematic drawing of the *miR-125b* OE vector. A sequence corresponding to *pre-miR-125b* was cloned downstream of the enhanced green fluorescent protein (eGFP) coding sequence (CDS) driven by a CAG promoter in the pcDNA6.2 vector **b)** Luciferase sensor assays after co-transfection of *miR-125b* OE vector and a sensor vector that a) does not contain any 3' UTR ("empty vector") or b) a sensor vector containing the 3' UTR of the predicted target genes at the 3' end of the Luciferase CDS showed luciferase activity reduction in all cases. Overexpression of *miR-125b* downregulated *Phox2b* 3'UTR-mediated luciferase expression by approximately 40 % (0.6 ± 0.09 , mean \pm sd) and *Sim1* 3'UTR-mediated luciferase expression by approximately 50 %. (0.5 ± 0.01 , mean \pm sd) (* $p < 0.05$; ** $p < 0.005$; *** $p < 0.0005$ in Student-T-test for repeated measurements). Value for the "empty vector" control was set as "1", and all other values were normalized to this control.

3.2.6. *MiR-125b* regulates the development of postmitotic *Phox2b*⁺/*Isl1*⁺ OM/TN neurons and of *Nkx6-1*⁺ BP progenitors *in vitro*

Thus far, I have shown that *miR-125b* displays a particularly strong expression in the mesencephalic and rostral metencephalic BP of the midgestational mouse embryo, which initially overlaps with the expression domains of two predicted and confirmed targets of this miRNA, *Phox2b* and *Sim1*, in the same brain region. Notably, the expression domains of *miR-125b* and *Phox2b* appear to segregate from each other at later developmental stages. I have also shown that *miR-125b*-mediated regulation of *Phox2b* and *Sim1* occurs via one conserved *miR-125b* binding site (seed sequence), respectively, within the 3'UTR of these two mRNAs. *Phox2b* expression is activated in postmitotic *Isl1*⁺ OM/TN MNs around E9.5-E10.5 (Pattyn et al., 1997), whereas *Sim1* expression is mostly confined to the VZ/SVZ of the midbrain/rostral hindbrain BP in what has been considered to be the progenitor domain of *Pou4f1*⁺ (*Brn3a*⁺) RN neurons (Nakatani et al., 2007). These mesencephalic/rostral metencephalic BP progenitors also express *Nkx6-1*, and *Nkx6-1* is required for the proper generation of RN and OM/TN neurons from these progenitors (Prakash et al., 2009). More recent overexpression data, however, indicate that *Nkx6-1* exerts a repressive effect on the expression of *Sim1* in BP progenitors and that *Nkx6-1* and *Sim1* have different activities in ventral midbrain development: *Nkx6-1* appears to suppress FP differentiation whereas *Sim1* appears to repress mdDA differentiation in the midbrain BP (Nakatani et al., 2010). Due to the lack of a working antibody against SIM1, I used NKX6-1 as another marker for the vMH BP progenitors and precursors. Altogether, my data so far suggest that *miR-125b* might be involved in the proper generation and/or maintenance of OM/TN neurons and/or *Sim1*⁺/*Nkx6-1*⁺ mesencephalic/rostral metencephalic BP progenitors in the developing mouse embryo.

In mice, *miR-125b* is encoded by two genes where *miR-125b-1* is located on chromosome 9 (intronic) and *miR-125b-2* is located on chromosome 16 (intergenic) and therefore makes an *in vivo* loss-of-function analysis of *miR-125b* very difficult and time-consuming. To obtain first insights into the biological function of *miR-125b*, I used the *in vitro* culture of primary ventral midbrain/hindbrain (vMH) cells from E11.5 wild-type (CD-1) mouse embryos, that were transduced with lentiviruses encoding either the *pre-miR-125b* (*miR-125b* OE lentivirus) (Edbauer et al., 2010) for gain-of-function

studies, or a *miR-125b* sponge lentivirus (Ebert et al., 2007) for loss-of function (knockdown) studies. Both viruses harboured an mCherry reporter gene for detection of the transduced cells (sketches for both lentiviral constructs are shown in Fig. 28b,c). Figure 28d depicts schematically the experimental design. In my experiments, the viral transduction efficiency was very high, and almost 100 % (in average 97%) of the cells expressed the mCherry reporter (Fig. 28e-m).

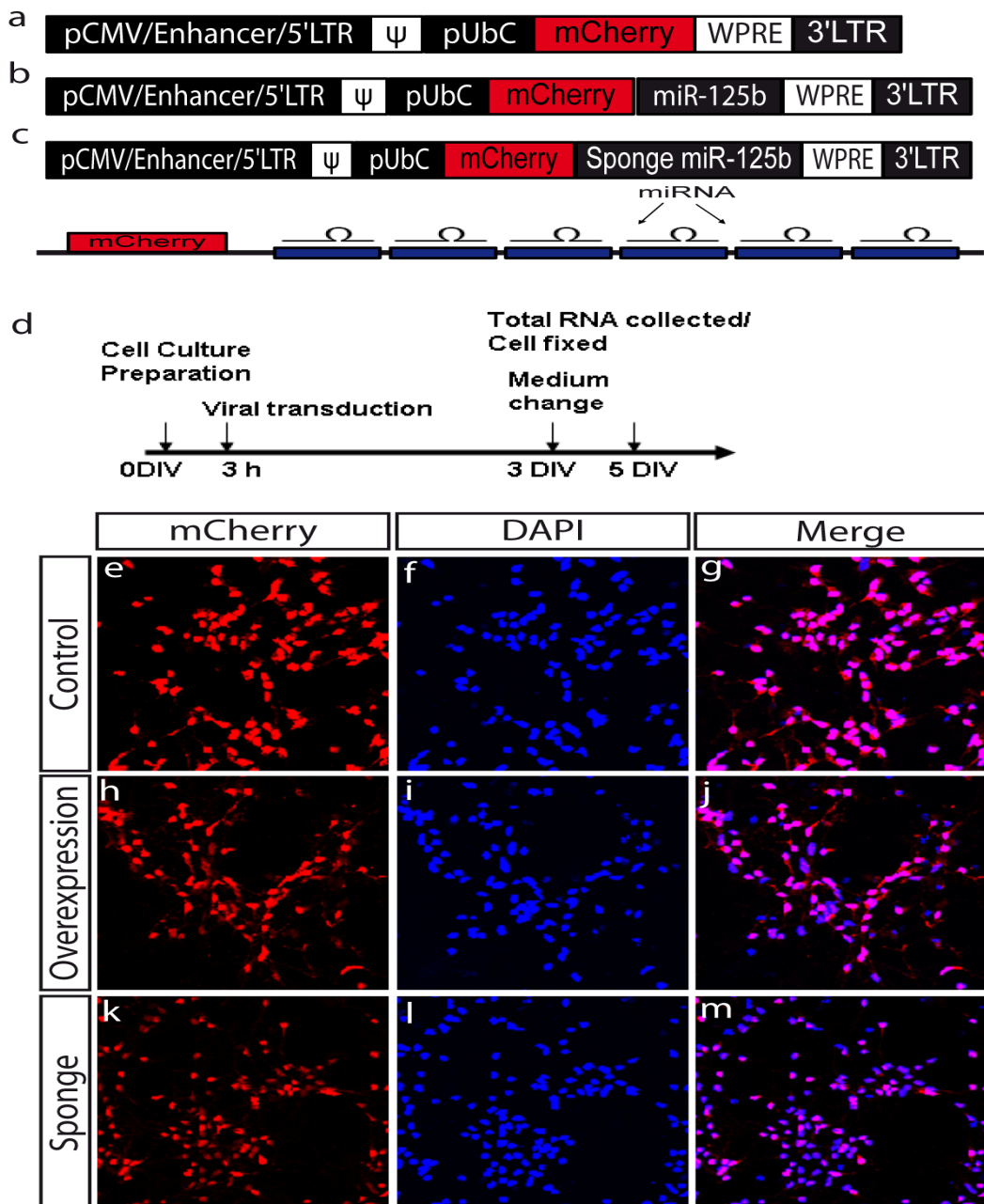


Figure 28. Viral constructs, experimental design and viral transduction efficiencies for control (empty backbone), *miR-125b* OE or sponge lentivirus of E11.5 primary vMH cell cultures. (a,b,c) Schematic diagrams depicting the viral vectors used as control (a), over-express the precursor *miR-125b*

(*miR-125b OE vector/lentivirus*) (b) or knock-down *miR-125b* (*mir-125b sponge vector/lentivirus*)(c) used in these experiments. The bottom diagram in (c) shows that the sequences (6 repeats within the mCherry 3'UTR) in the *mir-125b sponge vector* are not fully complementary to the mature *miR-125b* sequence and contain two central mismatches, thereby leading to a *miR-125b* bulge formation that prevents the cleavage (degradation) of the sponge RNA by AGO2. (d) Schematic depiction of the experimental design. E11.5 primary vMH cell cultures were prepared on day 0, infected with the viral vectors depicted in (a) (b) or (c) 3 hours after plating, and harvested for fixation or preparation of total RNA after 3 or 5 DIV. (e-m) E11.5 primary vMH cultures transduced with control (empty backbone + mCherry reporter) lentivirus (e-g), *miR-125b OE lentivirus* (h-j) and *mir-125b sponge lentivirus* (k-m) revealed that a transduction efficiency of almost 100 % was achieved in all cultures after 3 DIV (mCherry⁺/DAPI⁺ cells: Control lentivirus, 96.85 %; *miR-125b OE* lentivirus, 96.75 %; *miR-125b sponge* lentivirus, 97.12 %). Cells were stained with anti-RFP antibody (e,h,k) and cell nuclei were visualised with DAPI (f,i,l) in blue. Merged images are shown in (g,j,m).

Quantification of Phox2b⁺ cells (OM/TN neurons) in the E11.5 vMH primary cultures transduced with the *miR-125b OE* lentivirus revealed a reduction of Phox2b⁺ cell numbers by 30 % as compared to the control-infected cultures after 3 DIV (Fig. 29a,b,g). A slight decrease of 2 % relative to the controls were observed in the *miR-125b sponge*-transduced cultures after 3 DIV (Fig. 29a,c,g). At 5 DIV, a reduction of 16 % in the Phox2b⁺ cell numbers after transduction with the *miR-125b OE* lentivirus, and an increase by 25 % in the Phox2b⁺ cell numbers after transduction with the *miR-125b sponge* lentivirus were observed in the E11.5 primary vMH cultures (Fig. 29d-f,h,j). To establish whether this reduction or increase in Phox2b⁺ cells after transduction of the *miR-125b OE* or *sponge* lentivirus, respectively, was due to a decrease or increase, respectively, of *Phox2b* mRNA levels in the infected cells, I performed an RT-qPCR experiment with *miR-125b OE*- and *sponge*-infected E11.5 vMH primary cultures after 3 and 5 DIV. At 3 DIV, *Phox2b* mRNA levels were reduced by 35 % in the *miR-125b OE*-infected primary cultures and increased by approximately 9 % in the *sponge*-infected primary cultures (Fig. 29i). Similarly at 5 DIV, *Phox2b* mRNA levels were reduced by 34 % in the *miR-125b OE*-infected cultures, but strongly increased by 77 % in the *miR-125b sponge*-infected cultures as compared to the control-infected cells (Fig. 29j), thus paralleling the Phox2b⁺ cell counting results.

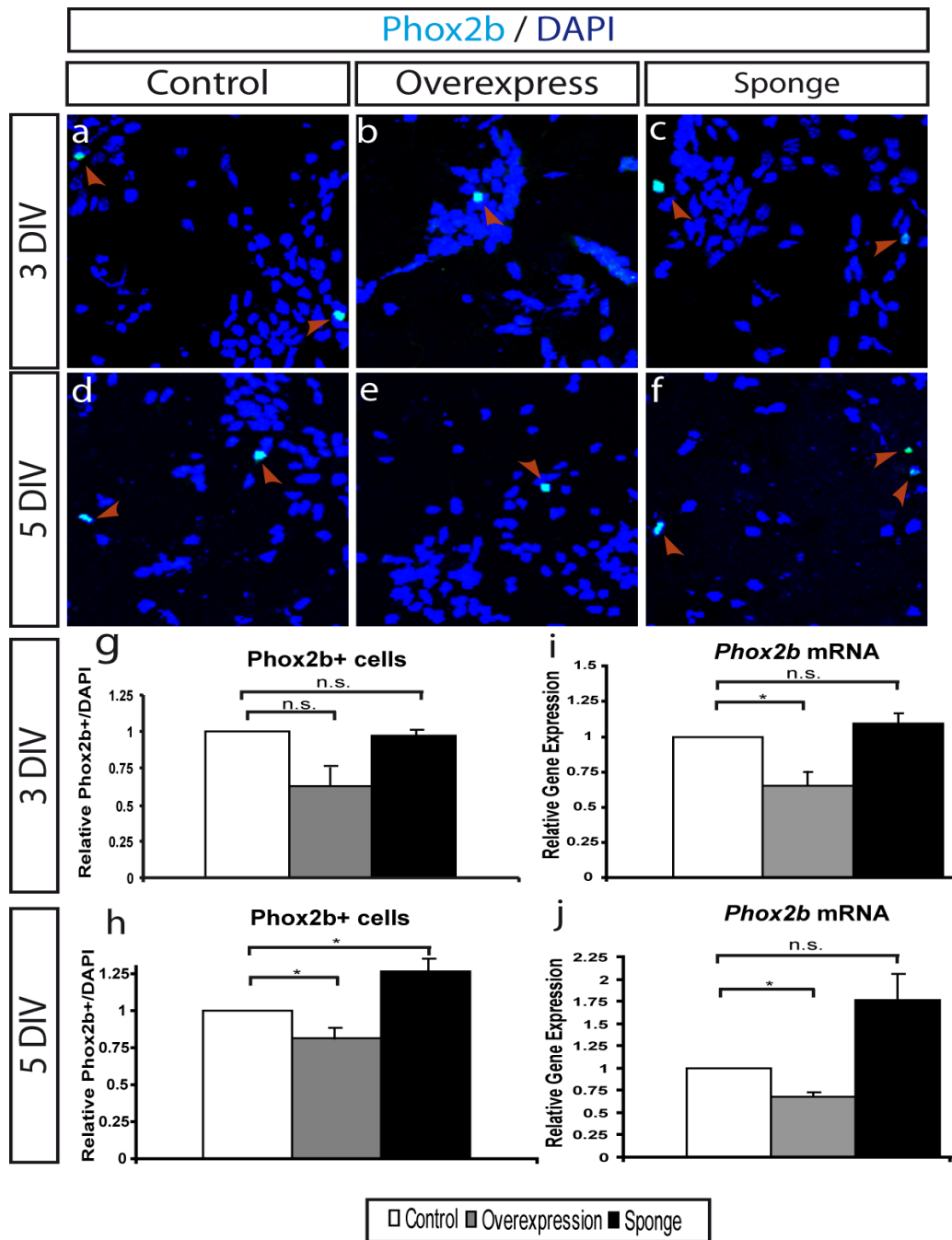


Figure 29. *MiR-125b* regulates the numbers of $Phox2b^+$ cells in E11.5 primary vMH cell cultures. (a-f) Representative pictures of primary vMH cultures derived from E11.5 CD-1 embryos transduced with control (a,d), *miR-125b* OE (b,e) and *miR-125b* sponge (c,f) lentiviruses and fixed after 3 DIV (a-c) or 5 DIV (d-f). (g, h) Quantification of $Phox2b^+/DAPI^+$ cells in these cultures showed a decrease of $Phox2b^+$ cells after *miR-125b* OE as compared to the controls ($Phox2b^+/DAPI^+$ cells, *miR-125b* OE: 3 DIV, 0.70 ± 0.116 ; 5 DIV, 0.84 ± 0.037 ; mean \pm SEM; n=3). An increase of $Phox2b^+$ cells after transduction with the *miR-125b* sponge lentivirus was observed only after 5 DIV ($Phox2b^+/DAPI^+$ cells, *miR-125b* sponge: 3 DIV, 0.98 ± 0.1 ; 5 DIV, 1.26 ± 0.083 ; mean \pm SEM; n=3). (i) RT-qPCR from primary vMH cultures at 3 DIV showed a significant reduction by 35 % of *Phox2b* mRNA after *miR-125b* overexpression and a

slight increase by 9 % of *Phox2b* mRNA levels after *miR-125b* knock-down (*Phox2b* mRNA 3 DIV: *miR-125b* OE, 0.65 ± 0.052 ; *miR-125b* sponge, 1.09 ± 0.1 ; mean \pm SEM; n=3). (j) RT-qPCR from primary vMH cultures at 5 DIV showed a significant reduction by 33% of *Phox2b* mRNA after *miR-125b* overexpression and an increase of *Phox2b* mRNA by 77 % after *miR-125b* knock-down in these cultures (*Phox2b* mRNA 5 DIV: *miR-125b* OE, 0.67 ± 0.052 ; *miR-125b* sponge, 1.77 ± 0.294 ; mean \pm SEM; n=3). Red arrowheads point at double-labelled Phox2b⁺ and DAPI⁺ cells. Phox2b⁺ cells and mRNA levels were normalized to the control, which was set as “1”. **P*<0.05 compared with corresponding control in the independent-samples *t* test.

As I have shown that *Phox2b* is a direct target of *miR-125b* (Fig.26), the reduction or increase of Phox2b⁺ cells and *Phox2b* mRNA levels after overexpression or knock-down, respectively, of *miR-125b* in primary vMH cells might just be due to the *miR-125b*-mediated downregulation or *miR-125b* sponge-mediated upregulation of *Phox2b* expression in these cells. To establish whether the overexpression or knockdown of *miR-125b* does indeed affect the generation of Phox2b⁺ OM/TN neurons in these cultures, I used another independent (not *miR-125b*-targeted) marker for these neurons, namely *Islet1* (*Isl1*) (Agarwala and Ragsdale, 2002).

Quantification of Isl1⁺ cells in the E11.5 primary vMH cultures after transduction with the *miR-125b* OE lentivirus revealed a significant decrease of Isl1⁺ cells by 32 % and 27 % after 3 and 5 DIV, respectively, whereas transduction with the *miR-125b* sponge lentivirus resulted in a 33 % increase of these cells relative to the controls only after 5 DIV, whereas no changes in Isl1⁺ cells were detected at 3 DIV (Fig. 30) after *miR-125b* knock-down. These results showed that overexpression or knockdown of *miR-125b* results in a reduction or increase, respectively, of Phox2b⁺ and Isl1⁺ cells in primary vMH cultures, indicating that *miR-125b* indeed controls the generation and/or survival of OM/TN neurons *in vitro* by negatively regulating the expression of *Phox2b* in these cells and in their postmitotic precursors.

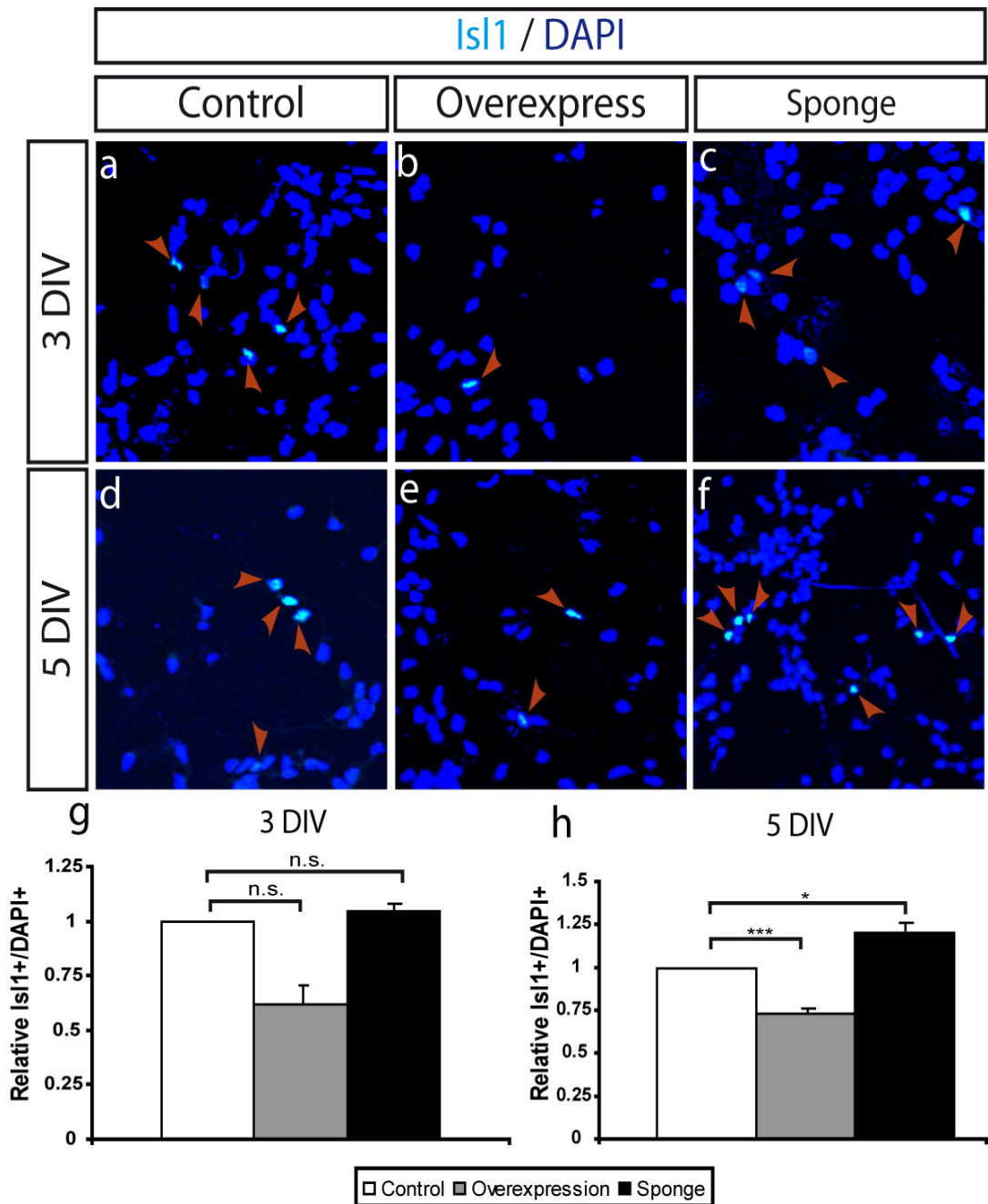


Figure 30. *MiR-125b* controls the generation of Isl1⁺ OM/TN neurons in E11.5 primary vMH cell cultures. (a-f) Primary VM cultures derived from E11.5 CD-1 embryos were transduced with control (a,d), *miR-125b* OE (b,e) and *miR-125b* sponge (c,f) lentiviruses and fixed after 3 DIV (a-c) and 5 DIV (d-f). (g) Quantification of Isl1⁺ cells in these cultures after 3 DIV showed a non-significant decrease of Isl1⁺ cells in the vMH cultures transduced with the *miR-125b* OE and *miR-125b* sponge lentiviruses compared to the controls (Isl1⁺/DAPI⁺ cells at 3 DIV: *miR-125b* OE, 0.68±0.126; *miR-125b* sponge, 1.06±0.1; mean±SEM; n=3). (h) In the vMH cultures at 5 DIV, a significant decrease by 27 % of Isl1⁺ cells was observed after transduction of the *miR-125b* OE lentivirus, and a significant increase by 33 % of Isl1⁺ cells was observed after transduction of the *miR-125b* sponge lentivirus (Isl1⁺/DAPI⁺ cells at 5 DIV: *miR-125b* OE: 0.73±0.015; *miR-125b* sponge: 1.33±0.116; mean±SEM; n=3). Red arrowheads point at

double-labelled $Isl1^+$ and $DAPI^+$ cells. $Isl1^+$ cells were normalized to the control, which was set as “1”. * $P < 0.05$, *** $P < 0.005$ compared with corresponding control in the independent-samples t test.

As the loss or gain of $Phox2b^+/Isl1^+$ cells after *miR-125b* OE or knock-down, respectively, pointed towards a *miR-125b* dosage-dependent reduction or increased generation of OM/TN neurons in the primary vMH cultures, I next aimed at determining the possible (cellular) mechanisms for this effect of *miR-125b*. There might be at least 3 possible mechanisms for *miR-125b* regulating the number of $Isl1^+$ OM/TN neurons generated in the vMH: (1) by directly selecting or repressing (in a dose-dependent manner) the $Sim1^+$ and/or $Nkx6-1^+$ BP progenitor and/or the $Phox2b^+$ OM/TN neuron fate over other possible progenitor/neuronal fates (such as the $Pou4f1/Brn3a^+$ RN fate, as these neurons arise from the same progenitor domain as the OM neurons, or the adjacent Th^+ mdDA fate (arising from the midbrain FP) and/or GABAergic fate (arising from the ABB and AP)) in the progenitors and/or postmitotic precursors in which *miR-125b* is expressed; (2) by dose-dependently regulating the proliferation of the $Sim1^+$ or $Nkx6-1^+$ BP progenitors that express *miR-125b* and generate the $Phox2b^+$ postmitotic OM/TN precursors; (3) by dose-dependently regulating the survival of the cells in which *miR-125b* is expressed ($Sim1^+/Nkx6-1^+$ BP progenitors and $Phox2b^+$ postmitotic OM/TN precursors).

To assess which one of these 3 possibilities apply in my case, I first determined the effects of *miR-125b* OE or knockdown on the $Sim1^+$ and/or $Nkx6-1^+$ mes-/rostral metencephalic BP progenitors/precursors in my primary vMH cultures. However, RT-qPCR of primary vMH cultures harvested after 5 DIV showed that *Sim1* mRNA levels were not altered significantly upon *miR-125b* OE or knockdown in these cultures (Fig. 31). It is worth noting at this point that miRNAs might exert their repressive effect on gene expression by either inducing the degradation or repressing the translation (in the absence of any degradation) or both of their target mRNA. In the case of *Sim1*, it appears that the confirmed interaction of *miR-125b* with the *Sim1* 3'UTR (see Fig. 26) in the luciferase sensor assays rather leads to a translational inhibition of this mRNA than to its degradation, as demonstrated by the luciferase sensor assays which I had performed (Fig- 26, 27) and by this qPCR result (fig.31). However, further confirmation of this result as soon as a *Sim1* antibody may become available is warranted.

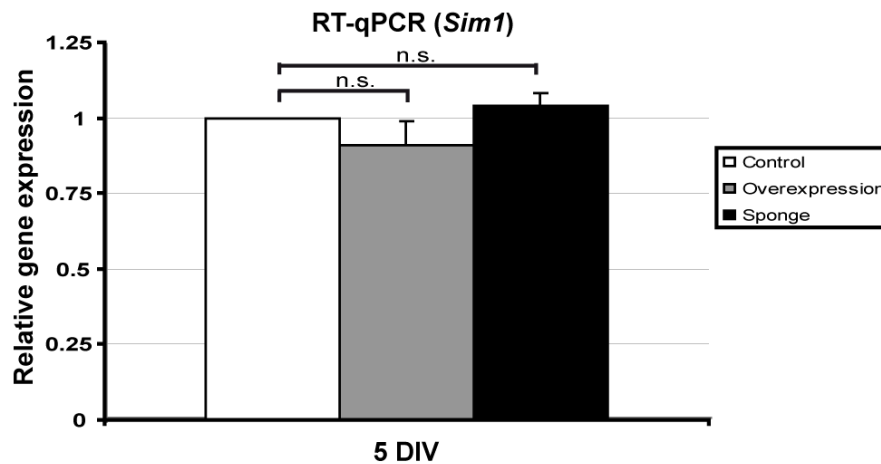


Figure 31. *Sim1* mRNA levels are not altered in E11.5 primary vMH cell cultures after *miR-125b* overexpression or knock-down. Quantitative RT-qPCR revealed that *Sim1* mRNA is not altered significantly relative to the control in primary vMH cultures transduced with *miR-125b OE* and *miR-125b sponge* lentiviruses after 5 DIV (*Sim1* mRNA 5 DIV: *miR-125b OE*, 0.67 ± 0.052 ; *miR-125b sponge*, 1.77 ± 0.294 ; mean \pm SEM; n=3). *Sim1* mRNA levels were normalized to the control, which was set as “1”. $P > 0.05$ compared with corresponding controls in the independent-samples *t* test.

Next, I quantified the numbers of $Nkx6-1^+$ cells in E11.5 primary vMH cultures transduced with *miR-125b OE* or *miR-125b sponge* lentiviruses. This revealed a significant decrease by 24 % of $Nkx6-1^+$ cells at 3 DIV after transduction of the *miR-125b OE* lentiviruses as compared to the controls, whereas transduction of the *miR-125b sponge* lentiviruses did not result in a significant change of $Nkx6-1^+$ cells relative to the control.

To establish whether the reduction in $Nkx6-1^+$ cells after the transduction of *miR-125b OE* lentivirus was due to decreased levels of *Nkx6-1* mRNA in the transduced cells, I performed RT-qPCR experiments on cultures that were treated in a similar manner. The RT-qPCR result revealed that *Nkx6-1* mRNA levels were reduced by 38 % and 37 %, at 3 and 5 DIV, respectively, after overexpression of *miR-125b*. However, *Nkx6-1* mRNA levels were not significantly altered after knock-down of *miR-125b* in these cultures, neither at 3 nor at 5 DIV (Fig. 32). These data suggest that *miR-125b* might in fact directly affect the numbers of $Nkx6-1^+$ BP progenitors by regulating their identity, proliferation, and/or survival in the murine vMH region. Therefore and to

assess this in more detail, I next determined the numbers of proliferating (EdU+) $Nkx6-1^+$ BP progenitors.

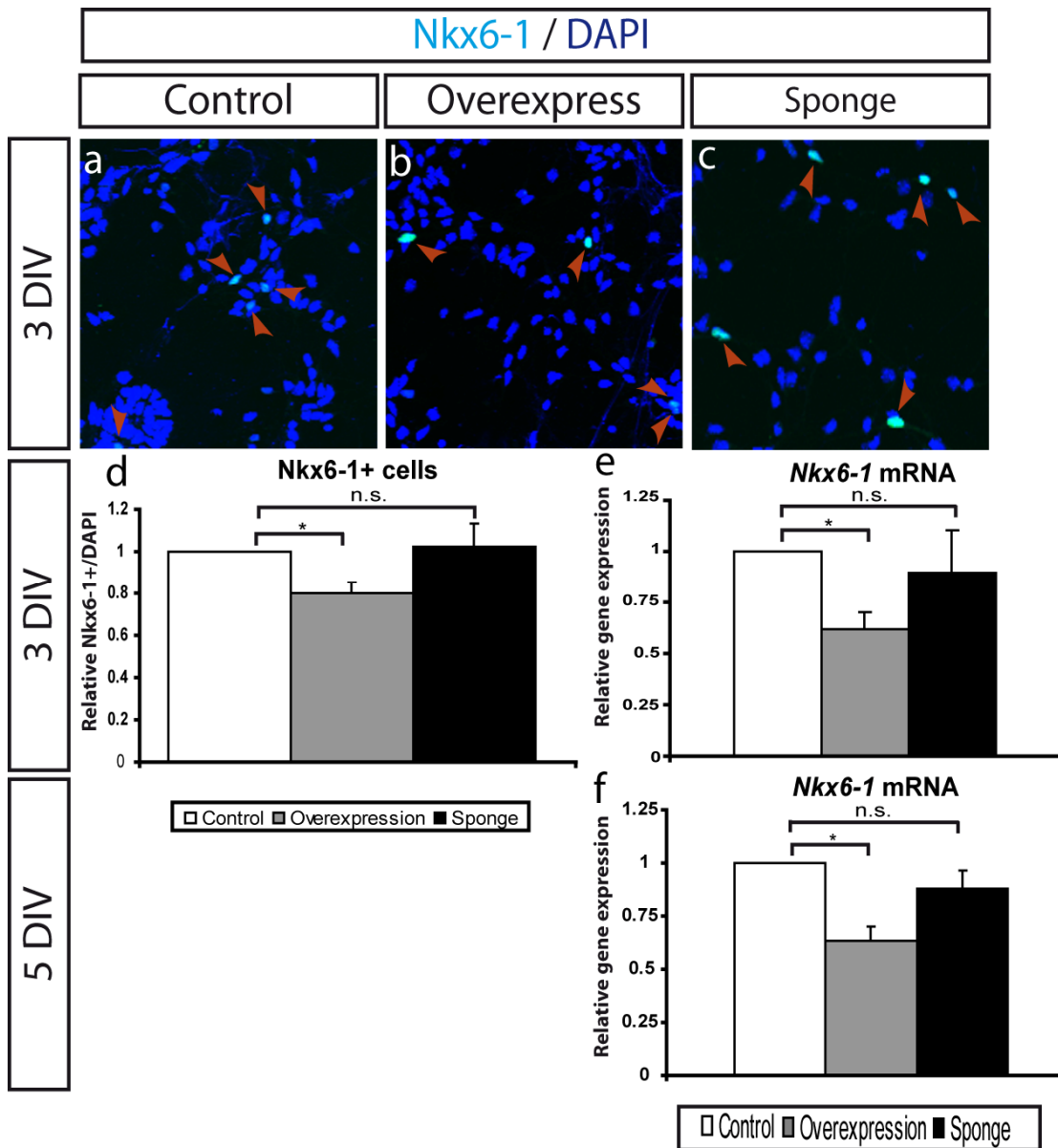


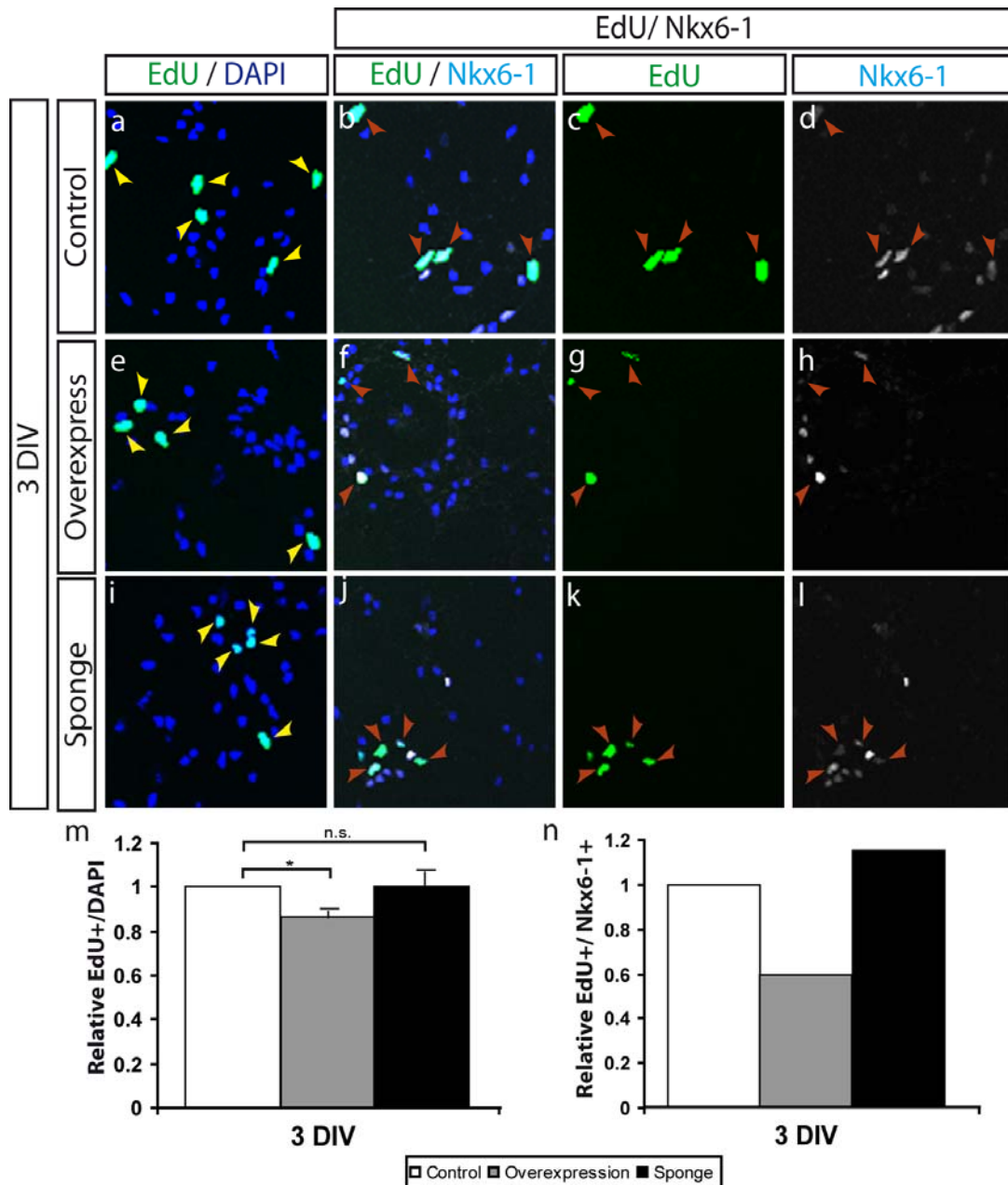
Figure 32. *miR-125b* appears to regulate the numbers of $Nkx6-1^+$ BP progenitors/precursors in E11.5 primary vMH cell cultures. (a-c) Primary vMH cultures derived from E11.5 CD-1 embryos were transduced with control (a), *miR-125b* OE (b) and *miR-125b* sponge (c) lentiviruses and fixed after 3 DIV. (d) Quantification of $Nkx6-1^+$ cells in these cultures showed a 24 % decrease at 3 DIV of $Nkx6-1^+$ cells after overexpression of *miR-125b* but no significant changes in $Nkx6-1^+$ cell numbers after knockdown of *miR-125b* in these cultures as compared to the control ($Nkx6-1^+/DAPI^+$ cells at 3 DIV: *miR-125b* OE, 0.76 ± 0.065 ; *miR-125b* sponge, 0.99 ± 0.1 ; mean \pm SEM n=3) (e,f) RT-qPCR from primary vMH cultures at 3 DIV (e) and 5 DIV (f) showed a significant reduction by 38 % of *Nkx6-1* mRNA levels after overexpression of *miR-125b* but no significant changes of *Nkx6-1* mRNA levels after knockdown of *miR-*

125b in these cultures as compared to controls (*Nkx6-1* mRNA 3 DIV: *miR-125b* OE, 0.62 ± 0.1 ; *miR-125b* sponge, 0.90 ± 0.1 ; *Nkx6-1* mRNA 5 DIV: *miR-125b* OE, 0.63 ± 0.07 ; *miR-125b* sponge, 0.88 ± 0.1 ; mean \pm SEM; n=3). Red arrowheads point at double-labelled *Nkx6-1*⁺ and DAPI⁺ cells. *Nkx6-1*⁺ cells and mRNA levels were normalized to the control, which was set as “1”. **P*<0.05 compared with corresponding controls in the independent-samples *t* test.

3.2.7. The numbers of proliferate cells in primary vMH cells including *Nkx6-1*⁺ BP progenitors are decreased by *miR-125b* overexpression

To assess if the proliferation of BP progenitors in the vMH region is affected by the overexpression or knock-down of *miR-125b*, I determined the numbers of proliferating using 5-ethynyl-2'-deoxyuridine (EdU), a thymidine analogue that incorporate into cellular DNA during replication and subsequently can be covalently attached by a small molecular fluorescent azide (without heat/acid DNA denaturing step), thus allowing DNA synthesis detection (Chehrehasa et al., 2009; Zeng et al., 2010). To assess if *Nkx6-1*⁺ progenitos are affected, I then co-labelled EdU⁺ and *Nkx6-1*⁺ (double-positive) cells in the *miR-125b* OE or sponge-transduced primary vMH cultures after 3 DIV.

I first quantified EdU-labelled proliferating cells in the E11.5 primary vMH cultures after transduced with the *miR-125b* OE and *miR-125b* sponge lentiviruses (fig. 33a,e,i). Quantification of EdU⁺ cells in the *miR-125b* OE primary cultures revealed a significant decrease of EdU⁺ cells by 12 % whereas no changes in the *miR-125b* sponge-transduced primary culture (Fig. 33m). Quantification of *Nkx6-1*/EdU double positive cells per total number of EdU⁺ cells (indicating the proportion of proliferating *Nkx6-1*⁺ BP progenitors among all proliferating cells) in the E11.5 primary vMH cultures after transduction with the *miR-125b* OE lentivirus revealed a significant decrease of *Nkx6-1*⁺/EdU⁺ cells by 37 % after 3 DIV, whereas transduction of the *miR-125b* sponge lentiviruses did not result in a significant change. My data suggest that an increased dosage of *miR-125b* indeed affects (reduces) the overall proliferation in primary vMH cultures but in particular the proliferation of *Nkx6-1*⁺ BP progenitors, thus contributing to the loss of postmitotic offspring (probably including the Phox2b⁺/Isl1⁺ OM/TN neurons but also RN neurons).



point at triple-labelled Nkx6-1⁺, EdU⁺ and DAPI⁺ cells. EdU⁺ and Nkx6-1⁺/EdU⁺ cells per total EdU⁺ cells were normalized to the controls, which were set as “1”. **P*<0.05 compared with corresponding controls in the independent-samples *t* test.

3.2.8. Reduction of the *miR-125b* dosage in vMH primary cultures also increases their survival

I next assessed whether *miR-125b* overexpression or knockdown would also affect the survival of ventral MH neural cells, including BP progenitors and postmitotic OM/TN precursors and/or neurons. Quantification of the numbers of cCasp3⁺ cells per DAPI⁺ cells in the E11.5 primary cultures after transduction of the *miR-125b* OE lentivirus did not reveal any significant changes, whereas transduction of the *miR-125b* sponge lentivirus revealed a significant decrease of cCasp3⁺ cells in these cultures by 29.5 % after 5 DIV but not at 3 DIV relative to the controls (Fig.34). This suggests that knockdown of *miR-125b* in the culture increased their survival.

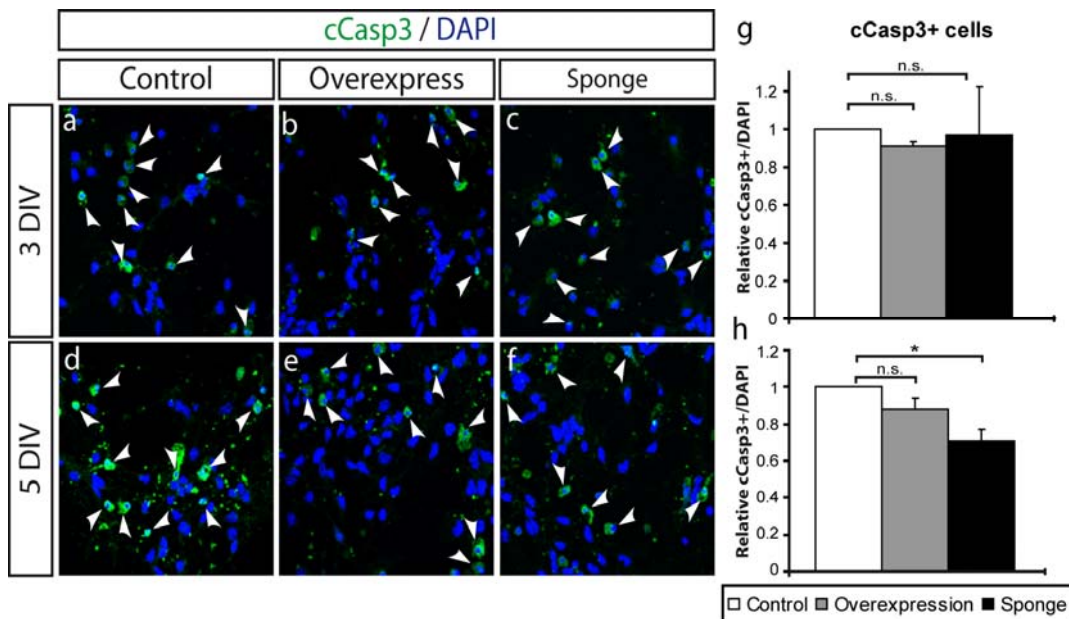


Figure 34. Reduction of *miR-125b* dosage in vMH primary cultures increases the survival of vMH cells. (a-f) Primary vMH cultures derived from E11.5 CD-1 embryos were transduced with control (a,d), *miR-125b* OE (b,e) and *miR-125b* sponge (c,f) lentiviruses and fixed after 3 DIV (a-c) and 5 DIV (d-f). (g,h) Quantification of cCasp3⁺/DAPI⁺ cells showed no alterations in apoptotic cell death in these cultures after 3 DIV (g) but showed a significant decrease of cCasp3⁺ cells after knockdown of *miR-125b* in these cultures at 5 DIV, whereas no changes in apoptotic cell death were detected after overexpression of *miR-125b* (h) (cCasp3⁺/DAPI⁺ cells at 3 DIV; *miR-125b* OE, 0.90±0.1; *miR-125b* sponge, 0.97±0.1;

cCasp3⁺/DAPI⁺ cells at 5 DIV: *miR-125b* OE, 0.88±0.1; *miR-125b sponge*, 0.71±0.067; mean±SEM; n=3). White arrowheads point at double-labelled cCasp3⁺ and DAPI⁺ cells. cCasp3⁺ cells were normalized to the control, which was set as “1”. **P*<0.05 compared with corresponding control in the independent-samples *t* test.

3.3. Generation of *Shh-Cre-SBE1* transgenic mice for the fate-mapping and inactivation of conditional alleles in the rostral midbrain/caudal diencephalon

Another aspect of my PhD work was dedicated to the generation of a transgenic mouse for the conditional inactivation of genes flanked by loxP-sites (“floxed” genes) in the murine ventral midbrain/caudal diencephalon, which is the putative progenitor domain of mdDA neurons (see section 2.2.1 in the Introduction). Epstein and colleagues (Epstein et al., 1999; Jeong and Epstein, 2003) previously had identified a regulatory sequence (enhancer) within the 2nd intron of the mouse *Shh* gene that restricts the expression of this gene to the rostral midbrain and caudal diencephalon in E9.5 embryos carrying a transgene containing this sequence (Fig. 35a,b). The corresponding transgene consisted of a *Shh* minimal promoter (a 1.261 kb fragment of the *Shh* promoter including the TATAA box) driving the expression of a bacterial *lacZ* gene (as reporter), and an evolutionarily conserved 535 bp fragment within intron 2 of the mouse *Shh* gene that was cloned at the 3’ end (after the 272 poly(A) signal) of the *lacZ* gene (Epstein et al., 1999). As the b-Gal expression of this transgene was restricted to the rostral midbrain and caudal diencephalon (and not detected in other regions where *Shh* is normally expressed in the mouse embryo, such as the caudal midbrain, hindbrain and spinal cord FP), the 535 bp enhancer fragment was subsequently named “*Shh brain enhancer 1*” (*SBE1*) by (Epstein et al., 1999). We therefore reasoned that this transgenic construct might also be used for the specific expression of other genes/cDNAs, including the Cre-recombinase cDNA, in the rostral midbrain/caudal diencephalon of the developing mouse embryo, by replacing the *lacZ* by the *Cre recombinase* CDS (Fig. 35c,d).

The transgenic construct was named *Shh-Cre-SBE1* (Fig. 35c), was constructed by Dr. Jordi Guimera in our lab. The linearized transgenic vector/construct was then used for pronuclear injection in C57BL/6J fertilized zygotes to produce *Shh-Cre-SBE1* transgenic mice. This was done at the Max Planck Institute of Molecular Cell Biology and Genetics (Transgenic Core Facility) in Dresden, Germany. The corresponding offspring was first screened for carrying the *Shh-Cre-SBE1* transgene by genomic PCR, and the PCR-positive founders were subsequently transferred to the HMGU in Munich and back-crossed to C57BL/6J mice. After verification of a successful germ-line

transmission of the transgene by the transgenic founders, breeding pairs with these founders and C57BL/6J mice were established. The offspring of these breeding pairs was then crossed to *ROSA beta geo26 (ROSA26)* reporter mice (Soriano, 1999), which harbour a stop codon flanked by *loxP* sites upstream of a *lacZ* reporter gene, under the control of the *Rosa26* promoter/locus. Expression of the Cre recombinase in the *Shh-Cre-SBE1* transgenic mice will excise the stop codon in front of the *lacZ* reporter gene, such that the *Rosa26* locus/promoter drives the expression of the *lacZ* reporter in all cells also expressing the Cre recombinase and their progeny, which will inherit the recombined *Rosa26* locus. Thereby, it is possible to determine the spatiotemporal origin of all cells that will activate Cre expression during the time period in which the *SBE1*-regulated *Shh* minimal promoter is active in the developing mouse embryo, and the fate of their offspring.

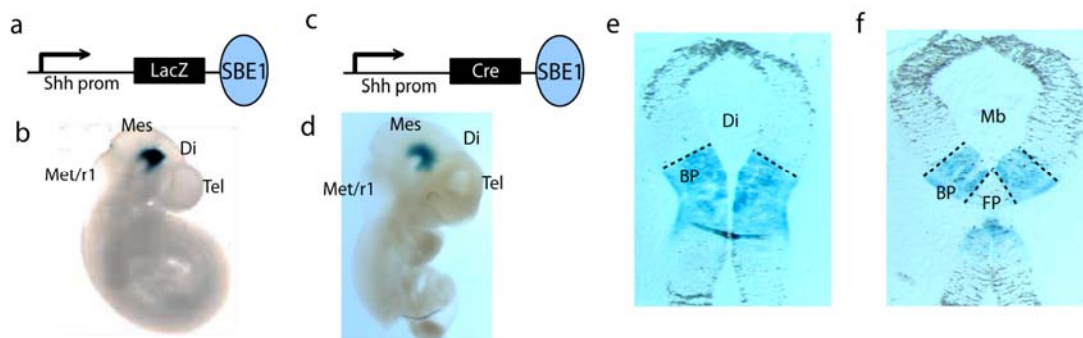


Figure 35 *Shh-Cre-SBE1* transgenic construct and beta-Gal expression pattern after *Shh-Cre-SBE1*-mediated recombination of the R26R reporter in transgenic embryos/mice. (a-b) Reporter construct used by (Epstein et al., 1999) consisting of a *Shh* minimal promoter, a *lacZ* reporter gene and the *SBE1* enhancer (a), to map the specific beta-Gal expression in the caudal diencephalon and rostral midbrain of the corresponding transgenic mouse embryos. (b). (c) *Shh-Cre-SBE1* construct generated by Dr. J.Guimera where the *LacZ* reporter gene was replaced by the *Cre* recombinase. (d) A representative E12.5 embryo derived from a *Shh-Cre-SBE1* x R26R intercross, showing a beta-Gal reporter expression pattern similar to the beta-Gal expression of *Shh-lacZ-SBE1* transgenic reporter mice shown in (b). (e,f) Coronal sections of such a *Shh-Cre-SBE1* x R26R transgenic mouse embryo at E12.5 revealed that beta-Gal activity is restricted to the FP and BP in the diencephalon (e) and only detected in the BP (sparing the FP) of the midbrain (f). Abbreviations: BP, basal plate; Di, diencephalon; Fb, forebrain; FP, floor plate; Hb, hindbrain; Mb, midbrain; Mes, mesencephalon; Met metencephalon; r1, rhombomere 1; Tel, telencephalon.

A total of 25 transgenic founder mice (11 males and 14 females) were obtained from the pronuclear injections at MPI of CBG in Dresden, Germany. Of these 25 founders, at least 4 founders transmitted the transgene through the germline. Breeding pairs with C57BL/6J females/males were set up with the four of the germline-transmitting founders, and all of their offspring was screened for correct/desired expression of the *lacZ* gene (in the *R26R* locus) after *Shh-Cre-SBE1*-mediated recombination in the rostral midbrain/caudal diencephalon.

The initial screens revealed that some transgenic E10.5 embryos derived from Founder male F412 showed beta-Gal expression in the caudal diencephalon and rostral midbrain as reported in (Epstein et al., 1999) (Fig. 35d), but other E10.5 embryos derived from the same male also showed beta-Galactosidase expression in other regions of the embryo such as midbrain, hindbrain, spinal cord or ubiquitous in the entire embryo (Fig. 36), thus suggesting that the *Shh-Cre-SBE1* transgene integrated at several sites within the genome. The *Shh-Cre-SBE1* transgene could also have come under the influence of another and stronger promoter or regulatory element that drives Cre expression to other than the desired sites in the rostral midbrain/caudal diencephalon. Nevertheless, this founder (F412) was subsequently used for the establishment of the *Shh-Cre-SBE1* transgenic mouse line by consecutive breedings of his offspring to C57BL/6J mice, as most of the embryos from F412 gave excluded expression in the caudal diencephalon and rostral midbrain (Fig. 35d). It was hoped that repeated breeding (backcrosses) to C57BL/6J mice might ‘dilute’ out the different copies/integration sites of the *Shh-Cre-SBE1* transgene in this founder to finally obtain a more or less “pure” transgenic mouse line in which the Cre-recombinase is expressed only in the rostral midbrain and caudal diencephalon. A genealogical tree showed the derivative offsprings from the founder 412 (Fig. 37). To genotype the *Shh-Cre-SBE1* transgenic mice, a primer pair was used where the forward primer is located within the Cre recombinase CDS and the reverse primer is located within the *SBE1* sequence, thus allowing for a transgene-specific amplification product (Table 7) of approximately 950 bp (Fig. 38).

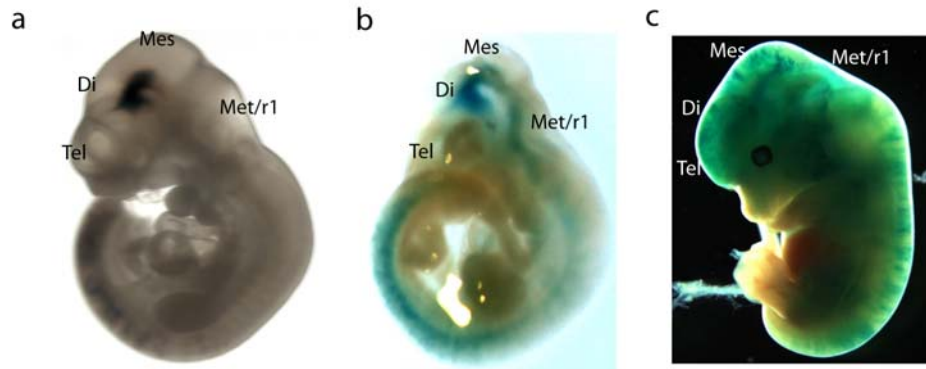


Figure 36. The offspring from *Shh-Cre-SBE1* transgenic founder male F412 shows both specific and ectopic beta-Gal expression patterns. (a) “Specific” beta-Gal expression after Cre-mediated recombination of the *R26R* locus was detected in the caudal diencephalon and rostral midbrain of this transgenic embryo. Small beta-Gal+ patches were also detected in the caudal spinal cord in this case. (b) Expression throughout the caudal diencephalon, ventral midbrain, ventral hindbrain and ventral spinal cord, thus recapitulating the *Shh* expression pattern in the entire mouse embryo at this stage. (c) A “completely ectopic” and patchy beta-Gal expression was found throughout this transgenic E12.5 embryo, representing rare cases of the screening.

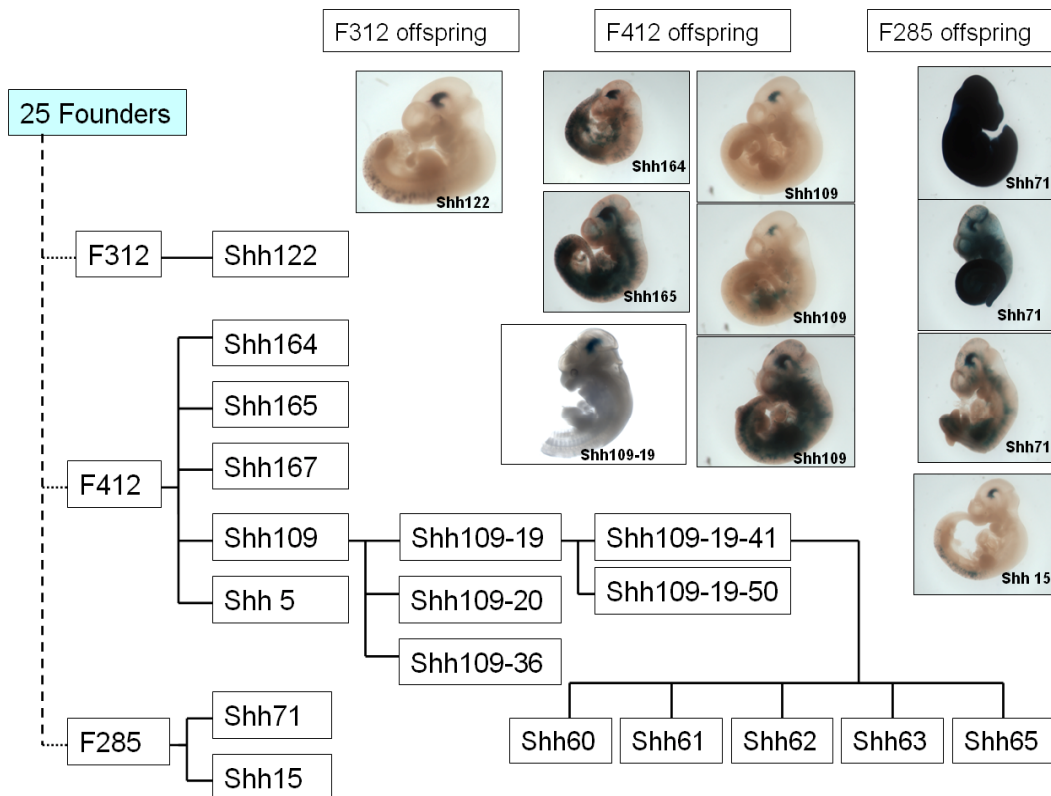


Figure 37. Genealogy tree showed the offsprings from three of the founders. Founder 412 (male) was used for subsequent establishment of the *Shh-Cre-SBE1* transgenic mouse line by consecutive breedings of his offspring to C57BL/6J mice, as most of the embryos from F412 gave excluded expression in the caudal diencephalon and rostral midbrain.

Table 7. Primer pairs and PCR conditions used to genotype *Shh-Cre-SBE1* transgenic mice.

Primer Name	Primer Sequence 5'-3'	PCR condition
Cre-SBE1-F	atgcaagctggtggctggac	94 °C 4 min, (94 °C 30 s, 60 °C 30 s, 65 °C 45 s, 72 °C 2 min, repeat 35 cycles) 72 °C 10 min.
Cre-SBE1-R	gccccttgactaccgctttac	

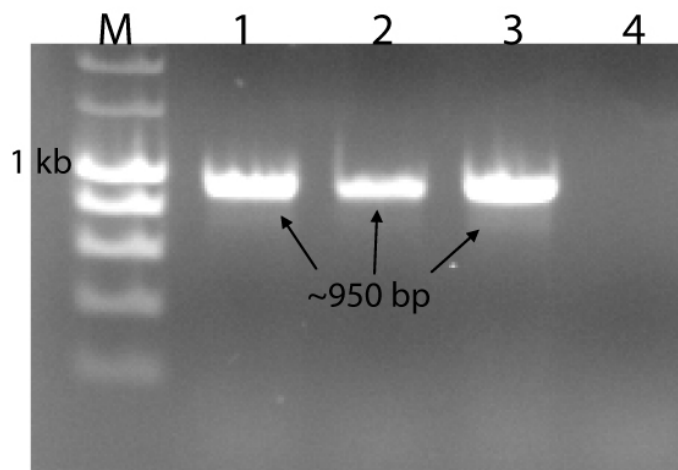


Figure 38 Genotyping PCR of *Shh-Cre-SBE1* transgenic mice. After PCR amplification of genomic DNA from *Shh-Cre-SBE1* transgenic offspring of founder F412 using the primers shown in Table 7, a positive amplification product of approximately 950 bp was obtained in 3 cases (lane 1-3), indicating that these mice (lane 1-3) carry the *Shh-Cre-SBE1* transgene. Lane 4 does not contain a PCR product (950 bp), indicating a negative transgene. M = marker.

4.0 Discussion

Here, I first showed that *in silico* prediction of several miRNAs supposedly targeting mRNAs involved in MHB or vMH neuron development (Table 2) could only be validated on a biological (cellular and molecular) level for a small subset of these miRNAs including *miR-709*, *miR-342-5p* and *miR-221* (predicted and validated to target the *Wnt1-3'UTR*), *miR-712* and *miR-714* (predicted and validated to target the *Wnt5b*- and *Lef1 3'UTR*, respectively). This approach was therefore not very useful to determine novel candidate miRNAs that might be involved in MHB and vMH neuron development. I therefore used another, experimental approach *in vitro* by profiling the expression of miRNAs during the differentiation of pluripotent mESCs into vMH neurons. This approach rendered one particular miRNA, *miR-125b*, that is expressed predominantly in the vMH region (particularly in the BP of the mid- and hindbrain) of the developing brain of the murine. From this particular *miR-125b* expression pattern in the developing vMH I deduced that this miRNA might be involved in the development of BP progenitors and of Phox2b⁺/Isl1⁺ postmitotic OM/TN neurons. In fact, I subsequently demonstrated using primary vMH cultures *in vitro*, that overexpression or knock-down of *miR-125b* in these cultures affected the numbers of Phox2b⁺/Isl1⁺ OM/TN neurons, the proliferation of Nkx6-1⁺ BP progenitors and the survival of vMH cells in these cultures. Finally, I showed the successful establishment and initial screening of a novel Cre-recombinase-expressing mouse, the *Shh-Cre-SBE1* transgenic mouse line.

4.1 Prediction of miRNAs with bioinformatics tools is still not a very reliable method to detect novel miRNAs and their functional interactions with target mRNAs

Determination of miRNA targets has been a major challenge despite the increasing important roles of miRNAs in various organisms such as plants and animals. Similarity-based approaches have higher performance in plant because miRNA:mRNA sequences are near perfect complementary. However, such approaches are not

appropriate for animal genomes because of the imperfect nature of the miRNA:mRNA interaction. Ago HITS-CLIP was developed recently to simultaneously identify Ago-bound miRNAs and the nearby mRNA sites with an anti-Ago antibody, thus could definitely distinguish direct from indirect miRNA-mRNA interactions (Liu and Kohane, 2009). However, the difficulty in identifying miRNA targets by experimental approaches has led to an enormous amount of available computational predictions for miRNA targets.

To date, various methods for *in silico* miRNA identification have been proposed to facilitate miRNA discovery, however the drawback of these current computational prediction methods is that they are based upon limited published biological data (if so), and so may not faithfully reflect the complexity of an actual biological situation. As such they are unlikely to uncover the unreported, novel miRNAs from the biological sample. Moreover, the common algorithms do not take into account the reported expression pattern of the miRNAs and of its predicted target genes. For instance, the negligence of co-expression information of miRNAs and their targeted mRNA(s) will include functionally irrelevant predictions in the algorithms, and thus lower the reliability of the computational prediction methods. An additional concern is that many computational predictions have used cell-based assays in which the miRNA and its putative targets are over-expressed to validate the mRNA targets. Although these “artificial” assays may aid in the validation of the predictions, they are unlikely to reflect conditions under which endogenous miRNAs function *in vivo*, and therefore might additionally skew predictions further away from *bona fide* mRNA targets.

It is worth noting that the computational algorithms used in this work are built on the general assumption that miRNAs bind to complementary sequences in the 3'UTRs of their target mRNAs (Bartel, 2004) and thereby induce mRNA degradation and/or repress protein translation. However, it was demonstrated that apart from the 3'UTR, miRNAs can also bind to the 5'UTR (Lytle et al., 2007) or within the CDS (protein coding region) (Duursma et al., 2008) of a mRNA, and repress this mRNA as efficiently as if the miRNA would bind to the 3'UTR. In my work, I validated only those miRNAs and their binding sites that were predicted within the 3'UTR, although some of my experiments showed that the miRNA seems indeed to target its predicted mRNA, the predicted binding sites could not be validated, or in even other cases, I

observed “off target” effects of a miRNA that might be mediated by sequences other than the predicted mRNA 3’UTR.

Knowing the drawbacks of each individual prediction programme/tool, we attempted to overcome some of their weaknesses by combining five different prediction algorithms. The idea behind this approach was that, by using the miRBase algorithm prediction tool to generate a list of potential candidates, only those miRNAs that were independently predicted by at least three different algorithms to target one and the same mRNA would be in fact “true” candidates to target this mRNA. However, and as my subsequent validation analyses showed, even this approach rendered too many “false-positive” miRNAs (miRNAs that were predicted to target a particular mRNA but could not be confirmed/validated on the experimental level) to be suitable for further applications. On the other hand, combining different prediction methods may not single out certain miRNAs that are correctly predicted by just one of the five algorithms, as it was already shown in the literature that different algorithms provide different results, and the degree of overlap between the different predictions (targets) is sometimes very poor or even absent (Sethupathy et al., 2006).

In my case, out of the 33 initially predicted miRNAs, only five showed distinct expression patterns in the CNS or liver, although expression was observed also in other regions/tissues of the developing mouse embryo (Fig. 8 & Fig. 10). Of these five distinct expression patterns, *miR-144* expression was observed in the liver, which was rather unexpected as the initial bioinformatics searches was focussed on genes involved in the development of the MHB GRN, mdDA neurons or other vMH neurons and in Parkinson’s disease (Table 2). Indeed, it has been shown that a single miRNA could potentially bind to tens, if not hundreds, of target mRNAs. In my miRNA ISH screens, some miRNAs expressions were not discernable in the developing embryo, thus making the interpretation difficult. These ‘not detectable’ miRNAs might be expressed in a low level to be detectable via ISH method or possibly these miRNAs are expressed in a tightly regulated spatio-temporal manner, and therefore was not observed/appeared in my screens. As for the ubiquitously expressed miRNAs which I observed in my screens, these miRNAs might be involved in regulating the constitutively expressed housekeeping genes. It is noteworthy that certain miRNAs have higher melting

temperature due to their GC-riched sequences, thus more stringent washing procedures during ISH are required to avoid ‘unspecific’ binding of miRNAs on the tissue samples.

The subsequent validation of these miRNAs and their predicted mRNA targets (Table 3) by functional analyses (luciferase sensor assays/site-directed mutagenesis of predicted binding sites) revealed that of these 33 miRNAs only five could be functionally validated and are thus in fact correctly predicted. In summary, only one miRNA (*miR-709*) of the originally predicted 33 miRNAs passed my initially postulated “necessary” three criteria: (1) the expression of the miRNA must be detectable in MHB tissues and/or in mdDA or other vMH neurons of the developing mouse embryo; (2) the miRNA must downregulate the mRNA/protein expression of its predicted target as assessed in luciferase sensor assays; and (3) site-directed mutagenesis of the predicted binding sites (seed sequence) of the miRNA in its target 3’UTR must abolish the miRNA-mediated downregulation of this target. The only one experimentally validated *miR-709* was correctly predicted and biologically relevant in the context of my studies, and thus also reflecting the still very high “false-positive” prediction rate of current bioinformatics prediction tools.

Although *miR-709* fulfilled all three criteria mentioned above, *miR-709* did not proceed for *in vivo* experiments due to several reasons/limitations. The next step in an experimental validation of *miR-709* to define its biological function/relevance for the regulation of *Wnt1* expression *in vivo* would be employing miRNA ablation (antagomir of *miR-709*) or overexpression (*pre-miR-709*) in the MHR of the developing mouse embryo (such as *in utero* electroporation). However, it is technically challenging to conduct the experiments as the formation of MHB occurs in the early developmental stage. Moreover, generation of conditional mutant for *miR-709* in the MHR/MHB would be an alternative. For instance, *En*^{+/*Cre*} deleter mice crossed with *miR-709*^{flox/flox} to obtain *En*^{+/*Cre*; *miR-709*^{flox/flox}} mice will allow the analysis of *miR-709* functions in the development of MHR including the MHB, mdDA and vMH neurons. Alternatively, *Wnt1*^{+/*Cre*} deleter mice cross with *miR-709*^{flox/flox} to obtain *Wnt1*^{+/*Cre*; *miR-709*^{flox/flox}} mice will allow the analysis of *miR-709* in the *Wnt1*-expressing domain particularly in the MHB. However, generating the conditional mutant mice would be very time consuming and these *in vivo* experiments are particularly technically challenging, difficult to conduct and to interpret because they often lead to severe phenotypes, and in some

cases, to early embryonic lethality. Therefore, a different experimental set-up to find miRNAs involved in MHR/MHB, mdDA and vMH neurons is required.

4.2 A conserved primate “miRNA recognition motif” was not validated on a functional level for the mouse

On a different note, I also tested the hypothesis of a conserved “miRNA recognition motif” within the 3'UTRs of primate but not other vertebrate mRNAs postulated by Dr. V. Stümpflen's group at the IBIS/HMGU. This motif was originally identified as a highly conserved sequence motif/element within the 3'UTRs of the majority of the primate mRNAs (10 %), which is however not found in the mRNA 3'UTRs of all other vertebrate/invertebrate species. This finding suggested that this sequence motif/element might be related to the evolution of primate species and might play a fundamental role in the posttranscriptional control of gene expression (mRNA stability, translation, degradation or even miRNA regulation) in primates. Surprisingly, and in contrast to all other species, this sequence element/motif was also found within the mouse *Wnt1* 3'UTR. Therefore, and in collaboration with V. Stümpflen's group, I tested the hypothesis that this sequence element/motif might be involved in the regulation of the murine *Wnt1* mRNA/3'UTR by miRNAs. However, functional analyses with luciferase sensor assays and site-directed mutagenesis of this sequence element/motif did not reveal any changes in luciferase expression from the mutated sensor vectors, thus arguing against any involvement of this sequence element/motif in the regulation of mouse *Wnt1* 3'UTR-mediated posttranscriptional regulation of gene expression, including regulation of the stability, degradation, translation of the luciferase-*Wnt1* 3'UTR fusion mRNA by endogenous factors or exogenous (transfected) *miR-709*, which was previously shown to target the *Wnt1* 3'UTR. It should be noted that these experiments were performed in the human HEK-293 cell line, such that any additional “primate” factors/machinery that might be necessary for the “function” of the ‘miRNA recognition’ motif/miRNA ‘target enhancer signal’ sequence element/motif should have been present in these cells.

4.3 NGS expression profiling of miRNAs during *in vitro* differentiation of mESCs into vMH neurons is a more reliable method for the identification and functional validation of miRNAs

In view of my previous results and the failure to find a miRNA with a specific expression pattern in the MHR that targets one of the key molecules involved in the development of this region and of mdDA neurons in a detectable margin, I turned to a different approach based on the profiling of miRNAs expressed at different steps of the differentiation of pluripotent mESCs into vMH neurons according to the protocol by (Lee et al., 2000). The mESC differentiation protocol according to (Lee et al., 2000) proceeds along 5 steps that correspond to distinct stages of embryogenesis, such as step1/stage 1: undifferentiated/pluripotent mESCs (inner cell mass of the blastocyst), step2/stage2: embryoid body (EB) formation (gastrulating embryo), step3/stage3: selection of nestin-positive vMH neural precursor cells (neural induction), step4/stage4: expansion of Nestin⁺ vMH neural precursor cells (neurulation), and step5/stage5: differentiation of these neural precursors into vMH neurons (generation of the different vMH neuronal subtypes). This approach was chosen because of 1) Easy/good accessibility to material (in contrast to embryos which could be contaminated with other tissues, loss of tissue, etc) and 2) defined timing of the developmental stage/all cells should be in more or less the same “stage” (in contrast to embryos that are not synchronized = one embryo is in a more advanced stage than another, it is impossible to isolate cells of just one defined developmental stage), 3) desired “material” (cells) can be expanded according to needs (in contrast to embryos, where I have to dissect primary material and pool it with all previously mentioned caveats (other tissues, different timing)). To profile the miRNAs (small RNAs) expressed during selected stages/steps (namely stage 1, 3 and 5 as “corner stones” during the differentiation procedure) of this differentiation protocol, I chose the next generation sequencing (NGS, also known as “deep sequencing”) technique because of its superiority to profile miRNAs over microarray and RT-qPCR. NGS is an array of high throughput tool compared to RT-qPCR. Compared to microarray, NGS costs lower, permits unlimited quantitative within a sample and allowing comprehensive interrogation of genomes without prior knowledge of sequence or annotation (Hurd and Nelson, 2009).

The sequence reads of this NGS approach revealed that miRNAs such as the *miR-290* family (in this specific case: *miR-291a/b*, *miR-292*, *miR-293*, *miR-294* and *miR-295*) were abundantly expressed in the undifferentiated/pluripotent mESCs, whereas their expression was markedly reduced in the differentiated vMH neurons. This miRNA family/cluster was in fact already described as an ESC-enriched miRNA playing a fundamental role in the control of proliferation/pluripotency and cell cycle exit of these cells and thus belonging to the so-called “ESC-specific cell cycle-regulating (ESCC)” miRNAs (Chen et al., 2007; Wang et al., 2008). The *miR-290* cluster (comprising *miR-290*, *miR-291a/b*, *miR-292*, *miR-293*, *miR-294* and *miR-295*) is co-transcribed as polycistronic primary transcripts from a common promoter (Suh et al., 2004), and it was therefore not surprising that most of its members were up-regulated in my undifferentiated mESC samples relative to the differentiated vMH neurons. However, I also detected differences in the abundance of individual members. For instance, a total of 13,826 and 152,066 reads for *miR-294* and *miR-295*, respectively, were detected in the pluripotent/undifferentiated mESCs, whereas only 38 and 110 reads of these miRNAs, respectively, were detected in the differentiated vMH neurons. On the other hand, 22,325 reads for *miR-292* were detected in the pluripotent/undifferentiated mESCs, whereas only 100 reads for *miR-292* were detected in the differentiated vMH neurons. Although it is not clear why co-transcribed miRNAs gave different read numbers in my experiments, however it was reported that like other RNAs, miRNA expression could potentially be controlled at the post-transcriptional level (Pillai, 2005; Obernosterer et al., 2006) and/or the stability of different half-lives of the mature miRNAs after processing within the cells.

Conversely, members of the *let-7* miRNA family (in this specific case *let7a-g*, *let7i*) and *miR-9* were particularly enriched (more than 200-fold) in my differentiated vMH neuron samples as compared to the undifferentiated/pluripotent mESCs. Indeed, *let-7* miRNAs have already been widely implicated in the induction of cell differentiation including neuronal differentiation by negatively regulating stem cell self renewal in a variety of tissues (Reinhart et al., 2000; Wang et al., 2009). Interestingly, the expression of *miR-9* was already upregulated more than 10-fold in the Nestin⁺ neural precursors (stage 3) (17,046 reads) as compared to the undifferentiated mESCs (stage 1) (1436 reads), in contrast to *let7* miRNAs, which were only abundant in

differentiated vMH neurons. It has already been shown that *mir-9* is upregulated during neural differentiation of mESCs (Krichevsky et al., 2006) and of adult neural stem cells (Zhao et al., 2009), and has therefore been implicated in the control of early neurogenic processes, including MHR patterning, (Leucht et al., 2008). Altogether, the enrichment of the *miR-290* family in my undifferentiated mESC samples and of the *let-7* family and *miR-9* in my differentiated vMH neuron samples confirmed the successful differentiation of mESCs into postmitotic neurons and the validity of my NGS approach to profile miRNA expression in my cultures.

To search for potential candidate miRNAs involved in MHB and vMH neuron development, I next determined the miRNAs that were mostly enriched in the differentiated vMH neurons as compared to the undifferentiated, pluripotent mESCs and the neural precursor cells. I found that *miR-125b* was the next most enriched/abundantly expressed miRNA in vMH neurons (after the *let7* family and *miR-9*), followed by *miR-181a*, *miR-206*, *miR-99a* and *miR-135a*, *miR-181b*, *miR-100*, *miR-137*, *miR-383* and *miR-153*. Notably, most of these “vMH neuron-enriched” miRNAs have already been reported to be associated with neuronal differentiation, maturation or function, as discussed below.

MiR-125b is an evolutionary conserved miRNA and is enriched in the brain of zebrafish, mice and humans (Ason et al., 2006; Le et al., 2009a), which is upregulated during neuronal differentiation of a variety of neural cells in vitro (Boissart et al., 2012), but *miR-125b* is also expressed in other non-neural tissues (Mizuno et al., 2008; Zhang et al., 2011). Lodish and colleagues demonstrated that *miR-125b* is upregulated during neuronal differentiation of a human neuroblastoma cell line (SH-SY5Y) and of human neural progenitor cells (ReNcell VM cells) (Le et al., 2009b). Moreover, overexpression of *miR-125b* in these cells promotes their neuronal differentiation and neurite outgrowth (Le et al., 2009b). *MiR-125b* is also upregulated during neuronal differentiation of P19 embryonal carcinoma cells and mESCs (Rybak et al., 2008), and more recently it was shown that *miR-125b* is also upregulated during the commitment of hESCs to neural precursors (Boissart et al., 2012). Overexpression of *miR-125b* in hESCs promoted their neural conversion by repressing the expression of the pluripotency factor and downstream effector of the Tgfbeta/BMP pathways, SMAD4, in these cells, whereas knockdown of *miR-125b* in hESCs had the opposite effect (Boissart et al., 2012).

Notably, *miR-125b* is the mammalian orthologue of *C. elegans lin-4* that targets the 3'UTR of the RNA-binding protein and pluripotency factor *lin28* mRNA (Wu and Belasco, 2005; Rybak et al., 2008). Upregulation of *miR-125b* during neuronal differentiation of P19 embryonal carcinoma cells and mESCs in fact downregulates the expression of *lin28* in these cells, thereby enabling the processing of *pre-let7* pre-miRNA into the mature *let7* miRNA that is otherwise inhibited by binding of *lin28* to the *pre-let7* stem loop (Wu and Belasco, 2005; Rybak et al., 2008). These findings together indicate that *miR-125b* plays a central role in promoting the commitment and differentiation of a neural progenitor/precursor cell to the neuronal fate. However, *miR-125b* is still highly expressed in the postnatal and adult brain (Edbauer et al., 2010), and Sheng and colleagues indeed revealed that *miR-125b* is associated with the synaptic RNA-binding protein FMRP, and is involved in synaptogenesis and the regulation of synaptic structure and function by targeting, among others, the NMDA receptor subunit NR2A (Edbauer et al., 2010). The human *miR-125b-2* gene is located on the human chromosome 21, and this miRNA is indeed overexpressed in fetal brains and hearts of individuals with Down syndrome (Trisomy 21) (Kuhn et al., 2008). By contrast, *miR-125b* was found to be downregulated in human medulloblastoma cells whereas it is upregulated during the neuronal differentiation of cerebellar granule cell precursors (GCPs) (Ferretti et al., 2008). *MiR-125b* targets the G-protein coupled receptor Smoothed (Smo) in this context, which transduces the Hedgehog signal during cerebellar development thus promoting the proliferation of GCPs. Downregulation of *miR-125b* in medulloblastoma therefore leads to high levels of Shh signaling and proliferation of these cells (Ferretti et al., 2008).

MiR-181a is highly enriched in synapses of the nucleus accumbens (NAc); a brain structure involved in motivational and rewarding behaviours and heavily innervated by dopaminergic neurons, and is induced in the rat NAc under chronic cocaine administration (Chandrasekar and Dreyer, 2011) and upon dopaminergic signaling in primary cortical/hippocampal neurons (Saba et al., 2012). In the latter context, *miR-181a* was shown to downregulate the expression of the glutamate AMPA receptor subunit GluA2 on the surface of hippocampal neurons, and to reduce the formation of synaptic spines as well as the frequency of mEPSCs (miniature excitatory postsynaptic currents) in these neurons (Saba et al., 2012).

MiR-206 is strongly induced in skeletal muscles of an Amyotrophic lateral sclerosis (ALS) mouse model and was shown to be required for the efficient regeneration of neuromuscular synapses after acute nerve injury by targeting histone deacetylase 4 (HDAC4) and thereby activating fibroblast growth factor signalling in denervated muscles (Williams et al., 2009). *MiR-206* was also shown to be upregulated during neuronal differentiation of human mesenchymal stem cells (derived from adult bone marrow) and to suppress the synthesis of the neurotransmitter substance P in these mesenchymal stem cell-derived neurons (Chang et al., 2011).

The human *miR-99a* gene is located on the human chromosome 21 and was in fact found to be overexpressed in the fetal brain and hearts of patients with Down syndrome (Trisomy 21) (Kuhn et al., 2008).

MiR-135a is enriched in glial cells and is downregulated in malignant glioma (Wu et al., 2011). Notably, it was shown that *miR-135a* selectively eliminates malignant glioma cells by inducing their apoptotic cell death through regulation of the Stat (signal transducer and activator of transcription) and Smad/Bmp signaling pathways in these cells (Wu et al., 2011).

MiR-137 is another brain-enriched miRNA that regulates neuronal maturation (dendritic morphogenesis, synaptic spine development) by targeting the ubiquitin ligase Mindbomb 1 (Smrt et al., 2010). Furthermore, *miR-137* was shown to be upregulated during neuronal differentiation of mesenchymal stem cells (Chang et al., 2011) and adult mouse neural stem cells as well as human glioblastoma-derived stem cells, and to induce the cell cycle arrest if overexpressed in the latter cells (Silber et al., 2008). Interestingly, it was also found that *miR-137* expression levels are significantly downregulated in the frontal cortex of a subgroup of sporadic Alzheimer Disease (AD) patients with elevated ceramide levels, and it was subsequently shown that *miR-137* indeed targets the rate-limiting enzyme in ceramide synthesis (Geekiyana and Chan, 2011). These findings suggest that the loss of *miR-137* expression in the brain increases the susceptibility to develop AD.

Lastly, *miR-100* is another miRNA that was enriched in neuronal progenitors after differentiation of human mesenchymal stem cells (Chang et al., 2011). However, other (functional data) are not available in the literature neither for *miR-100* nor for the

other two miRNAs found among the top 10 upregulated candidates in the differentiated vMH neurons (final differentiation stage), *miR-181b* and *miR-383*

4.3.1 *MiR-125b* is expressed in a very specific spatiotemporal pattern in the developing murine MHR that correlates with the expression of its direct targets *Phox2b* and *Sim1*

The NGS expression profiling revealed that apart from *let7* and *miR-9*, *miR-125b* and *miR-181a* were the third and fourth, respectively, most enriched/abundant miRNAs in differentiated vMH neurons as compared to the undifferentiated mESCs, whereas all other (following) miRNAs showed a significant drop of read numbers in the differentiated vs. the undifferentiated stage (Fig. 21). Due to their widespread or almost ubiquitous expression in the developing murine CNS (eg see Fig. 7) and their already well known and characterized functions in CNS development and neuronal differentiation (Bak et al., 2008; Leucht et al., 2008), I discarded the *let7* family and *miR-9* from further analyses/experiments. However, the previously mentioned literature already suggested a fundamental but not fully characterized role of *miR-125b* and *miR-181a* in neural development and homeostasis, and a preliminary search for predicted targets of these two (*miR-125b* and *miR-181a*) and of the other eight miRNAs indicated that among these predicted targets are indeed some with a potential (known) function in vMH neuron development (see below). Therefore, and to narrow down the selection of miRNA(s) for further functional studies *in vitro* and/or *in vivo*, I applied again my three main criteria already established for the validation of predicted miRNAs (see sections 3.1 & 3.2.3 in the Results and 4.1 in the Discussion) and focuses in particular on *miR-125b* and *miR-181a*: 1) the expression of the miRNA must be detectable in MHB tissues and/or in mesDA or other vMH neurons of the developing mouse embryo; (2) the miRNA must downregulate the mRNA/protein expression of its predicted target as assessed in luciferase sensor assays (see section 3.2.5); and (3) site-directed mutagenesis of the predicted binding sites (seed sequence) of the miRNA in its target 3'UTR must abolish the miRNA-mediated downregulation of this target (see section 3.2.5).

While I could not detect a signal for *miR-181a* using both DIG and radioactive LNA-based, *miR-125b* exhibited a prominent and spatiotemporally distinct expression in the MHR of the developing mouse embryo. For this reason, *miR-181a* was discarded for further analyses. Initially, at midgestational stages of E10.5, *miR-125b* was predominantly expressed throughout the neuroepithelium in the ventral MHR, including progenitor cells (higher expression as shown by DIG-labeled ISH in Fig. 22) and postmitotic neurons (lower expression as shown by radioactive ISH in Fig. 23a). However, at later stages (E12.5), *miR-125b* expression is mostly restricted to the VZ/SVZ in the mid/hindbrain BP. Notably, *miR-125b* expression strongly correlated with the expression of two of its predicted (and confirmed, see below) targets, namely *Phox2b* and *Sim1*, in the ventral MHR of the developing mouse embryo. While *miR-125b* initially overlapped with the expression of these two genes in BP progenitors (located in the VZ/SVZ), as is the case for *Sim1*, and postmitotic OM/TN neurons (located in the MZ), as is the case for *Phox2b*, it later refined to a continued co-expression of *miR-125b* and *Sim1* in BP progenitors but an apparently mutually exclusive expression of *miR-125b* and *Phox2b* in postmitotic OM/TN neurons within the MZ of the MH BP. Subsequent luciferase sensor and site-directed mutagenesis assays indeed confirmed that the *Sim1* and *Phox2b* 3'UTRs, each containing one highly conserved binding site (seed sequence) for *miR-125b* across several mammalian species, are directly targeted by *miR-125b*.

Altogether, these data indicated that *miR-125b* and *Sim1/Phox2b* are initially co-expressed in vMH (BP) progenitors but later, and probably due to the negative posttranscriptional regulation exerted by *miR-125b*, at least in the case of *Phox2b* mRNAs, segregate to distinct domains within the vMHR. The subsequent expression segregation between *miR-125b* and *Sim1* was not observed, such as occurs at E12.5 between *miR-125b* and *Phox2b*, might be due to the regulation of *miR-125b* on *Sim1* occurs on protein translational level but not mRNA expression level, as I have shown *Sim1* mRNA expression level did not change after overexpression/knockdown of *miR-125b* in the primary cultures as revealed by RT-qPCR (Fig. 31) but *Sim1*-3'UTR-mediated luciferase activity was reduced (Fig. 26 & Fig. 27). Moreover, radioactive ISH does not provide cellular resolution (due to scattering of the silver grains), therefore it is difficult to detect single cells expressing *miR-125b* in which *Sim1* might be

downregulated. Due to the lack of working *Sim1* antibody, the direct correlation of *miR-125b* and *Sim1* could not be elucidated.

Therefore, I concluded that apart from its known role/function in promoting generic neuronal differentiation of BP progenitors in the murine MHR into vMH neurons and reported target genes in relation to cell cycle/apoptosis context/pathways such as p53 in promoting both apoptosis and proliferation (Le et al., 2009b; Le et al., 2011), p53-apoptosis mediators *Bak1*, *Igfbp3*, *Itch*, *Puma*, *Prkra*, *Tp53inp1*, *Tp53*, *Zac1* (Le et al., 2011), cell cycle regulator such as *E2F3* (Huang et al., 2010), cyclin *C*, *Cdc25c*, *Cdkn2c* and so on in p53 network (Le et al., 2011), Shh receptor *Smo* (Ferretti et al., 2008), *lin28* (Sempere et al., 2004; Rybak et al., 2008) and NMDA receptor subunit *NR2A* (Edbauer et al., 2010), *miR-125b* might also play a more specific role in the generation and/or selection of distinct vMH neuronal cell fates, such as OM/TN neurons, RN neurons and other neuronal populations derived from vMH BP progenitors (Puelles, 2007), and/or in the repression of alternative neuronal cell fates (such as Th^+ mdDA neurons arising from the midbrain FP or GABAergic neurons arising from the midbrain AP (Lin et al., 2009). To assess whether *miR-125b* exerts such a potential specific function of in vMH neurogenesis, I used a primary vMH cell culture-based *in vitro* assay described in more detail below.

4.3.2. Analyses of *miR-125b* function in mouse vMH neural development

To study the function of *miR-125b* in the developing ventral midbrain/rostral hindbrain, I performed gain-of-function experiments by overexpressing *miR-125b* and loss-of-function experiments by knocking down *miR-125b* expression with a so-called “sponge” vector in primary vMH cell cultures. To this end, I used lentiviruses encoding either the *pre-mmu-miR-125b* sequence (*miR-125b OE* lentivirus) or a concatemeric sequence (5 sequence repeats) within the mCherry reporter 3’UTR that is not fully complementary to the mature *miR-125b* sequence and contains two central mismatches, thereby leading to a *miR-125b* bulge formation that prevents the cleavage (degradation) of the sponge RNA by AGO2 (*mir-125b sponge* lentivirus) that were kindly provided by Dr. D. Edbauer (DZNE, Munich). The primary vMH cultures were derived from the ventral MHR at E11.5 and are expected to contain both neural progenitors and

postmitotic neurons that are found at this time-point within this region, including the Sim1⁺ BP progenitors and Phox2b⁺ postmitotic OM/TN precursors/neurons in which *miR-125b* is initially expressed. In fact, qPCR to detect *miR-125b* expression in these primary cultures revealed *miR-125b* indeed expressed in these cultures. Therefore, these primary vMH cultures are well-suited to study the effects of both *miR-125b* overexpression and knock-down on vMH neuron development. It should be noted that due to the heterogeneous neural progenitor composition (comprising FP and BP progenitors from the midbrain and rostral hindbrain that will give rise to different neuronal subtypes) of these primary cultures, the amount of the different neuronal subtypes generated in these cultures reflects their proportion *in vivo*, i.e. OM/TN neurons will only make up a minority (approx. 2 %) of all neurons in the cultures as compared to other (larger) neuronal populations such as mdDA, RN or GABAergic neurons.

Initially, I focussed my analyses on the generation of Phox2b⁺ OM/TN neurons in the primary vMH cultures as *Phox2b* is a confirmed target of *miR-125b* and any change in *miR-125b* expression levels is expected to impinge on the expression of *Phox2b* in these cultures. Notably, overexpression of *miR-125b* in primary vMH cultures led to a significant 30 % and 16 % reduction of Phox2b⁺ cells that correlated with a similar 35 % and 34% reduction of *Phox2b* mRNA levels in these cultures after 3 and 5 DIV, respectively. This strongly suggests that binding of *miR-125b* to its BS within the *Phox2b* 3'UTR (as previously shown by luciferase sensor assays and confirmed by site-directed mutagenesis of this BS) induces the degradation of *Phox2b* mRNA. However and based on this finding, the loss of Phox2b⁺ cells in the *miR-125b* OE vector/lentivirus-transduced primary vMH cultures might have been due to a loss or downregulation of *Phox2b* expression (on both the mRNA and protein levels) in the corresponding cells (postmitotic OM/TN precursors and mature OM/TN neurons), but not due to the loss of the OM/TN neuronal cells themselves. To assess whether this is the case, I used another independent marker for the postmitotic OM/TN neurons, *Isl1*, which is not predicted as a target of *miR-125b*. The number of Isl1⁺ cells was also significantly reduced by a very similar 32 % and 27% after 3 and 5 DIV, respectively, after *miR-125b* overexpression in the primary vMH cultures, indicating that the loss of Phox2b⁺ cells after *miR-125b* overexpression is in fact due to the loss of the

corresponding postmitotic $Isl1^+$ OM/TN neurons. Remarkably, the opposite effect was noted when *miR-125b* expression was reduced in the primary vMH cells: sponge-mediated knockdown of *miR-125b* in these cultures resulted in a significant 25% increase of $Phox2b^+$ cells and 33% increase of $Isl1^+$ cells in these cultures, albeit only after 5 DIV. One reason for this delayed increase of $Phox2b^+$ and $Isl1^+$ cells might be that knockdown of *miR-125b* in the primary vMH cultures only affects the specification of the $Phox2b^+$ and $Isl1^+$ cell fate in proliferating mesencephalic BP progenitors that still have to differentiate into $Phox2b^+$ and $Isl1^+$ OM/TN neurons. The mature OM/TN neurons already expressing *Phox2b* and *Isl1* are not expected to be affected by the knockdown of *miR-125b* as this miRNA is not expressed anymore in these cells (see Fig. 24). Another reason might be that the sponge-mediated knockdown of *miR-125b* in primary vMH cells only becomes effective after some time/a longer incubation period. In fact and in support of the latter possibility, *Phox2b* mRNA levels were increased by 9% in *miR-125b* sponge lentivirus-transduced primary vMH cells after 3 DIV but reached a significant 77% increase only after 5 DIV. Altogether, these data strongly suggested a function of *miR-125b* in vMH cell fate specification, in particular by regulating the appropriate amount of postmitotic $Phox2b^+/Isl1^+$ OM/TN neuronal progeny generated from vMH BP progenitors expressing this miRNA.

If this were truly the case, it was expected that *miR-125b* overexpression selects another cell fate over the $Phox2b^+/Isl1^+$ OM/TN neuron fate whereas *miR-125b* knockdown selects the $Phox2b^+/Isl1^+$ OM/TN neuron fate over other (possible) vMH neuronal fates. Two very likely candidates for these alternative fate choices were the $Brn3a$ ($Pou4f1$)⁺ RN and the 5-HT ($Sert$)⁺ dorsal raphe serotonergic neuron fates, as OM and RN neurons arise from the same BP progenitor domain in the mesencephalon (Nakatani et al., 2007; Prakash et al., 2009), and TN and dorsal raphe 5-HT neurons arise from the same BP progenitor domain in the rostral metencephalon (r1) (Prakash et al., 2009; Deneris and Wyler, 2012) (NP, personal communication). The postmitotic $Phox2b^+/Isl1^+$ OM/TN neurons are derived from *Phox2a*-expressing BP progenitors in the mes- and metencephalon, respectively, and *Phox2a* is necessary for the generation of these neurons (Pattyn et al., 1997). Although it was suggested that $Brn3a/Pou4f1^+$ RN neurons are derived from the $Sim1^+$ BP progenitors in the ventral midbrain (Nakatani et al., 2010), and dorsal raphe 5-HT/ $Sert^+$ neurons are derived from $Nkx2-2/Nkx2-9^+$ BP

progenitors in the rostral hindbrain (r1) (Deneris and Wyler, 2012), the precise identity of the progenitors of these two vMH neuronal subtypes is still unclear as *Sim1* and *Nkx2-9* LOF data in this context have not been reported so far, and *Nkx2-2* LOF does not affect the generation of 5-HT/Sert⁺ neurons (Deneris and Wyler, 2012). In fact, the loss of *Nkx6-1* in mes-/metencephalic BP progenitors of the *Nkx6-1*^{-/-} mice results in an approx. 70% reduction of Brn3a (Pou4f1)⁺ RN neurons (Prakash et al., 2009) and a loss of dorsal raphe Sert⁺ neurons (NP, personal communication), indicating that although *Nkx6-1* is not expressed in the corresponding postmitotic neurons, it is required in the corresponding progenitors to generate the proper amount of postmitotic progeny. These results therefore also indicate that Brn3a(Pou4f1)⁺ RN neurons and dorsal raphe Sert⁺ neurons both arise from the *Nkx6-1*⁺ BP progenitors in the mes- and metencephalon. As the co-expression on a single-cell level of *Phox2a/b*, *Sim1*, *Nkx6-1* and serotonergic precursor markers has not been assessed so far, in part due to the lack of working antibodies for some of these markers, it might well be that *Phox2b*⁺/*Isl1*⁺ OM/TN neurons, Brn3a⁺ (Pou4f1⁺) RN neurons and dorsal raphe 5-HT⁺/Sert⁺ neurons all arise from *Nkx6-1*⁺ BP progenitors in the ventral MHR. Thus, other mechanisms must be in place to select the corresponding neuronal fate in *Nkx6-1*⁺ BP progenitors, and posttranscriptional regulation of *Phox2b* and *Sim1* expression in at least a subset of these progenitors was/is a very attractive hypothesis.

Therefore and to test this hypothesis, I assessed the numbers of Brn3a⁺ (Pou4f1⁺) RN neurons, 5-HT⁺/Sert⁺ serotonergic neurons but also of Th⁺ mdDA neurons arising from the adjacent FP in the ventral midbrain after overexpression or knockdown of *miR-125b* in my primary cultures. However, these experiments are currently still in progress and therefore a conclusive remarks could not be made at this point.

Based on the previous results, I next determined the effects of *miR-125b* overexpression or knockdown on the numbers and cellular behaviours (proliferation, apoptosis and generation of alternative cell fates) of vMH neural progenitors. The other predicted and confirmed (my own data, see Fig. 26) target of *miR-125b*, *Sim1*, is expressed in mesencephalic BP progenitors (my own data and (Nakatani et al., 2007; Nakatani et al., 2010), suggested that these may be the progenitors of Brn3a (Pou4f1)⁺ RN neurons. Due to the lack of a working *Sim1* antibody, I could only determine the expression levels of *Sim1* mRNA in my control, *miR-125b* OE and *miR-125b* sponge

lentivirus-transduced cultures. However, quantitative PCR revealed that *Sim1* mRNA levels were not affected by the overexpression or knockdown of *miR-125b*. Therefore, I could not use *Sim1* as an appropriate marker for these experiments. However, another TF, namely *Nkx6-1*, is also expressed in mesencephalic/metencephalic BP progenitors and was shown to be required for the proper generation of Brn3a (Pou4f1)⁺ RN neurons (Prakash et al., 2009) and of Sert⁺ dorsal raphe serotonergic neurons (NP, personal communication) by these progenitors, as previously mentioned. Overexpression of *miR-125b* in vMH cells in fact significantly reduced the numbers of Nkx6-1⁺ cells by 24 % at 3 DIV that correlated with a 38% and 37% decrease in *Nkx6-1* mRNA levels after 3 and 5 DIV, respectively. Remarkably, the Nkx6-1⁺ cell numbers and *Nkx6-1* mRNA levels were not changed in these cultures after sponge-mediated knockdown of *miR-125b* neither at 3 nor at 5 DIV, indicating that the effects of *miR-125b* OE on the Nkx6-1⁺ cell numbers and mRNA levels are most likely indirect and not due to a direct downregulation of *Nkx6-1* expression by *miR-125b*.

As *Nkx6-1* is also expressed in postmitotic Isl1⁺ OM/TN neurons and required for the proper positioning/migration and axonal outgrowth of these neurons in the vMH region (Prakash et al., 2009), it remained unclear from these data whether the reduction of Nkx6-1⁺ cell numbers and mRNA levels truly reflected a reduction of BP progenitors or was merely due to the loss of Phox2b/Isl1⁺ OM/TN neurons after *miR-125b* overexpression. To establish if *miR-125b* overexpression also affects the vMH BP progenitor cell numbers (by affecting their proliferation, survival or fate specification), I used EdU co-labelling with *Nkx6-1* to distinguish between proliferating BP progenitors (EdU⁺ and Nkx6-1⁺ cells) and postmitotic OM/TN precursors and neurons (EdU⁻ but Nkx6-1⁺ cells). The number of EdU⁺/Nkx6-1⁺ double-labelled cells (BP progenitors) per total number of EdU⁺ single-labelled (proliferating) cells was indeed reduced by 37 % whereas the total number of proliferating (EdU⁺) cells per se was only reduced by 12% relative to the controls after *miR-125b* overexpression in primary vMH cultures and a 3 hour-pulse of EdU at 3 DIV, indicating that the overexpression of *miR-125b* in these cultures selectively decreased the proportion of proliferating Nkx6-1⁺ BP progenitors among all proliferating vMH cells. Notably, knockdown of *miR-125b* in primary vMH cultures did not affect neither the numbers of proliferating Nkx6-1⁺ BP progenitors nor the total numbers of proliferating cells in the primary vMH cultures,

indicating that reduction/depletion of *miR-125b* in these cultures does not affect the proliferation and cell cycle progression of vMH cells.

Apart from the previously discussed (see section 4.3) ample literature about *miR-125b* promoting the cell cycle exit and neuronal differentiation of a wide selection of stem and neural progenitor cells both *in vivo* and *in vitro* by targeting pluripotency factors such as *SMAD4* and *lin28* (Lee et al., 2005; Boissart et al., 2012; Wong et al., 2012), *miR-125b* has also been implicated in the negative regulation of cell differentiation in other non-neural contexts. Thus, overexpression of *miR-125b* in murine mesenchymal stem cells inhibited their proliferation but also differentiation into osteoblasts whereas *miR-125b* knockdown had the opposite effect in these cells, but the precise targets mediating these effects of *miR-125b* remained unclear from this study (Mizuno et al., 2008). *MiR-125b* is downregulated in many bladder cancer tissues and cell lines, and overexpression of *miR-125b* in these cells inhibited their proliferation and suppressed their ability to form tumours *in vitro* and *in vivo* (Huang et al., 2010). Notably, the cell cycle regulatory transcription factor *E2F3* (that promotes the transition from G1 to S-phase of the cell cycle (Peng, Ng et al., manuscript in submission), was identified in this study as a direct target of *miR-125b* (Huang et al., 2010). Finally, *miR-125b* was recently shown to be highly expressed in skin stem cells and sharply downregulated when these cells initiate differentiation (Zhang et al., 2011). Overexpression of *miR-125b* in skin stem cells *in vivo* in fact repressed their differentiation into the corresponding progeny whereas it had no effect on stem cell homeostasis itself, indicating that *miR-125b* might act by balancing the self-renewal (proliferation) of stem/progenitor cells and their early lineage commitment (differentiation) (Zhang et al., 2011). Therefore, it is possible that instead of or apart from a specific function of *miR-125b* in the promotion of the specific/generic neuronal differentiation of Nkx6-1⁺ BP/vMH progenitors into OM/TN neurons/vMH neurons by regulating the expression of *Sim1* and *Phox2b* or other more generic neural targets, (Le et al., 2009b) in these cells, *miR-125b* suppresses both the proliferation of Nkx6-1⁺ BP/vMH progenitors and their differentiation into OM/TN neurons/vMH neurons by regulating these or other targets (including cell cycle regulatory proteins such as E2F3 (Huang et al., 2010), cyclin C, Cdc25c, Cdkn2c and other mediators of the p53 network (see below) (Le et al., 2011)) in these cells. As the outcome of these two scenarios would be the same after

miR-125b overexpression/gain-of-function in primary vMH cultures (reduced proliferation and reduced numbers of Nkx6-1⁺ BP progenitors as well as reduced numbers of postmitotic Phox2b⁺/Isl1⁺ and/or vMH neurons which in fact I observed in my cultures), it is impossible at present to distinguish between these two possibilities in this case. However, the fact that *miR-125b* knockdown/loss-of-function in primary vMH cultures did not result in an increased proliferation of vMH cells or even an increased number of Nkx6-1⁺ BP progenitors strongly suggests that *miR-125b* does not regulate the cell cycle progression/self-renewal of Nkx6-1⁺ BP/vMH neural progenitors themselves. Nevertheless, the fact that Phox2b⁺/Isl1⁺ OM/TN neuron (or other vMH neuron) numbers were increased after *miR-125b* knockdown in these cultures could still imply a repressive function of this miRNA on OM/TN (or other vMH) neurons differentiation in particular/in general.

The selective decrease or increase of Phox2b⁺/Isl1⁺ (and possibly other vMH neurons) cell numbers as well as the selective decrease but not increase of Nkx6-1⁺ cells and of proliferating (EdU⁺) vMH progenitors and Nkx6-1⁺ BP progenitors after overexpression or knockdown, respectively, of *miR-125b* in primary vMH cultures suggested that the survival of these cells was compromised at least after overexpression of *miR-125b* in these cultures. I therefore assessed the number of apoptotic cells in the primary vMH cultures after overexpression or knockdown of *miR-125b*. Notably, knockdown of *miR-125b* in primary vMH cultures significantly decreased the numbers of apoptotic (cCasp3⁺) cells in these cultures, indicating that overall cell survival was increased/ enhanced by reducing the *miR-125b* dosage. Surprisingly however, overexpression of *miR-125b* did not result in an increased number of apoptotic vMH cells and a rather decreased (albeit not significant) number of apoptotic cells was also detected in these cultures. It is therefore highly unlikely that the reduced numbers of Phox2b⁺/Isl1⁺ cells (and possibly other vMH neurons) of Nkx6-1⁺ cells and of proliferating (EdU⁺) vMH progenitors/Nkx6-1⁺ BP progenitors after overexpression of *miR-125b* are due to a decreased survival/increased death of these cells, which is also in line with the finding that *Phox2b* LOF does not result in a decreased survival of OM/TN neurons (*Phox2b* knock-out embryos do not display a loss of OM/TN neurons at least until birth (Pattyn et al., 2000b)). However, the increased numbers of Phox2b⁺/Isl1⁺ cells (and possibly other vMH neurons) but not of Nkx6-1⁺ cells or of proliferating (EdU⁺)

vMH progenitors/Nkx6-1⁺ BP progenitors after knockdown of *miR-125b* might in fact be due to a selectively enhanced survival/decreased death of Phox2b⁺/Isl1⁺ cells (and possibly other vMH neurons) in the absence of *miR-125b*. These anti-apoptotic effects after reduction of *miR-125b* levels in primary vMH cells are unlikely to be mediated by the previously established (*Sim1* and *Phox2b*) and known targets (SMAD4, Lin28 (Rybak et al., 2008), E2F3 (Huang et al., 2010), cyclinC, Cdc25c, Cdkn2c, (Le et al., 2011) of *miR-125b*, as an (demonstrated or expected) increased expression of these targets after *miR-125b* knockdown is not expected to enhance the survival of the corresponding cells. In fact, an increased expression of cell cycle regulatory proteins such as E2F3 has even been shown to increase apoptotic cell death (Dyson, 1998; Helin, 1998; Muller et al., 2001), thus contradicting my own results. Although the reason for this contradicting result and the potential underlying mechanism for the apparently pro-apoptotic function of *miR-125b* in vMH cells remain unclear at present, it has been proposed that *miR-125* buffers and fine-tunes the p53 network by regulating the dose of both proliferative and apoptotic regulators of this network (Le et al., 2011). It might therefore be that reduction of the *miR-125b* dosage in vMH cells rather promotes/facilitates that anti-apoptotic “branch” of the p53 network/pathway, but further experiments are needed to establish whether this is indeed the case.

4.4 Outlook: *miR-125b* function in vMH neuron development

Further work need to be done before a more complete picture of *miR-125b* functions could be elucidated. Thus far, I have shown by using NGS, *miR-125b* expression is induced during neural induction stage and is enriched in the differentiated neurons. I also demonstrated that *miR-125b* distinct expression within the BP of the mesencephalon and rostral metencephalon (MHB region). I have further shown that two predicted *miR-125b* target genes, *Phox2b* and *Sim1*, their expressions overlap with *miR-125b* initially in the same brain region, but at least for *Phox2b*, *miR-125b* and *Phox2b* expressions segregate at later stage. I showed for the first time, both *Phox2b* and *Sim1* are experimentally validated downstream targets of *miR-125b*, where *miR-125b* exerts its repressive effect via its seed sequencing within *Phox2b*- and *Sim1* 3'UTR. Gain-of-functions and loss-of-functions of *miR-125b* in E11.5 primary cultures showed that *Phox2b*⁺ and *Isl1*⁺ cells OM/TN neurons are affected by *miR-125b* overexpression or knockdown. I further demonstrated that *Nkx6-1*⁺ cells were reduced upon *miR-125b* overexpression. Moreover, overexpression of *miR-125b* decreased the proliferation of these *Nkx6-1*⁺ BP progenitors as well as overall proliferation of VMH cells, whereas the knockdown of *miR-125b* did not affect cell proliferation in these cultures. Surprisingly, apoptotic cell death was decreased upon *miR-125b* knock-down, albeit an opposing effect was not observed after *miR-125b* overexpression.

To answer if other nearby neuron populations such as RN (*Pou4f1*⁺ /*Brn3a*⁺ cells), mdDA neurons (*Th*⁺ cells) and/or serotonergic neurons (*5-HT*⁺) are affected by the overexpressing or knockdown of *miR-125b*, gain/loss-of-functions studies on E11.5 primary cultures will need to be done.

5.0 Materials and Methods

5.1. Materials

5.1.1. General equipments

Table 8. List of equipments used.

Name	Model/ Cat No.	Manufacturer
Microscopes		
Confocal microscope	IX81	Olympus
High Resolution Microscopy Camera	AxioCam HRC	Carl Zeiss AG
Inverted Microscope	Axiovert 200	Carl Zeiss AG
Microscope	Axioplan 2	Carl Zeiss AG
Stereomicroscope	MZ8	Leica Microsystems AG
Stereomicroscope	Stemi SV 6	Carl Zeiss AG
Stereomicroscope	MZ7.5	Leica Microsystems AG
Stereomicroscope		
Histology		
Electronic, motorized rotary microtome	HM 355 S	Microm GmbH
Embedding center, dispenser + hot plate	EG1160	Leica Microsystems AG
Fiber Optic Illuminator	KL 1500	Leica Microsystems AG
Flattening table	HI1220	Leica Microsystems AG
Centrifuges		
Microcentrifuge	5415 D	Eppendorf AG
	5702	Eppendorf AG
	5417R	Eppendorf AG
MasterCycler Gradient	950000015	Eppendorf AG
Ultra centrifuge	Sorvall Evol. RC	Thermo Scientific
Centrifuge	Varifuge 3.0R	Thermo Scientific
PCR		
Thermocycler	Mastercycler®	Eppendorf AG

	gradient	
RT-qPCR Sequence Detection System	ABI Prism 7900HT	Applied Biosystems
Softwares		
Gel Documentation System	E.A.S.Y Win32	Herolab GmbH
ISH pictures	Axiovision 4.6	Zeiss, Germany
Confocal picture	FV10-ASW 2.0	Olympus
Adobe Photoshop	CS3	Adobe Systems Inc.,
Adobe Illustrator	CS3	USA
SigmaStat	3.5	Adobe Systems Inc.,
Sigma Plot	12.0	USA
		Aspire Software, USA
		Aspire Software, USA
Cell Culture		
Incubator	400	Memmert GmbH Co.KG
hemocytometer		Neubauer, Germany
ISH		
Film processor	Curix 60	AGFA
Hybridizer Incubator	HB100	UVP, UK
Water bath	WPE45	Memmert
Luminometer	Centro LB 960	Berthold Technologies/ Germany
pH-Meter	inoLab pH 720	WTW GmbH
Precision Balance	LC 6201 S	Sartorius AG
Tumbler	Polymax 1040	Heidolph Instruments GmbH & Co. KG
Ultrapure Water System	Milli-Q® Biocel	Millipore Corporation
Water Bath Square 220 Volt	1451	Sakura Finetek Europe B.V.

5.1.2. Consumables

Table 9. List of consumables used.

Name	Model/ Cat No.	Manufacturer
Histology		
Embedding cassettes	TurbOflow II MC-	McCormick Scientific
Peel-A-Way® Embedding	510	Polysciences, Inc
Molds	Square - S22	Polysciences, USA
Poly AquaMount	18606	Thermo Scientific
Microscope slide	J1800AMNZ	
ISH		
microspin™ S-300 HR Column	275130	Amersham Biosciences
[α-35S] dATP	NEG039H001MC	UK
35S-uridine triphosphate	NEG034H001MC	Perkin Elmer
ISH buffer (for LNA ISH)	B8807G	Perkin Elmer
BioMax MR	Z350389-50EA	Ambion, USA
Developer	G153	Sigma Aldrich, USA
Rapid Fixer	G354	AGFA AGFA
Cell culture		
Cover slips	H878	Carl Roth GmbH + Co.
Ampicilin	A5354	KG
Kanamycin	K1377	Sigma Aldrich, USA
DMEM	31053044	Sigma Aldrich, USA
Knock out DMEM	10829018	Invitrogen, USA
DMEMF/12	11320074	Invitrogen, USA
Poly-D-Lysine	P6407	Invitrogen, USA
LIF	<u>AF-250-NA</u>	Sigma Aldrich, USA
bFGF	3139-FB	R&D Systems, USA
Laminin (50 µg/mL)	11243217001	R&D Systems, USA
Poly-L-Ornithine (100 µg/mL)	P5899	Roche, Switzerland
Insulin	12585014	Sigma Aldrich, USA
Transferin	T1428	Invitrogen, USA
Human Fibronectin	1918-FN	Sigma Aldrich, USA

B27	0080085SA	R&D Systems, USA
N2 Supplement	5000959	Invitrogen, USA
SHH	Bulk 461-SH	Invitrogen, USA
FGF8	423-F8-025	R&D Systems, USA
Ascorbic acid	A4403	R&D Systems, USA
BDNF	248-BD-025	Sigma Aldrich, USA
		R&D Systems, USA
PCR		
PCR nucleotide mix (dNTP)	11814362001	Roche, Switzerland
DMSO	D9170	Sigma Aldrich, USA
Taqman RT-PCR Master Mix Kit	4309169	Applied Biosystems

5.1.3. Chemicals

Table 10. List of chemicals used.

Name	Provider	Cat. No.
Acetic acid	Merck KGaA	100063
Agarose	SERVA GmbH	11406
Aqua-Poly/Mount	Polysciences, Inc	18606
BSA	Sigma-Aldrich, Inc.	A3059
Chloroform	Merck KGaA	1070242500
Citric acid monohydrate	Merck KGaA	100244
Ethanol	Merck KGaA	100983
Ethidiumbromide	Carl Roth GmbH + Co. KG	2218.2
Ethylenediaminetetraacetic acid disodium salt	Sigma-Aldrich, Inc.	E5134
GIBCO FBS	Invitrogen GmbH	10106-169
Magnesium chloride hexahydrate	Merck KGaA	105833
Milk (Blotting-Grade Blocker)	Biorad	170-6404
N,N-Dimethylformamide	Sigma-Aldrich, Inc.	D4551
NEG-50™ Frozen Section Medium	Richard-Allan Scientific	6502
Nonidet™ P 40 Substitute	Sigma-Aldrich, Inc.	74385

Paraformaldehyde	Sigma-Aldrich, Inc.	P6148
Phenol	Merck KGaA	516724
Potassium chloride	Merck KGaA	104936
Potassium ferricyanide K ₃ Fe(CN) ₆	Sigma-Aldrich, Inc.	60299
Potassium ferrocyanide K ₄ Fe(CN) ₆	Sigma-Aldrich, Inc.	60279
Potassium phosphate monobasic	Sigma-Aldrich, Inc.	P5655
Roti®-Histol	Carl Roth GmbH + Co. KG	6640
Sodium chloride	Merck KGaA	106404
Sodium citrate tribasic dihydrate	Sigma-Aldrich, Inc.	S4641
Sodium hydroxide	Carl Roth GmbH + Co. KG	6771
Sodium phosphate dibasic dihydrate	Sigma-Aldrich, Inc.	30412
Sucrose	Sigma-Aldrich, Inc.	S0389
Trizma® hydrochloride	Sigma-Aldrich, Inc.	T3253
<u>TRIzol® Reagent</u>	Invitrogen GmbH	15596-026
TWEEN® 20	Sigma-Aldrich, Inc.	P1379
X-Gal	Fermentas GmbH	R0404
Xylol	Merck KGaA	108681

5.1.4. Commercial kits

Table 11. List of commercial kits used.

Name	Provider	Catalogue No.
Terminal transferase labelling kit	Roche	03333566001
iScript cDNA synthesis kit	Biorad	170-8890
TOPO TA cloning kit	Invitrogen	K4500-01
One Shot TOP10 Chemically <i>E.coli</i> competent cell	Invitrogen	C4040-10
Quick Change Site Directed Mutagenesis Kit	Stratagene	200519
Dual-Luciferase® Reporter Assay system	Promega	E1910
<u>Click-iT™ Edu Imaging Kits</u>	Invitrogen	C10337
DIG Oligonucleotide 3'-End Labeling Kit	Roche	03353575910

5.1.5. Enzymes

Table 12. List of enzymes used.

Name	Provider	Catalogue No.
Proteinase K	AppliChem GmbH	A3830
REDTaq® DNA Polymerase	Sigma-Aldrich, Inc	D4309
T4 DNA Ligase	Roche	10716359001
Alkaline Phosphatase (CIP)	NEB	M0290L
<i>Xba</i> I	Invitrogen	15226012
<i>Bgl</i> II	Invitrogen	15213010
<i>Bam</i> HI	Invitrogen	15201023

5.1.6. Antibodies

Table 13. List of antibodies used.

Antigen	Species	Host	Conjugate	Dilution	Provider	Cat No.
RFP		rabbit	-	1:500	Rockland	600-401-379
Phox2b		rabbit	-	1:800	Dr.Brunnet	Gift
Isl1		mouse	-	1:100	DSHB	40.2D6-c
Nkx6-1		mouse	-	1:200	DSHB	F65A2-c
cCasp3		rabbit	-	1:100	Cell signaling	9661
Th		mouse	-	1:600	Chemicon	MAB318
Brn3a		mouse	-	1:200	Santa Cruz	SC-8429
Nkx2-2		mouse	-	1:200	DSHB	74.5A5-c
Tuj1		mouse	-	1:500	Sigma Aldrich	T8660
IgG (H+L)	Rabbit	Donkey	Alexa594(red)	1:500	Molecular Probes	A21207
IgG (H+L)	Rabbit	Donkey	Alexa488(green)	1:500	Molecular Probes	A21206
IgG (H+L)	Rabbit	Donkey	Cy5	1:250	Jackson	711-176-152
IgG (H+L)	Mouse	Donkey	Alexa594(red)	1:500	Molecular Probes	A21203
IgG (H+L)	Mouse	Donkey	Alexa594(green)	1:500	Molecular	A21202

					Probes	
IgG (H+L)	Mouse	Goat	DyLight649 (Cy5)	1:250	Jackson	115-496-003

5.1.7. Buffers and solutions

Table 14. List of buffers and solutions used.

Name	Composition/Final Concentration	Amount
10 x PBS	NaCl KCl, Na ₂ HPO ₄ KH ₂ PO ₄ adjust pH to 7.4, fill up to 1 L with H ₂ O, autoclave	80 g 2 g 26.28g 2.4 g
10 x TAE	Tris-HCl Acetic Acid 0.5 M EDTA, pH 8.0 Fill up to 1L with H ₂ O, autoclave	48.4 g 11.42 ml 20 ml
20 % PFA in PBS	PFA, pH 7.4 Add NaoH cookies till solution is crystal clear. Adjust pH to 7.4 with HCl	200 g
Blocking solution	1 % BSA 10 % FCS 5 % milk 0.05 % Triton-X Fill up with PBS	
Fix solution (for ICC and IHC)	4 % PFA in PBS (pH 7.4) 100 mM EGTA (pH 7.4) 1 M MgCl ₂	47.4 ml 2.5 ml 0.1 ml
Fix solution (for X-Gal staining)	5 mM EDTA pH 7.4 2 mM MgCl ₂ dissolved in 4%PFA in PBS (pH 7.4)	
Wash buffer (for X-gal staining)	1 M MgCl ₂ 2 % NP40 PBS pH 7.4	0.4 ml 2 ml 197.6 ml

X-Gal stain	1 mg/ml X-Gal stock (dissolved in DMF) 5 mM Potassium ferrocyanide 5 mM Potassium ferricyanide Wash buffer	
1X Buffer I (for DIG-labelled LNA probe)	Tris NaCl ddH ₂ O to 1 litre Note: Adjust pH to 7.5	12.1 g 8.7 g
1X Buffer II (for DIG-labelled LNA probe)	Tris NaCl ddH ₂ O to 1 litre Note: Adjust pH to 9.5	12.1 g 8.7 g
Tail lysis buffer	1 M Tris-HCl pH8 KCl MgCl ₂ .6H ₂ O NP-40 Tween 20 Gelatine ddH ₂ O to 100 ml	1 ml 0,374 g 51 mg 0,45 ml 0,45 ml 10 mg
Hybridization Buffer (for RNA ISH)	50 % formamide 20 mM Tris-HCl pH8.0 300 mM NaCl 5 mM EDTA pH 8.0 10 % dextran sulphate 0.02 % Ficoll 400 0.02 % PVP40 0.02 % BSA 0.5 mg/ml tRNA 0.2 mg/ml carrier DNA	250 ml of 100 % formamide 10 ml of 1 M Tris-HCl pH 8.0 30 ml 5 M NaCl 5 ml of 0.5 M EDTA 100 ml of 50 % dextran sulphate 50 ml of 10x Polymers contains Ficoll 400, PVP 40, BSA. 25 ml 10 mg/ml tRNA 10 ml carrier DNA,

	200 mM DTT	acid cleaved, 10 mg/ml 20 ml of 5 M DTT
20X SSC	150 mM NaCl 15 mM Sodium Citrate ddH ₂ O to 1 litre Note: Adjust pH to 7	175.3 g 88.2 g

5.1.8. LNA oligo probe to detect miRNA expression

Table 15. LNA oligo probe used to detect miRNA expression. Hybridization for each LNA detection probe was done at 21 °C below T_m.

LNA probe	Catalogue No.	T _m (°C)	LNA probe	Catalogue No.	T _m (°C)
miR scrambled	99004-00	75	<i>mmu-miR-300</i>	39143-00	77
<i>mmu-miR-9</i>	39459-00	71	<i>mmu-miR-320</i>	39554-00	79
<i>mmu-miR-7b</i>	39564-00	72	<i>mmu-miR-328</i>	39163-00	87
<i>mmu-miR-17</i>	39545-00	75	<i>mmu-miR-342-5p</i>	39538-00	76
<i>mmu-miR-22</i>	39114-00	74	<i>mmu-miR-350</i>	39542-00	71
<i>mmu-miR-30a</i>	39449-00	73	<i>mmu-miR-365</i>	39215-00	67
<i>mmu-miR-34a</i>	39519-00	81	<i>mmu-miR-378</i>	39569-00	75
<i>hsa-miR-125b</i>	18022-00	77	<i>mmu-miR-449a</i>	39589-00	76
<i>mmu-miR-132</i>	39033-00	76	<i>mmu-miR-449b</i>	39715-00	77
<i>mmu-miR-133a</i>	39460-00	80	<i>mmu-miR-449c</i>	39641-00	80
<i>mmu-miR-133b</i>	39573-00	81	<i>mmu-miR-452</i>	39226-00	74
<i>mmu-miR-135a</i>	39037-00	69	<i>mmu-miR-469</i>	39233-00	81
<i>mmu-miR-135b</i>	39543-00	72	<i>mmu-miR-674</i>	39384-00	75
<i>mmu-miR-138</i>	39418-00	84	<i>mmu-miR-679</i>	39281-00	82
<i>mmu-miR-144</i>	39464-00	64	<i>mmu-miR-684</i>	39288-00	66
<i>hsa-miR-181a</i>	18066-00	77	<i>mmu-miR-689</i>	39294-00	92
<i>mmu-miR-182</i>	39474-00	78	<i>mmu-miR-693-3p</i>	39387-00	77
<i>mmu-miR-210</i>	39104-00	87	<i>mmu-miR-705</i>	39320-00	88
<i>mmu-miR-212</i>	39550-00	81	<i>mmu-miR-709</i>	39324-00	77
<i>mmu-miR-221</i>	39556-00	80	<i>mmu-miR-712</i>	39327-00	82

<i>mmu-miR-224</i>	39558-00	73	<i>mmu-miR-714</i>	39329-00	88
<i>mmu-miR-877</i>	39723-00	77			

N.B. All LNA ISH probes were bought from Exiqon, Denmark. *hsa-miR-125b* also targets *mmu-miR-125b-5p* as annotated in miRBase 10.0.

5.1.9. Riboprobes to detect mRNA

Table 16. Riboprobes used in RNA ISH.

Template	cDNA size (bp)	Linearized with	Transcribed with	Provided by	Accession number
<i>Sim1</i>	1328	HindIII	T7	S.Götz	NM_011376
<i>Phox2b</i>	1506	EcoRI	T3	MHB Team	NM_008888

5.1.10. Precursor miRNAs for luciferase assay

Table 17. precursor miRNAs used in luciferase sensor assays

Name	Provider	Catalogue No.
<i>mmu-miR-7b</i>	Ambion	PM13116
<i>hsa-miR-34a</i>	Ambion	PM11030
<i>hsa-miR-125b</i>	Ambion	PM10148
<i>mmu-miR-135b</i>	Ambion	PM13044
<i>hsa-miR-221</i>	Ambion	PM10337
<i>mmu-miR-342-5p</i>	Ambion	PM12538
<i>mmu-miR-449a</i>	Ambion	PM11127
<i>mmu-miR-449b</i>	Ambion	PM12675
<i>mmu-miR-449c</i>	Ambion	PM11430
<i>mmu-miR-705</i>	Ambion	PM11392
<i>mmu-miR-709</i>	Ambion	PM11496
<i>mmu-miR-712</i>	Ambion	PM11561
<i>mmu-miR-714</i>	Ambion	PM11590
<i>mmu-miR-877</i>	Qiagen	MSY0004861
Negative Control 1	Ambion	AM17110

5.1.11. Vectors

Table 18. Vectors used for cloning

Vector	Catalogue	Provider
Renilla luciferase (pRL-SV40 Vector)	E2231	Promega
pGL3 Promoter vector	E1761	Promega
pcDNA6.2-EmGFP	Plasmid 22741	Addgene

5.1.12. Primers

5.1.12.1. Genotyping

Table 19. Primers used for mouse genotyping

Primer Name	Primer Sequence 5'-3'
R26R-D1	caaagtcgctctgagttgtatc
R26R-R1	cacaccaggttagccttaagc
R26R-Mutant	gcgaagagttgtcctca

5.1.12.2. luciferase sensor vectors

Table 20. List of primer pairs used to generate candidate genes 3'UTR PCR fragment.

Gene 3'UTR	length (bp)	Primer Sequence
<i>Wnt1</i>	857	Forward 5' -GCTCTAGACTCGCTGGTCCTGATGTTTG-3'
		Reverse 5' -TCTCTAGACCTCAGAGGAAGATACTACATTGGT-3'
<i>Pitx3</i>	271	Forward 5' -GCTCTAGAGACAGGGGTTCGCCTAGACTG-3'
		Reverse 5' -TCTCTAGAAGTCCGCGCACGTTTATTTTC-3'
<i>Lef1</i>	1197	Forward 5' -GCTCTAGATAAGAGAAGCTCCTTCCCAACG-3'
		Reverse 5' -TCTCTAGAAATGCTCAGCACGTTAACTCAAAC-3'
<i>Wnt5a</i>	314	Forward 5' -GCTCTAGAAGGTGTAGGAGCCATTTTCT-3'
		Reverse 5' -TCTCTAGAAATACACACACACACACACC-3'
<i>Wnt5b</i>	815	Forward 5' -GCTCTAGATCCTCTCCGCCTCACAAAAG-3'
		Reverse 5' -TCTCTAGAAAGGGACGCTGTACATGTGG-3'

<i>Wnt6</i>	653	Forward	5' -GCTCTAGAACCTCTGGGCCATCTACAGG-3'
		Reverse	5' -TCTCTAGATCATGACCGTTAATTTTCATCATG-3'
<i>Otx2</i>	358	Forward	5' -GCTCTAGAGAAAAAGGAAGGGGCCTTAG-3'
		Reverse	5' -GCATCTAGACAATCAGTCGCACAATCCAC-3'
<i>Sim1</i>	1328	Forward	5' -ATGTCTAGAAGGAAAGGGCAGAGCAGAGT-3'
		Reverse	5' -ATGTCTAGAGCCCCAAAATACAAATTCATCG-3'
<i>Phox2b</i>	1506	Forward	5' -ATGTCTAGAAGTGGGCGAGTGGGTAGAC-3'
		Reverse	5' -ATGTCTAGATGACGCTCATGTTCCAAAAC-3'

5.1.12.3. Site-directed mutagenesis on luciferase vector

Table 21. List of primer pairs used to generate site-directed mutagenesis on luciferase vector.

Name	miRNA	Mutated primer sequence
<i>Wnt1</i>	<i>miR-709(1)</i>	Sense 5'-caaaacctacattctccttgctg <u>gagggt</u> gggagccattgaacagc-3'
		Antisense 5'-gctgttcaatggctcc <u>ccctc</u> agacaaggagaatgtagggtttg-3'
	<i>miR-709(2)</i>	Sense 5'- cctcctcccacccttctctgct <u>gagggt</u> gctcatcactgtgtaa -3'
		Antisense 5'- ttacacagtgatgag <u>ccctc</u> gacaggaaggggtgggaggagg -3'
<i>Phox2b</i>	<i>miR-125b</i>	Sense 5'GTGAGCTTGGACTTCGGGGCACT <u>GACTTCCG</u> GCTGTGTCTGAG TGACG-3' Antisense 5'- CGTCACTCAGACACAGCC <u>GGAAGT</u> CAGTGCCCCGAAGTCCA AGCTCAC -3'
<i>Sim1</i>	<i>miR-125b</i>	Sense 5'- GATAATTATGAAATCATTACTTGGCATTGGACAG <u>GCCGCC</u> CAT TAGTACTGTATTTTCATCACTCAACATGATC-3' Antisense 5'- GATCATGTTGAGTGATGAAAATACAGTACTAAT <u>GGGCGG</u> CT GTCCAATGCCAAGTAATGATTTTCATAATTATC -3'

N.B. Mutated nucleotides were underlined and bolded.

5.1.12.4. Site-directed mutagenesis for *Wnt1* 3'UTR 'miRNA recognition motive'

Table 22. Primers used for 'motive-recognition' motive experiment

Name	Location	Primer Sequence
Mut.Mot .1	Both stems	Sense 5'- gcgatccatctctcccact <u>ttactactttgggactcttgaacct</u> acttgctgagtcggctc -3' Antisense 5'- gagccgactcaggcaagt <u>aggttcaagagtccc</u> aagtag <u>taagt</u> gggagagatggat cgc-3'
Mut.Mot .2	Left stem	Sense 5'- catagcgatccatctctcccact <u>ttactactttg</u> agactcctgaaceacttgctg -3' Antisense 5'- caggcaagtggttcaggagctc <u>caagtagta</u> agtgggagagatggatcgtatg-3'
Mut.Mot .3	Right stem	Sense 5'- cacctctacctggggactct <u>ttgaacat</u> atttgctgagtcggctcgaac -3' Antisense 5'- gttcgagccgactcaggcaaa <u>atattgttca</u> agagtccccaggtaggaggtg -3'

N.B. Mutated nucleotides were underlined and bolded.

5.1.12.5. miRNA overexpressing (OE) construct

Table 23. DNA insert sequences.

Name	Primer Sequence
<i>miR-125b-5p</i>	Forward 5'- GGATCCTGGAGGCTTGCTGAAGGCTGTATGCTGGCCTAGTCCCTGAGACC <u>CTAACTTGTG</u> AGGTATTTTAGTAACATCACAAAGTCAGGTTCTTGGGACCT AGGCCAGGACACAAGGCCTGTTACTAGCACTCACATGGAACAAATGGCCC AGATCT-3' Reverse 5'- AGATCTGGGCCATTTGTTCCATGTGAGTGCTAGTAACAGGCCTTGTGTCCTGGCCTA GGTCCCAAGAACCTGACTTGTGATGTTACTAAAATACCTCACAAGTTAGGGTCTCAG <u>GGACT</u> AGGCCAGCATAACAGCCTTCAGCAAGCCTCCAGGATCC-3'

N.B. mature microRNA sequences were bolded and underlined.

5.1.12.6. Lentivirus constructs

Table 24. Primers used to generate *miR-125b* DNA insert for lentivirus constructs

Name	Primer Sequence
<i>miR-125b-5p</i>	Forward Primer 5'-GATGCTAGCCTAGCCCCGCAGACACTAGC-3' Reverse Primer 5'-CATGGCGCGCCCCGCCTCCTCTTGCTCTGTATC-3'
<i>miR-125b Sp</i>	5' - <u>ccggcCGACCATGGCACCGACTGTTA</u> tc-3'

N.B. mature microRNA sequences were bolded and underlined.

5.1.12.7. RT-qPCR Taqman primers

Table 25. DNA insert sequences.

Name	Catalogue	Amplicon length	Provider
<i>Phox2b</i>	4331182	91	Applied Biosystems
<i>Sim1</i>	4331182	102	Applied Biosystems
<i>Nkx6-1</i>	4331182	69	Applied Biosystems
<i>Th</i>	4331182	61	Applied Biosystems

N.B. mature microRNA sequences were bolded and underlined.

5.1.13. Cell culture medium

Table 26. List of mediums for cell culture.

Name	Final composition	Volume
LB Medium	Bacto-Tryptone	10 g
	Bacto-yeast extract	5 g
	NaCl	10 g
	ddH2O to 1 litre	
	Note: adjust pH to 7.0, autoclave	
HEK293T Medium	10 % FCS	50 ml
	DMEM	450 ml
Diffentiation medium (For primary culture)	DMEM F12	9.5 ml
	L-Glutamine	100 µl
	50x B27	200 µl

	1 % FCS	100 μ l
	Pen/Strep	100 μ l
ES medium (500 ml)	Knockout™ DMEM	415 ml
	2 mM L-Glutamine	2.5
	0.001 % β -mercap. ethanol	2.5
	15 % FCS	75 ml
	LIF	45 μ l
EB medium (500 ml)	Knock out DMEM	440 ml
	10 % FCS	50 ml
	0.001 % β -mercap. ethanol	5 ml
	1x L-Glutamine	5 ml
ITSFn medium (10 ml)	DMEM/F12	9.8 ml
	Insulin	10 μ l
	Transferin	250 μ l
	Sodium selenium	1 μ l
	Fibronectin	44.6 μ l
	1x L-glutamine	100 μ l
N2 medium (10 ml)	DMEMF/12	9.8 ml
	100X L-Glutamine	50 μ l
	N2 Supplement	100 μ l
DA1 medium (10 ml)	N2 medium	10 ml
	Laminin	20 μ l
	bFGF	1 μ l
	SHH (500 ng/ml)	15 μ l
	FGF8 (100 ng/ml)	40 μ l
	0.5 mM Ascorbic acid	10 μ l
DA2 medium (10 ml)	N2 medium	10 ml
	BDNF	6 μ l
	0.5 mM Ascorbic acid	3 μ l

N.B. mature microRNA sequences were bolded and underlined.

5.2 Methods

5.2.1. Experimental animals

Outbred CD-1 mice were purchased from Charles River (Kisslegg, Germany) and kept under a 12-12 light-dark cycle under standard conditions. Mice were given *ad libitum* access to food and water. Animal treatment was conducted in accordance with the federal guidelines as approved by the HMGU Institutional Animal Care and Use Committee (Munich, Germany).

Mice bearing *Sonic Hedgehog* (*Shh*) minimal promoter, Cre and a *Shh* enhancer (SBE1) were designated as Shh-Cre-SBE1. Transgenic *Shh-Cre-SBE1* mice were kept in a C57BL/6 background. For cell fate-mapping experiments, male *Shh-Cre-SBE1* transgenic mice were crossed with female R26R reporter mice (Soriano et al., 1999) to obtain *Shh-Cre-SBE1*;R26R offspring.

5.2.2 Genotyping

5.2.2.1 Isolation of genomic DNA

Mouse tails (~0.5 cm) were cut with clean scissors and incubated overnight at 55 °C in tail lysis buffer (Table 14) with Proteinase K (final concentration: 100 µg/ml). Proteinase K was heat inactivated the next day by incubation at 94°C for 15 min. Tail lysis samples were then centrifuged for 12,000 rpm for 5 min.

5.2.2.2 PCR-genotyping

Genotyping PCRs were set-up as follows, using the allele-specific primers as indicated in Table 19:

14 µl H₂O (ad 20 µl)
2 µl 10x buffer (ad 1x)
1 µl genomic DNA
0.5 µl 10 mM dNTPs (ad 250 µM)
1 µl 10pmol/ µl forward primer (ad 10 nM)
1 µl 10pmol/ µl reverse primer (ad 10 nM)

0.5 µl Red-Taq Polymerase (ad 0.5 Units)

5.2.2.3 R26R reporter mice-genotyping

Primer pair R26R-D1 and R26R-R1 amplified a 253 bp PCR product detecting wild-type R26R allele. Primer pair R26R-D1 and R26R-Mutant amplified a 300 bp PCR product detecting targeted R26R allele (mutant). In each PCR reaction, 2 µl R26R-D1, 0.5 µl R26R-R1 and 1.5 µl R26R-Mutant primers were used, allowing detection of both wild type and mutant R26R allele in a single PCR reaction. Primer sequences were shown in Table 19. PCR conditions used were as follows:

95 °C	4 min	} 42 cycles
95 °C	30 sec	
50 °C	35 sec	
75 °C	35 sec	
72 °C	10 min	

5.2.3 Histology

5.2.3.1 Dissection of mouse embryos/brains

Collection of embryonic stages was done from timed-pregnant females, morning of the day of vaginal plug detection was designated as embryonic day 0.5 (E0.5). Embryos were staged according to Theiler (1989) (<http://www.emouseatlas.org/Databases/Anatomy/MAstaging.html>). Pregnant mice were killed by CO₂ asphyxiation. Uteri horns were removed and kept in cold phosphate buffered saline (PBS) before dissection. Embryos/brains were microdissected in cold PBS and fixed in 4 % paraformaldehyde (PFA) overnight at 4 °C.

5.2.3.2 Paraffin embedding of mouse embryos

Embryos/brains were dehydrated in an ascending ethanol series (30 %, 60 %, 70 %, 85%, 95%, 100%, 1 hour each), cleared in xylene (6-14 min depending on embryo stage) and embedded in paraffin, and sectioned on a microtome at 8 µm thicknesses. Sections

were processed following two different protocols depending on the detection probe used (LNA-ISH or RNA-ISH) as shown in Tables 15 and Table 16, respectively.

5.2.4 In Situ Hybridization (ISH) on paraffin sections

5.2.4.1 Labelling of Locked Nucleic Acid (LNA) oligo detection probe

5.2.4.1.1 DIG-labeled LNA oligo detection probe

The unlabeled LNA modified probes (Table 15) were DIG-labeled (ddUTP) with a single nucleotide at the 3' end using DIG Oligonucleotide 3'-End Labelling Kit according to the manufacturer's instructions. Labelling conditions are shown in Table 15. Incubation was performed at 37 °C for 15 min, then placed on ice. Labelling reaction was terminated by adding 2 µl 0.2 M EDTA (pH 8).

Table 27. 3'-end labelling of LNA-modified detection probe

Reagent	Volume (µl)	Final Conc.
LNA oligo template	4	0.3 µM
DIG-ddUTP solution (1 mM)	1	0.05 mM
5 x Terminal Transferase Buffer	4	1x
CoCl ₂ (25 mM)	2	2.5 mM
Terminal Transferase	1	400 U
H ₂ O	1	
Total	20	

5.2.4.1.2 Radioactive-labeled LNA oligo detection probe

The unlabeled LNA-modified probes were tailed at the 3'-end with [α -³⁵S] dATP using Terminal Transferase Labelling Kit according to the manufacturer's instructions with some modifications as shown in Table 28. Labelling conditions are shown in Table 27. Incubation was performed at 37 °C for 30 min. Labelling reaction was terminated by adding 2 µl 0.2 M EDTA (pH 8). Sterile H₂O was added to make up to 30 µl final

volume. Labelled LNA-modified DNA probe was purified from free nucleotides with microspin™ S-300 HR Column according to the manufacturer's instructions.

Table 28. Tailing of LNA modified oligo detection probe

Reagent	Volume (µl)	Final Conc.
LNA oligo (0.5 µM)	6	0.15 µM
[α-35S] dATP (1mCi/ml)	6	
5 x Terminal Transferase Buffer	4	1x
CoCl ₂ (15 mM)	2	1.5 mM
Terminal Transferase	1	400 U
H ₂ O	1	
Total	20	

5.2.4.2 Riboprobes for RNA ISH

5.2.4.2.1 Cloning of riboprobes

The riboprobes were generated previously in the lab. In general, cDNA was reverse transcribed from E12.5 CD1 mouse embryo head total RNA using iScript cDNA synthesis kit according to the manufacturer's instructions. Gene-specific primers were designed and the cDNA was PCR amplified to obtain gene-specific fragments as indicated in Table 16. The amplified band was subcloned into pCRII TOPO (for *Sim1*) or pKSII+ Bluescript (for *Phox2b*) vector carrying Sp6/T7 or T3 RNA Polymerase promoters, and verified by sequencing.

5.2.4.2.2 Labelling of riboprobes

In vitro transcription of plasmids containing the *Phox2b* and *Sim1* cDNA was performed with T3 or T7 RNA polymerase in the presence of ³⁵S-uridine triphosphate (UTP). In brief, 20 µg plasmid were linearised with the corresponding restriction enzyme overnight at 37 °C. The linearised plasmid was used as a template to set up the RNA transcription reaction (Table 29), and incubated at 37 °C for 3 hours. RNA polymerase (0.5 µl) was added again to the reaction mixture after one hour. RNase-free

DNaseI (2 μ l) was added at the end of the reaction to destroy the DNA template. The RNA transcript (probe) was purified with RNeasy mini kit according to standard procedures.

Table 29. RNA probe labelling.

Reagent	Volume (μ l)
Linearised plasmid	x
H2O	Add to 30
10x transcription buffer	3
NTP-mix (rATP/rCTP/rGTP 10 mM each)	3
DTT (0.5 M)	1
RNAse inhibitor (40 U/ μ l)	1
35S-thio-rUTP (1mCi/ml)	8
T7/SP6 RNA polymerase (20 U/ μ l)	1

5.2.4.3 Processing of paraffin sections for LNA ISH and RNA ISH

Paraffin-embedded embryos were sectioned on a microtome at 8 μ m thickness. Slides were dried in a 37 °C incubator overnight and stored at 4 °C until use. The ISH procedure was as described in Fischer et al., 2007 with minor modifications. In brief, sections were deparaffinised in xylol (20 min twice), rehydrated in a descending ethanol series (100 %, 95 %, 70 %, 5 min each), washed briefly in water followed by PBS, post-fixed in 4 % PFA for 20 min, washed shortly with PBS, treated with Proteinase-K (7 min), post-fixed in 4% PFA, acetylated in triethanolamine (10 min), washed in 1X SSC (5 min twice), and rehydrated in an ascending ethanol series (60 %, 70 %, 95 % and 100 %, 5 min each) and finally air dried. For LNA ISH, the Proteinase K treatment step was omitted.

5.2.4.4 ISH detection of miRNAs with LNA probes on paraffin sections

5.2.4.4.1 DIG-labelled LNA detection probes

After 1 hour of pre-hybridization with Hybmix (Ambion), hybridization was performed overnight at 21 °C below the melting temperature (T_m) of the corresponding LNA detection probe. Approximately 100 μ l Hybmix (Ambion) containing 0.5 pmol DIG-labelled LNA detection probe was applied onto each slide. Stringent washes (2X SSC, 1X SSC, 0.2X SSC (with 0.1 % Tween 20 and 1 mM DTT) and PBS, 15 min each) were performed on the next day followed by immunological detection. Briefly, slides were pre-blocked in blocking buffer (1 h) and incubated with anti-DIG Fab antibody (1:2000) overnight at 4 °C. The next day, sections were washed thrice with PBS (5 min), twice with Buffer I and once with Buffer II (10 min each) before performing NBT/BCIP staining in a dark, humidified chamber for 1-4 days, depending on the signal strength. TE buffer was added to stop the reaction before mounting of the slides.

5.2.4.4.2 Radioactively labelled LNA detection probes

After 1 hour of pre-hybridization with Hybmix (Ambion), hybridization was performed overnight at 21 °C below the melting temperature (T_m) of the corresponding LNA detection probe. Approximately 1 million c.p.m. LNA detection probe (or at least 700,000 c.p.m./ slide) were applied in 150 μ l Hybmix (Ambion). Stringent washes were performed on the next day (once with 1X SSC and four times with 0.2X SSC containing 0.05 % Tween 20 and 500 μ l 1 M DTT, 15 min each, twice with 0.1X SSC and once with water for 5 min each), followed by dehydration in an ascending ethanol series (70 %, 95 % and 100 %, 2 min each). Slides were air dried for 30 min.

5.2.4.5 mRNA ISH with radioactive riboprobes on paraffin sections

Pre-hybridization (1 hour) and hybridization (overnight) were performed at 60 °C with hybmix buffer (Table 14). Approximately 7 million c.p.m. riboprobe/slide was applied. Stringent washes were performed on the next day (four times with 4X SSC, 5 min each, once with RNaseA containing NTE buffer at 37 °C for 20 min, twice with 2X SSC, once with 1X SSC and 0.5X SSC with 1 mM DTT, twice with 0.1X SSC with 1 mM DTT at 64 °C for 30 min each, twice with 0.1 X SSC for 10 min each). Slides were dehydrated

in an ascending ethanol series (30 %, 50 %, 70 %, 95 % and 100 %, 1 min each) and air dried for 30 min.

5.2.4.6 Exposure and developing of radioactively labelled sections

Slides were exposed on a Kodak BioMax MR X-ray film overnight, and dipped in NTB Emulsion (Kodak) following standard procedures. For miRNA ISH, sections were exposed for 5-14 days. For mRNA ISH, sections were exposed for 4-6 weeks, depending on the signal strength. Slides were developed using developer (at RT, 3 min in the dark), rinsed in water (30 seconds) and fixed in fixative (Rapid Fixer, Kodak) at RT for 5 min in the dark, afterwards rinsed under running tap water for 25 min and air-dried for 1 hour. Sections were counterstained with 0.5 % Cresyl Violet prior to mounting.

5.2.5 Immunohistochemistry

Paraffin-embedded sections were processed as follows: sections were deparaffinised and rehydrated in a descending ethanol series (100%, 90 %, 85 %, 60 %, 30 %, 4 min each) and washed thrice in H₂O. Antigen retrieval was done by heating the sections in 10 mM sodium-citrate buffer, pH 6.0, in a microwave oven (630W, 15min). The sections were washed 5min each in H₂O followed by PBS, and blocked for 60 min in blocking solution (see 5.1.7). Sections were incubated in primary antibody in blocking solution overnight at 4 °C, rinsed thrice in PBS and incubated in secondary antibody in blocking solution for 90 min at RT. Sections were rinsed thrice in PBS (5 min each) before mounting the slides in Poly AquaMount with DAPI (Vector Labs).

5.2.6 Vector Constructs

5.2.6.1 Luciferase sensor vectors

Luciferase sensor vectors were constructed by cloning the 3'-UTR of the genes of interest into the *Xba*I site downstream of the Luciferase coding sequence (CDS) of

pGL3 Promoter vector (Promega). The 3'UTR sequences of candidate mRNAs were PCR amplified from E12.5 CD1 embryonic head cDNA with primers containing *Xba*I sequences at the 5' end as shown in Table 20. The nucleotide sequences of the generated plasmids were confirmed by DNA sequencing.

5.2.6.2 Site-directed Mutagenesis of luciferase sensor vectors

Site-directed mutagenesis of the predicted microRNA seed sequences within the 3' UTR fragments of the sensor vectors was done using the Quick Change Multi-Site Directed Mutagenesis Kit (Stratagene) according to the manufacturer's instructions. Mutagenic primers are shown in Table 21. The nucleotide sequences of the generated plasmids were confirmed by DNA sequencing.

5.2.6.3 Site-directed mutagenesis for *Wnt1* 3'UTR “miRNA recognition motif”

Mutated plasmids were generated using the Quick Change Multi-Site Directed Mutagenesis Kit according to the manufacturer's instructions. Mutagenic primers are shown in Table 22. The nucleotide sequences of the generated plasmids were confirmed by DNA sequencing.

5.2.6.4 miRNA overexpression (OE) construct

For overexpression of *pre-miR-125b-5p*, double stranded DNA oligos of *pre-miR-125b* sequence were annealed and inserted into vector pcDNA6.2-GW/EmGFP-miR (Invitrogen) using the BLOCK-iT™ Pol II miR RNAi Expression Vector kit (Invitrogen) according to the manufacturer's instructions. DNA sequences of the oligonucleotides are shown in Table 23.

5.2.6.5. Lentiviral vector construction and lentivirus production

The *miR-125b* OE lentivirus and *miR-125b* sponge lentivirus were constructed and produced in Dr. D. Edbauer lab (Edbauer et al., 2010). Briefly, for the *miR-125b* OE construct, the precursor miR-125b was PCR-amplified (primer pair shown in Table 24) from rat genomic DNA and cloned into the 3'UTR of mCherry driven by a human ubiquitin C promoter in FUW plasmid (Lois et al., 2002). For sequestration of endogenous *miR-125b* from E11.5 vMH primary cultures (by using *miR-125b* sponge), five artificial miRNA binding sites with two central mismatches and a deletion (sequences shown in Table 24) were subcloned downstream of the stop codon/polyA signal of mCherry driven by a human ubiquitin C promoter in FUW plasmid, thus acting as a sponge (Ebert et al., 2007; Edbauer et al., 2010). Viral particles were packaged using a second-generation system. 293FT cells (Invitrogen) were transiently co-transfected with the lentiviral expression vector (4.8 µg per 10 cm plate) and pSPAX2 (3.7 µg) and pVSVG (2.1 µg) using Lipofectamine 2000. Virus released into the culture supernatant was concentrated by ultracentrifugation (64,000 g, 2.5 h) and resuspended overnight in 50 µl Neurobasal media per 10 cm dish.

5.2.7 Restriction enzyme digestion/blunting/kinasing

In general, 0.5 U of restriction enzymes and Klenow/ µg vector DNA was incubated for 60 min (overnight for restriction enzyme digestion) at 37 °C. Enzymes were heat inactivated at 65 °C for 5 min. DNA was purified by gel purification or spin-column purification.

5.2.8 Ligations

Rapid DNA ligation kit (Roche) was used for sticky and blunt end ligations. In general, approximately 1 µl vector backbone and 3 µl insert DNA were mixed with 2 µl 10x T4 DNA ligation buffer and 1 µl T4 DNA ligase in a final volume of 20 µl. Ligation was performed at 16 °C overnight.

5.2.9 Transformation into competent bacteria

In general, 4 µl circular DNA was used to transform into competent bacterial cells (One Shot TOP10 Chemically competent *E.coli*) according to the manufacturer's instructions. Cells were plated onto LB-Agar containing the corresponding antibiotic.

5.2.10 DNA mini- and maxi-preps

For minipreps, one bacterial colony was picked from the agar plate to inoculate 5 ml LB medium and grown overnight at 37°C. For maxipreps, 100 µl bacterial suspensions was used to inoculate 250 ml LB-medium. The bacterial culture was grown overnight at 37 °C. DNA was subsequently purified using Qiagen Midi or Maxi kits according to the manufacturer's instructions.

5.2.11 Sequencing of DNA

All sequencing was carried out by GATC Biotech (Germany).

5.2.12 Luciferase sensor assay

HEK293T cells (1×10^5 cells/ well) were plated on a 24-well plate 24 hours before transfection. 300 ng from each sensor vector (*Wnt1*, *Pitx3*, *Lef1*, *Wnt5a*, *Wnt5b*, *Wnt6*, *Otx2*) was cotransfected with 30ng renilla luciferase vector (as internal transfection control (Table 18) and 10, 30, and/or 50 nM precursor miRNA (Table 17). For *miR-125b-5p* predicted target genes (*Sim1* and *Phox2b*), 900ng from each sensor vector was cotransfected with 30ng renilla luciferase and 30 nM precursor miRNA (Table 17). For overexpression of *miR-125b-5p* (*miR-125b OE*), 300ng sensor vector and 900ng *miR-125b OE* vector were cotransfected with 30ng renilla luciferase. All transfections were done using Lipofectamine 2000 according to the manufacturer's instructions. 48 hours after transfection, cells were lysed in passive lysis buffer and chemiluminescence was quantified with Dual-Glo Luciferase Assay (Promega) according to manufacturer's instructions. At least three individual experiments were performed in triplicate for each

condition. Control experiments were performed with Pre-miR Negative Control 1/2 (Table 17) or transfecting precursor miRNA and the “empty” pGL3 Promoter vector (without 3’UTR cloned into it).

5.2.13 Differentiation of mESCs into vMH neurons

The mESC line JM8 (C57BL/6N agouti) was propagated and maintained on gelatine-coated dishes in ES medium (Table 26). mESC differentiation into ventral mid-/hindbrain neuronal populations was carried out as described by (Lee et al., 2000) with minor modifications. Briefly, to induce EB formation (stage 2), the cells were dissociated into a single-cell suspension by 0.05 % trypsin treatment and plated on non-adherent bacterial culture dishes at a density of 2×10^6 cells/6 cm petri dish in EB medium. EB formation proceeded for four days, EBs were then plated onto an adhesive tissue culture surface (6 cm petri dish) coated with gelatin in EB cell medium. After 24 h of culture, selection of Nestin-positive cells (neural precursors, stage 3) was initiated by replacing the EB medium by serum-free Insulin/Transferrin/Selenium/Fibronectin (ITSFn) medium (Okabe et al., 1996) and proceeded for 6 days. Half of the ITSFn medium in each well was changed every third day. At stage 4 (expansion of Nestin⁺ neural precursors), cells were dissociated by treatment with 0.05% trypsin/0.04% EDTA, and plated on tissue culture plastic or glass coverslips at a concentration of $3-5 \times 10^5$ cells/6 cm petri dish in N2 medium modified according to (Johe et al., 1996) (DA neuron medium 1). Before cell plating, dishes and coverslips were pre-coated with polyornithine (15 mg/ml) and laminin (1 μ g/ml). Nestin⁺ cells were expanded for 4-6 days and medium was changed every third day. Finally, neuron differentiation (stage 5) was induced by removal of bFGF and cultured in DA neuron Medium 2 for 6 days.

5.2.14 Primary cell culture

5.2.14.1 Cover slip treatment and coating

12 mm Ø coverslips were washed with 100 % ethanol with a drop of HCl (32 %), microwave heated for 3 min, washed twice with 100 % ethanol and air dried before

autoclaving. Coverslips were incubated in Poly-D-Lysine (20 µg/ml) at 37 °C for 48 hours before plating of cells.

5.2.14.2 Primary vMH culture

Tissues comprising the ventral MHR were microdissected from E11.5 CD-1 embryos as described in (Pruszek et al., 2009) with some minor changes. Briefly, embryos were freed from extraembryonic membranes, approx. half of the midbrain and of the rostral hindbrain (including the MHB) were excised without prior skin removal, the neural tube was cut open dorsally to obtain an “open book” preparation as described in (Pruszek et al., 2009), and the skin/epidermis tissues were removed leaving only ‘open’ neural tube. Ventral part of the MH tissues was isolated by cutting along the sulcus limitans. The vMH tissue was incubated in 0.01 % trypsin with DNaseI for 5 min at 37°C, and triturated with a 1 ml pipette to obtain a single-cell suspension. Living cells were counted by Trypan blue exclusion in a hemocytometer. Approximately 4×10^5 cells per well were plated on Poly-D-Lysin coated coverslips in a 24-well plate and kept in differentiation medium (Table 26). Three hours after plating, cells were transduced/infected with the corresponding virus (see section 5.2.6.5). Cells were fixed for immunostaining (see 2.2.14.3) or total RNA was collected (see 2.2.15) after 3 or 5 days *in vitro* (DIV).

5.2.14.3 EdU treatment and staining

Three hours before harvesting primary cultures of 3/5 days, 1 µl of EdU (10 mM) was added into incubating cells. Cover slips were then fixed in 4 % paraffin for 15 min, immediately processed using the Click-iTTM EdU Alexa Fluor® 488 Imaging Kit according to the manufacturer’s instructions, and double-labeled with Nkx6-1 antibody.

5.2.14.4 Immunocytochemistry

Primary vMH and differentiated mESCs on coverslips were fixed in 4% PFA for 15 min, rinsed in PBS, permeabilized in 0.05 % Triton-X100, and incubated in blocking solution (see Table 14) for 10 min at RT. Cover slips were incubated in the primary antibody in blocking solution overnight at 4 °C, rinsed twice in PBS and incubated in the secondary antibody in blocking solution for 90 min at RT. Subsequently, cover slips were rinsed twice in PBS (5 min each), and incubated with DAPI for nuclear staining before mounting the coverslips in Poly Aqua Mount.

5.2.14.5 Cell counting

Cells from primary vMH cultures were counted in 25-30 random fields per coverslip/treatment, and data were collected from at least three independent experiments.

5.2.15 Isolation of total RNA

Total RNA was extracted from primary vMH cells or differentiating mESCs using TRIzol reagent according to the manufacturer's instructions.

5.2.16 cDNA synthesis

1µg total RNA was reverse transcribed into cDNA using iScript cDNA synthesis kit according to the manufacturer's protocol. Reverse transcription without reverse transcriptase served as negative control.

5.2.17 Quantitative RT-PCR (qPCR) for detection of mRNAs

Quantitative (real time) PCR was performed on an ABI PRISM 7900HT Sequence Detection System (Applied Biosystems), using Taqman Real Time PCR Master Mix kit (Applied Biosystems), cDNA (appr. 15 ng/well) and the primers indicated in Table 25. The amplification conditions were an initial step at 95 °C for 10 min, followed by 45

cycles of 20 s at 95°C and 1 min at 60°C. All reactions were done in triplicate, and each experiment was repeated at least 3 times. The Ct value was recorded for each reaction, and the expression level of each mRNA was calculated relative to *Actb* (*b-actin*). Data are presented as target gene expression = $2^{-\Delta Ct}$, with $\Delta Ct = (\text{target gene Ct} - \text{Actb Ct})$ according to the $2^{-\Delta Ct}$ method described by (Livak and Schmittgen, 2001). Reactions without cDNA/template served as a negative control.

5.2.18 Next generation sequencing (NGS) for miRNA expression profiling of differentiating mESC

All next generation sequencing assays were performed in the lab of Dr. W. Chen at the Max Delbrück Centre for Molecular Medicine (MDC), Berlin. In brief, samples (cells from a 6 cm Ø dish or from 2 wells of 6-well plate) were collected from JM8 (C57BL/6N agouti) mESC (Pettitt et al., 2009) (Stage 1), Nestin⁺ neural precursor cells (Stage 3) and differentiated neurons (Stage 5), and total RNA was extracted/isolated using Trizol Reagent. The small RNA fraction with a size range of 10–40 nt was separated using flashPAGE Fractionator (Ambion, USA) according to the manufacturer's instructions, ligated with synthetic RNA adapters, reverse transcribed and amplified using Illumina (Illumina, USA) sequencing primers. The adapter-ligated libraries were sequenced for 36 cycles on the Illumina/GAII sequencer according to the manufacturer's instructions. For the mapping of small RNA sequencing reads, 3' adapter sequences were first removed from the sequencing reads using an in-house Perl script (MDC Berlin, Germany). The reads between 17 and 30 nt were retained and mapped to known mouse pre-miRNA sequences deposited in miRBase (v16.0) (Kozomara and Griffiths-Jones), without any mismatches using soap.short software (Li et al., 2008). Down- or upregulated miRNAs in the different stages of the mESC differentiation paradigm (Lee et al., 2000) were determined by comparing terminally differentiated neuron (stage 5) to undifferentiated mESCs (Stage 1) samples, after excluding the very low-abundance miRNAs (<10 sequencing reads in the control sample).

5.2.19 Statistical Analyses

Cell countings, luminescence and qPCR values were averaged according to treatment, and luminescence and qPCR values were normalized to the internal control. All data are expressed as the mean±SEM or mean±sd from at least three independent experiments unless otherwise stated. The Student's *t*-Test (two-tailed, two-sample equal variance) was used to evaluate the significance of differences in experimental results. Differences were considered statistically significant at $p < 0.05$. One asterisk corresponds to $p < 0.05$, two asterisks correspond to $p < 0.01$ and three asterisks correspond to $p < 0.001$.

5.2.20 X-Gal histochemistry

5.2.20.1 Whole mount X-gal staining

Embryos were fixed in 4% PFA for 10-20 min depending on age (E9.5-E14.5), washed once in Wash Buffer (Table 14) for 15 min and stained with X-Gal buffer (Table 14) for 3-24 hours protected from light. After successful staining, embryos were rinsed in Wash Buffer and post-fixed in 4 % PFA. For storage, the embryos were transferred into PBS. Embryos selected for sectioning were dehydrated and sectioned as described before (section 5.2.3.2).

5.2.20.2 X-Gal staining on cryosections

For X-Gal staining on cryosections, the embryos/brains were dissection in cold PBS and cryoprotected in 20% sucrose overnight (storage possible). Cryoprotected embryos/brains were embedded in NEG-50™, and sectioned on a cryotome at 20 μm. After mounting on microscope slides and before staining, the sections were fixed for 30 min with 4 % PFA in PBS and washed with Wash Buffer (Table 14) 3 times for 5 minutes. X-Gal staining solution (Table 14) was applied on the slides and incubated overnight in a humid chamber in the dark. After successful staining, the slides were rinsed in Wash Buffer (Table 14) for 30 s and fixed overnight in 4% PFA in PBS. The next day, the slides were washed in 3 times in PBS (5 minutes each) and mounted with Aqua-Poly/Mount.

5.2.21 Microscopy

Images were taken using bright and dark field optics on an Axioplan2 microscope, AxioCam MRc camera, and Axiovision 4.6 software (Zeiss) and processed with Adobe Photoshop 7.0 or CS3 and Illustrator software (Adobe Systems). Graphs and statistical analyses were generated with Microsoft Excel or SigmaPlot 12.0, or SigmaStat 3.5 software.

6.0 References

- Agarwala S, Ragsdale CW (2002) A role for midbrain arcs in nucleogenesis. *Development* 129:5779-5788.
- Altmann CR, Brivanlou AH (2001) Neural patterning in the vertebrate embryo. *Int Rev Cytol* 203:447-482.
- Ang SL (2006) Transcriptional control of midbrain dopaminergic neuron development. *Development* 133:3499-3506.
- Ason B, Darnell DK, Wittbrodt B, Berezikov E, Kloosterman WP, Wittbrodt J, Antin PB, Plasterk RH (2006) Differences in vertebrate microRNA expression. *Proc Natl Acad Sci U S A* 103:14385-14389.
- Bak M, Silahatoglu A, Moller M, Christensen M, Rath MF, Skryabin B, Tommerup N, Kauppinen S (2008) MicroRNA expression in the adult mouse central nervous system. *Rna* 14:432-444.
- Bartel DP (2004) MicroRNAs: genomics, biogenesis, mechanism, and function. *Cell* 116:281-297.
- Bartel DP, Chen CZ (2004) Micromanagers of gene expression: the potentially widespread influence of metazoan microRNAs. *Nat Rev Genet* 5:396-400.
- Bibel M, Richter J, Schrenk K, Tucker KL, Staiger V, Korte M, Goetz M, Barde YA (2004) Differentiation of mouse embryonic stem cells into a defined neuronal lineage. *Nat Neurosci* 7:1003-1009.
- Bohnsack MT, Czaplinski K, Gorlich D (2004) Exportin 5 is a RanGTP-dependent dsRNA-binding protein that mediates nuclear export of pre-miRNAs. *Rna* 10:185-191.
- Boissart C, Nissan X, Giraud-Triboult K, Peschanski M, Benchoua A (2012) miR-125 potentiates early neural specification of human embryonic stem cells. *Development* 139:1247-1257.
- Bosley TM, Oystreck DT, Robertson RL, al Awad A, Abu-Amero K, Engle EC (2006) Neurological features of congenital fibrosis of the extraocular muscles type 2 with mutations in PHOX2A. *Brain* 129:2363-2374.
- Briscoe J, Pierani A, Jessell TM, Ericson J (2000) A homeodomain protein code specifies progenitor cell identity and neuronal fate in the ventral neural tube. *Cell* 101:435-445.
- Broihier HT, Kuzin A, Zhu Y, Odenwald W, Skeath JB (2004) Drosophila homeodomain protein Nkx6 coordinates motoneuron subtype identity and axonogenesis. *Development* 131:5233-5242.
- Cambronero F, Puelles L (2000) Rostrocaudal nuclear relationships in the avian medulla oblongata: a fate map with quail chick chimeras. *J Comp Neurol* 427:522-545.
- Chandrasekar V, Dreyer JL (2011) Regulation of MiR-124, Let-7d, and MiR-181a in the accumbens affects the expression, extinction, and reinstatement of cocaine-induced conditioned place preference. *Neuropsychopharmacology* 36:1149-1164.
- Chang SJ, Weng SL, Hsieh JY, Wang TY, Chang MD, Wang HW (2011) MicroRNA-34a modulates genes involved in cellular motility and oxidative phosphorylation in neural precursors derived from human umbilical cord mesenchymal stem cells. *BMC Med Genomics* 4:65.
- Chao J, Nestler EJ (2004) Molecular neurobiology of drug addiction. *Annu Rev Med* 55:113-132.
- Chehrehasa F, Meedeniya AC, Dwyer P, Abrahamsen G, Mackay-Sim A (2009) EdU, a new thymidine analogue for labelling proliferating cells in the nervous system. *J Neurosci Methods* 177:122-130.
- Chen C, Ridzon D, Lee CT, Blake J, Sun Y, Strauss WM (2007) Defining embryonic stem cell identity using differentiation-related microRNAs and their potential targets. *Mamm Genome* 18:316-327.

- Chiang C, Litingtung Y, Lee E, Young KE, Corden JL, Westphal H, Beachy PA (1996) Cyclopia and defective axial patterning in mice lacking Sonic hedgehog gene function. *Nature* 383:407-413.
- Coppola E, Pattyn A, Guthrie SC, Goridis C, Studer M (2005) Reciprocal gene replacements reveal unique functions for Phox2 genes during neural differentiation. *Embo J* 24:4392-4403.
- Crossley PH, Martin GR (1995) The mouse Fgf8 gene encodes a family of polypeptides and is expressed in regions that direct outgrowth and patterning in the developing embryo. *Development* 121:439-451.
- Davis TH, Cuellar TL, Koch SM, Barker AJ, Harfe BD, McManus MT, Ullian EM (2008) Conditional loss of Dicer disrupts cellular and tissue morphogenesis in the cortex and hippocampus. *J Neurosci* 28:4322-4330.
- Deneris ES, Wyler SC (2012) Serotonergic transcriptional networks and potential importance to mental health. *Nat Neurosci* 15:519-527.
- Denli AM, Tops BB, Plasterk RH, Ketting RF, Hannon GJ (2004) Processing of primary microRNAs by the Microprocessor complex. *Nature* 432:231-235.
- Dogini DB, Ribeiro PA, Rocha C, Pereira TC, Lopes-Cendes I (2008) MicroRNA expression profile in murine central nervous system development. *J Mol Neurosci* 35:331-337.
- Duursma AM, Kedde M, Schrier M, le Sage C, Agami R (2008) miR-148 targets human DNMT3b protein coding region. *Rna* 14:872-877.
- Dyson N (1998) The regulation of E2F by pRB-family proteins. *Genes Dev* 12:2245-2262.
- Ebert MS, Neilson JR, Sharp PA (2007) MicroRNA sponges: competitive inhibitors of small RNAs in mammalian cells. *Nat Methods* 4:721-726.
- Echelard Y, Epstein DJ, St-Jacques B, Shen L, Mohler J, McMahon JA, McMahon AP (1993) Sonic hedgehog, a member of a family of putative signaling molecules, is implicated in the regulation of CNS polarity. *Cell* 75:1417-1430.
- Echevarria D, Vieira C, Gimeno L, Martinez S (2003) Neuroepithelial secondary organizers and cell fate specification in the developing brain. *Brain Res Brain Res Rev* 43:179-191.
- Edbauer D, Neilson JR, Foster KA, Wang CF, Seeburg DP, Batterson MN, Tada T, Dolan BM, Sharp PA, Sheng M (2010) Regulation of synaptic structure and function by FMRP-associated microRNAs miR-125b and miR-132. *Neuron* 65:373-384.
- Epstein DJ, McMahon AP, Joyner AL (1999) Regionalization of Sonic hedgehog transcription along the anteroposterior axis of the mouse central nervous system is regulated by Hnf3-dependent and -independent mechanisms. *Development* 126:281-292.
- Evinger C (1988) Extraocular motor nuclei: location, morphology and afferents. *Rev Oculomot Res* 2:81-117.
- Fan CM, Kuwana E, Bulfone A, Fletcher CF, Copeland NG, Jenkins NA, Crews S, Martinez S, Puellas L, Rubenstein JL, Tessier-Lavigne M (1996) Expression patterns of two murine homologs of *Drosophila* single-minded suggest possible roles in embryonic patterning and in the pathogenesis of Down syndrome. *Mol Cell Neurosci* 7:1-16.
- Ferretti E, De Smaele E, Miele E, Laneve P, Po A, Pelloni M, Paganelli A, Di Marcotullio L, Caffarelli E, Screpanti I, Bozzoni I, Gulino A (2008) Concerted microRNA control of Hedgehog signalling in cerebellar neuronal progenitor and tumour cells. *Embo J* 27:2616-2627.
- Friedman RC, Farh KK, Burge CB, Bartel DP (2009) Most mammalian mRNAs are conserved targets of microRNAs. *Genome Res* 19:92-105.
- Geekiyana H, Chan C (2011) MicroRNA-137/181c regulates serine palmitoyltransferase and in turn amyloid beta, novel targets in sporadic Alzheimer's disease. *J Neurosci* 31:14820-14830.
- Gregory RI, Shiekhattar R (2005) MicroRNA biogenesis and cancer. *Cancer Res* 65:3509-3512.

- Griffiths-Jones S, Grocock RJ, van Dongen S, Bateman A, Enright AJ (2006) miRBase: microRNA sequences, targets and gene nomenclature. *Nucleic Acids Res* 34:D140-144.
- Guo S, Brush J, Teraoka H, Goddard A, Wilson SW, Mullins MC, Rosenthal A (1999) Development of noradrenergic neurons in the zebrafish hindbrain requires BMP, FGF8, and the homeodomain protein soulless/Phox2a. *Neuron* 24:555-566.
- Helin K (1998) Regulation of cell proliferation by the E2F transcription factors. *Curr Opin Genet Dev* 8:28-35.
- Hornykiewicz O (1978) Psychopharmacological implications of dopamine and dopamine antagonists: a critical evaluation of current evidence. *Neuroscience* 3:773-783.
- Hsu PW, Huang HD, Hsu SD, Lin LZ, Tsou AP, Tseng CP, Stadler PF, Washietl S, Hofacker IL (2006) miRNAMap: genomic maps of microRNA genes and their target genes in mammalian genomes. *Nucleic Acids Res* 34:D135-139.
- Hsu SD, Chu CH, Tsou AP, Chen SJ, Chen HC, Hsu PW, Wong YH, Chen YH, Chen GH, Huang HD (2008) miRNAMap 2.0: genomic maps of microRNAs in metazoan genomes. *Nucleic Acids Res* 36:D165-169.
- Huang L, Luo J, Cai Q, Pan Q, Zeng H, Guo Z, Dong W, Huang J, Lin T (2010) MicroRNA-125b suppresses the development of bladder cancer by targeting E2F3. *Int J Cancer* 128:1758-1769.
- Hurd PJ, Nelson CJ (2009) Advantages of next-generation sequencing versus the microarray in epigenetic research. *Brief Funct Genomic Proteomic* 8:174-183.
- Hutchinson SA, Cheesman SE, Hale LA, Boone JQ, Eisen JS (2007) Nkx6 proteins specify one zebrafish primary motoneuron subtype by regulating late islet1 expression. *Development* 134:1671-1677.
- Hutvagner G, McLachlan J, Pasquinelli AE, Balint E, Tuschl T, Zamore PD (2001) A cellular function for the RNA-interference enzyme Dicer in the maturation of the let-7 small temporal RNA. *Science* 293:834-838.
- Hynes M, Porter JA, Chiang C, Chang D, Tessier-Lavigne M, Beachy PA, Rosenthal A (1995) Induction of midbrain dopaminergic neurons by Sonic hedgehog. *Neuron* 15:35-44.
- Jeong Y, Epstein DJ (2003) Distinct regulators of Shh transcription in the floor plate and notochord indicate separate origins for these tissues in the mouse node. *Development* 130:3891-3902.
- Johe KK, Hazel TG, Muller T, Dugich-Djordjevic MM, McKay RD (1996) Single factors direct the differentiation of stem cells from the fetal and adult central nervous system. *Genes Dev* 10:3129-3140.
- Jopling CL, Yi M, Lancaster AM, Lemon SM, Sarnow P (2005) Modulation of hepatitis C virus RNA abundance by a liver-specific MicroRNA. *Science* 309:1577-1581.
- Kapsimali M, Kloosterman WP, de Bruijn E, Rosa F, Plasterk RH, Wilson SW (2007) MicroRNAs show a wide diversity of expression profiles in the developing and mature central nervous system. *Genome Biol* 8:R173.
- Ketting RF (2011) microRNA Biogenesis and Function : An overview. *Adv Exp Med Biol* 700:1-14.
- Khvorova A, Reynolds A, Jayasena SD (2003) Functional siRNAs and miRNAs exhibit strand bias. *Cell* 115:209-216.
- Kim J, Krichevsky A, Grad Y, Hayes GD, Kosik KS, Church GM, Ruvkun G (2004) Identification of many microRNAs that copurify with polyribosomes in mammalian neurons. *Proc Natl Acad Sci U S A* 101:360-365.
- Kim J, Inoue K, Ishii J, Vanti WB, Voronov SV, Murchison E, Hannon G, Abeliovich A (2007) A MicroRNA feedback circuit in midbrain dopamine neurons. *Science* 317:1220-1224.
- Kozomara A, Griffiths-Jones S miRBase: integrating microRNA annotation and deep-sequencing data. *Nucleic Acids Res* 39:D152-157.

- Kozomara A, Griffiths-Jones S (2011) miRBase: integrating microRNA annotation and deep-sequencing data. *Nucleic Acids Res* 39:D152-157.
- Krek A, Grun D, Poy MN, Wolf R, Rosenberg L, Epstein EJ, MacMenamin P, da Piedade I, Gunsalus KC, Stoffel M, Rajewsky N (2005) Combinatorial microRNA target predictions. *Nat Genet* 37:495-500.
- Krichevsky AM, Sonntag KC, Isacson O, Kosik KS (2006) Specific microRNAs modulate embryonic stem cell-derived neurogenesis. *Stem Cells* 24:857-864.
- Kuhn DE, Nuovo GJ, Martin MM, Malana GE, Pleister AP, Jiang J, Schmittgen TD, Terry AV, Jr., Gardiner K, Head E, Feldman DS, Elton TS (2008) Human chromosome 21-derived miRNAs are overexpressed in down syndrome brains and hearts. *Biochem Biophys Res Commun* 370:473-477.
- Lagos-Quintana M, Rauhut R, Yalcin A, Meyer J, Lendeckel W, Tuschl T (2002) Identification of tissue-specific microRNAs from mouse. *Curr Biol* 12:735-739.
- Lau P, Verrier JD, Nielsen JA, Johnson KR, Notterpek L, Hudson LD (2008) Identification of dynamically regulated microRNA and mRNA networks in developing oligodendrocytes. *J Neurosci* 28:11720-11730.
- Le MT, Teh C, Shyh-Chang N, Xie H, Zhou B, Korzh V, Lodish HF, Lim B (2009a) MicroRNA-125b is a novel negative regulator of p53. *Genes Dev* 23:862-876.
- Le MT, Xie H, Zhou B, Chia PH, Rizk P, Um M, Udolph G, Yang H, Lim B, Lodish HF (2009b) MicroRNA-125b promotes neuronal differentiation in human cells by repressing multiple targets. *Mol Cell Biol* 29:5290-5305.
- Le MT, Shyh-Chang N, Khaw SL, Chin L, Teh C, Tay J, O'Day E, Korzh V, Yang H, Lal A, Lieberman J, Lodish HF, Lim B (2011) Conserved regulation of p53 network dosage by microRNA-125b occurs through evolving miRNA-target gene pairs. *PLoS Genet* 7:e1002242.
- Lee KJ, Jessell TM (1999) The specification of dorsal cell fates in the vertebrate central nervous system. *Annu Rev Neurosci* 22:261-294.
- Lee RC, Feinbaum RL, Ambros V (1993) The *C. elegans* heterochronic gene *lin-4* encodes small RNAs with antisense complementarity to *lin-14*. *Cell* 75:843-854.
- Lee SH, Lumelsky N, Studer L, Auerbach JM, McKay RD (2000) Efficient generation of midbrain and hindbrain neurons from mouse embryonic stem cells. *Nat Biotechnol* 18:675-679.
- Lee YS, Kim HK, Chung S, Kim KS, Dutta A (2005) Depletion of human micro-RNA miR-125b reveals that it is critical for the proliferation of differentiated cells but not for the down-regulation of putative targets during differentiation. *J Biol Chem* 280:16635-16641.
- Leucht C, Stigloher C, Wizenmann A, Klafke R, Folchert A, Bally-Cuif L (2008) MicroRNA-9 directs late organizer activity of the midbrain-hindbrain boundary. *Nat Neurosci* 11:641-648.
- Li R, Li Y, Kristiansen K, Wang J (2008) SOAP: short oligonucleotide alignment program. *Bioinformatics* 24:713-714.
- Lin W, Metzakopian E, Mavromatakis YE, Gao N, Balaskas N, Sasaki H, Briscoe J, Whitsett JA, Goulding M, Kaestner KH, Ang SL (2009) *Foxa1* and *Foxa2* function both upstream of and cooperatively with *Lmx1a* and *Lmx1b* in a feedforward loop promoting mesodiencephalic dopaminergic neuron development. *Dev Biol* 333:386-396.
- Liu H, Kohane IS (2009) Tissue and process specific microRNA-mRNA co-expression in mammalian development and malignancy. *PLoS One* 4:e5436.
- Livak KJ, Schmittgen TD (2001) Analysis of relative gene expression data using real-time quantitative PCR and the 2⁻(Delta Delta C(T)) Method. *Methods* 25:402-408.
- Lo L, Morin X, Brunet JF, Anderson DJ (1999) Specification of neurotransmitter identity by *Phox2* proteins in neural crest stem cells. *Neuron* 22:693-705.

- Lois C, Hong EJ, Pease S, Brown EJ, Baltimore D (2002) Germline transmission and tissue-specific expression of transgenes delivered by lentiviral vectors. *Science* 295:868-872.
- Lugli G, Torvik VI, Larson J, Smalheiser NR (2008) Expression of microRNAs and their precursors in synaptic fractions of adult mouse forebrain. *J Neurochem* 106:650-661.
- Lumsden A (2004) Segmentation and compartment in the early avian hindbrain. *Mech Dev* 121:1081-1088.
- Lytle JR, Yario TA, Steitz JA (2007) Target mRNAs are repressed as efficiently by microRNA-binding sites in the 5' UTR as in the 3' UTR. *Proc Natl Acad Sci U S A* 104:9667-9672.
- Martinez S (2001) The isthmus organizer and brain regionalization. *Int J Dev Biol* 45:367-371.
- Massion J (1967) The mammalian red nucleus. *Physiol Rev* 47:383-436.
- McMahon AP (2000) Neural patterning: the role of Nkx genes in the ventral spinal cord. *Genes Dev* 14:2261-2264.
- McMahon AP, Moon RT (1989) int-1--a proto-oncogene involved in cell signalling. *Development* 107 Suppl:161-167.
- Miranda KC, Huynh T, Tay Y, Ang YS, Tam WL, Thomson AM, Lim B, Rigoutsos I (2006) A pattern-based method for the identification of MicroRNA binding sites and their corresponding heteroduplexes. *Cell* 126:1203-1217.
- Mishima T, Mizuguchi Y, Kawahigashi Y, Takizawa T, Takizawa T (2007) RT-PCR-based analysis of microRNA (miR-1 and -124) expression in mouse CNS. *Brain Res* 1131:37-43.
- Mizuno Y, Yagi K, Tokuzawa Y, Kanasaki-Yatsuka Y, Suda T, Katagiri T, Fukuda T, Maruyama M, Okuda A, Amemiya T, Kondoh Y, Tashiro H, Okazaki Y (2008) miR-125b inhibits osteoblastic differentiation by down-regulation of cell proliferation. *Biochem Biophys Res Commun* 368:267-272.
- Morin X, Cremer H, Hirsch MR, Kapur RP, Goridis C, Brunet JF (1997) Defects in sensory and autonomic ganglia and absence of locus coeruleus in mice deficient for the homeobox gene Phox2a. *Neuron* 18:411-423.
- Morton SU, Scherz PJ, Cordes KR, Ivey KN, Stainier DY, Srivastava D (2008) microRNA-138 modulates cardiac patterning during embryonic development. *Proc Natl Acad Sci U S A* 105:17830-17835.
- Muller H, Bracken AP, Vernell R, Moroni MC, Christians F, Grassilli E, Prosperini E, Vigo E, Oliner JD, Helin K (2001) E2Fs regulate the expression of genes involved in differentiation, development, proliferation, and apoptosis. *Genes Dev* 15:267-285.
- Nakatani T, Minaki Y, Kumai M, Ono Y (2007) Helt determines GABAergic over glutamatergic neuronal fate by repressing Ngn genes in the developing mesencephalon. *Development* 134:2783-2793.
- Nakatani T, Kumai M, Mizuhara E, Minaki Y, Ono Y (2010) Lmx1a and Lmx1b cooperate with Foxa2 to coordinate the specification of dopaminergic neurons and control of floor plate cell differentiation in the developing mesencephalon. *Dev Biol* 339:101-113.
- O'Rourke JR, Swanson MS, Harfe BD (2006) MicroRNAs in mammalian development and tumorigenesis. *Birth Defects Res C Embryo Today* 78:172-179.
- Obernosterer G, Leuschner PJ, Alenius M, Martinez J (2006) Post-transcriptional regulation of microRNA expression. *Rna* 12:1161-1167.
- Okabe S, Forsberg-Nilsson K, Spiro AC, Segal M, McKay RD (1996) Development of neuronal precursor cells and functional postmitotic neurons from embryonic stem cells in vitro. *Mech Dev* 59:89-102.
- Orom UA, Nielsen FC, Lund AH (2008) MicroRNA-10a binds the 5'UTR of ribosomal protein mRNAs and enhances their translation. *Mol Cell* 30:460-471.
- Pattyn A, Goridis C, Brunet JF (2000a) Specification of the central noradrenergic phenotype by the homeobox gene Phox2b. *Mol Cell Neurosci* 15:235-243.

- Pattyn A, Hirsch M, Goridis C, Brunet JF (2000b) Control of hindbrain motor neuron differentiation by the homeobox gene *Phox2b*. *Development* 127:1349-1358.
- Pattyn A, Morin X, Cremer H, Goridis C, Brunet JF (1997) Expression and interactions of the two closely related homeobox genes *Phox2a* and *Phox2b* during neurogenesis. *Development* 124:4065-4075.
- Pattyn A, Simplicio N, van Doorninck JH, Goridis C, Guillemot F, Brunet JF (2004) *Ascl1/Mash1* is required for the development of central serotonergic neurons. *Nat Neurosci* 7:589-595.
- Pellegrini M, Pantano S, Fumi MP, Lucchini F, Forabosco A (2001) Agenesis of the scapula in *Emx2* homozygous mutants. *Dev Biol* 232:149-156.
- Perez-Balaguer A, Puelles E, Wurst W, Martinez S (2009) Shh dependent and independent maintenance of basal midbrain. *Mech Dev* 126:301-313.
- Pettitt SJ, Liang Q, Rairdan XY, Moran JL, Prosser HM, Beier DR, Lloyd KC, Bradley A, Skarnes WC (2009) Agouti C57BL/6N embryonic stem cells for mouse genetic resources. *Nat Methods* 6:493-495.
- Pillai RS (2005) MicroRNA function: multiple mechanisms for a tiny RNA? *Rna* 11:1753-1761.
- Prakash N, Wurst W (2006) Genetic networks controlling the development of midbrain dopaminergic neurons. *J Physiol* 575:403-410.
- Prakash N, Puelles E, Freude K, Trumbach D, Omodei D, Di Salvio M, Sussel L, Ericson J, Sander M, Simeone A, Wurst W (2009) *Nkx6-1* controls the identity and fate of red nucleus and oculomotor neurons in the mouse midbrain. *Development* 136:2545-2555.
- Prakash N, Brodski C, Naserke T, Puelles E, Gogoi R, Hall A, Panhuysen M, Echevarria D, Sussel L, Weisenhorn DM, Martinez S, Arenas E, Simeone A, Wurst W (2006) A *Wnt1*-regulated genetic network controls the identity and fate of midbrain-dopaminergic progenitors in vivo. *Development* 133:89-98.
- Pruszk J, Just L, Isacson O, Nikkhah G (2009) Isolation and culture of ventral mesencephalic precursor cells and dopaminergic neurons from rodent brains. *Curr Protoc Stem Cell Biol* Chapter 2:Unit 2D 5.
- Puelles E (2007) Genetic control of basal midbrain development. *J Neurosci Res* 85:3530-3534.
- Puelles E, Annino A, Tuorto F, Usiello A, Acampora D, Czerny T, Brodski C, Ang SL, Wurst W, Simeone A (2004) *Otx2* regulates the extent, identity and fate of neuronal progenitor domains in the ventral midbrain. *Development* 131:2037-2048.
- Puelles L, Rubenstein JL (2003) Forebrain gene expression domains and the evolving prosomeric model. *Trends Neurosci* 26:469-476.
- Reinhart BJ, Slack FJ, Basson M, Pasquinelli AE, Bettinger JC, Rougvie AE, Horvitz HR, Ruvkun G (2000) The 21-nucleotide *let-7* RNA regulates developmental timing in *Caenorhabditis elegans*. *Nature* 403:901-906.
- Rybak A, Fuchs H, Smirnova L, Brandt C, Pohl EE, Nitsch R, Wulczyn FG (2008) A feedback loop comprising *lin-28* and *let-7* controls pre-*let-7* maturation during neural stem-cell commitment. *Nat Cell Biol* 10:987-993.
- Saba R, Storchel PH, Aksoy-Aksel A, Kepura F, Lippi G, Plant TD, Schrott GM (2012) Dopamine-Regulated MicroRNA *MiR-181a* Controls *GluA2* Surface Expression in Hippocampal Neurons. *Mol Cell Biol* 32:619-632.
- Sander M, Paydar S, Ericson J, Briscoe J, Berber E, German M, Jessell TM, Rubenstein JL (2000) Ventral neural patterning by *Nkx* homeobox genes: *Nkx6.1* controls somatic motor neuron and ventral interneuron fates. *Genes Dev* 14:2134-2139.
- Schmidt T, Mewes HW, Stumpflen V (2009) A novel putative miRNA target enhancer signal. *PLoS One* 4:e6473.

- Sempere LF, Freemantle S, Pitha-Rowe I, Moss E, Dmitrovsky E, Ambros V (2004) Expression profiling of mammalian microRNAs uncovers a subset of brain-expressed microRNAs with possible roles in murine and human neuronal differentiation. *Genome Biol* 5:R13.
- Sethupathy P, Megraw M, Hatzigeorgiou AG (2006) A guide through present computational approaches for the identification of mammalian microRNA targets. *Nat Methods* 3:881-886.
- Shimamura K, Hartigan DJ, Martinez S, Puellas L, Rubenstein JL (1995) Longitudinal organization of the anterior neural plate and neural tube. *Development* 121:3923-3933.
- Silber J, Lim DA, Petritsch C, Persson AI, Maunakea AK, Yu M, Vandenberg SR, Ginzinger DG, James CD, Costello JF, Bergers G, Weiss WA, Alvarez-Buylla A, Hodgson JG (2008) miR-124 and miR-137 inhibit proliferation of glioblastoma multiforme cells and induce differentiation of brain tumor stem cells. *BMC Med* 6:14.
- Simeone A (2005) Genetic control of dopaminergic neuron differentiation. *Trends Neurosci* 28:62-65; discussion 65-66.
- Smidt MP, Burbach JP (2007) How to make a mesodiencephalic dopaminergic neuron. *Nat Rev Neurosci* 8:21-32.
- Smits SM, Burbach JP, Smidt MP (2006) Developmental origin and fate of meso-diencephalic dopamine neurons. *Prog Neurobiol* 78:1-16.
- Smrt RD, Szulwach KE, Pfeiffer RL, Li X, Guo W, Pathania M, Teng ZQ, Luo Y, Peng J, Bordey A, Jin P, Zhao X (2010) MicroRNA miR-137 regulates neuronal maturation by targeting ubiquitin ligase mind bomb-1. *Stem Cells* 28:1060-1070.
- Soriano P (1999) Generalized lacZ expression with the ROSA26 Cre reporter strain. *Nat Genet* 21:70-71.
- Stanke M, Junghans D, Geissen M, Goridis C, Ernsberger U, Rohrer H (1999) The Phox2 homeodomain proteins are sufficient to promote the development of sympathetic neurons. *Development* 126:4087-4094.
- Stark KL, Xu B, Bagchi A, Lai WS, Liu H, Hsu R, Wan X, Pavlidis P, Mills AA, Karayiorgou M, Gogos JA (2008) Altered brain microRNA biogenesis contributes to phenotypic deficits in a 22q11-deletion mouse model. *Nat Genet* 40:751-760.
- Suh MR, Lee Y, Kim JY, Kim SK, Moon SH, Lee JY, Cha KY, Chung HM, Yoon HS, Moon SY, Kim VN, Kim KS (2004) Human embryonic stem cells express a unique set of microRNAs. *Dev Biol* 270:488-498.
- Tay Y, Zhang J, Thomson AM, Lim B, Rigoutsos I (2008) MicroRNAs to Nanog, Oct4 and Sox2 coding regions modulate embryonic stem cell differentiation. *Nature* 455:1124-1128.
- Thomas SA, Matsumoto AM, Palmiter RD (1995) Noradrenaline is essential for mouse fetal development. *Nature* 374:643-646.
- Tomari Y, Zamore PD (2005) MicroRNA biogenesis: drosha can't cut it without a partner. *Curr Biol* 15:R61-64.
- Valarche I, Tissier-Seta JP, Hirsch MR, Martinez S, Goridis C, Brunet JF (1993) The mouse homeodomain protein Phox2 regulates Ncam promoter activity in concert with Cux/CDP and is a putative determinant of neurotransmitter phenotype. *Development* 119:881-896.
- Vallstedt A, Muhr J, Pattyn A, Pierani A, Mendelsohn M, Sander M, Jessell TM, Ericson J (2001) Different levels of repressor activity assign redundant and specific roles to Nkx6 genes in motor neuron and interneuron specification. *Neuron* 31:743-755.
- Wang Y, Keys DN, Au-Young JK, Chen C (2009) MicroRNAs in embryonic stem cells. *J Cell Physiol* 218:251-255.

- Wang Y, Baskerville S, Shenoy A, Babiarz JE, Baehner L, Blelloch R (2008) Embryonic stem cell-specific microRNAs regulate the G1-S transition and promote rapid proliferation. *Nat Genet* 40:1478-1483.
- Wightman B, Ha I, Ruvkun G (1993) Posttranscriptional regulation of the heterochronic gene *lin-14* by *lin-4* mediates temporal pattern formation in *C. elegans*. *Cell* 75:855-862.
- Williams AH, Valdez G, Moresi V, Qi X, McAnally J, Elliott JL, Bassel-Duby R, Sanes JR, Olson EN (2009) MicroRNA-206 delays ALS progression and promotes regeneration of neuromuscular synapses in mice. *Science* 326:1549-1554.
- Winkler C, Kirik D, Bjorklund A (2005) Cell transplantation in Parkinson's disease: how can we make it work? *Trends Neurosci* 28:86-92.
- Wong SS, Ritner C, Ramachandran S, Aurigui J, Pitt C, Chandra P, Ling VB, Yabut O, Bernstein HS (2012) miR-125b Promotes Early Germ Layer Specification through *Lin28/let-7d* and Preferential Differentiation of Mesoderm in Human Embryonic Stem Cells. *PLoS One* 7:e36121.
- Wu L, Belasco JG (2005) Micro-RNA regulation of the mammalian *lin-28* gene during neuronal differentiation of embryonal carcinoma cells. *Mol Cell Biol* 25:9198-9208.
- Wu S, Lin Y, Xu D, Chen J, Shu M, Zhou Y, Zhu W, Su X, Zhou Y, Qiu P, Yan G (2011) MiR-135a functions as a selective killer of malignant glioma. *Oncogene*.
- Yang Z, Wu J (2006) Small RNAs and development. *Med Sci Monit* 12:RA125-129.
- Ye W, Shimamura K, Rubenstein JL, Hynes MA, Rosenthal A (1998) FGF and Shh signals control dopaminergic and serotonergic cell fate in the anterior neural plate. *Cell* 93:755-766.
- Zeng C, Pan F, Jones LA, Lim MM, Griffin EA, Sheline YI, Mintun MA, Holtzman DM, Mach RH (2010) Evaluation of 5-ethynyl-2'-deoxyuridine staining as a sensitive and reliable method for studying cell proliferation in the adult nervous system. *Brain Res* 1319:21-32.
- Zhang L, Stokes N, Polak L, Fuchs E (2011) Specific microRNAs are preferentially expressed by skin stem cells to balance self-renewal and early lineage commitment. *Cell Stem Cell* 8:294-308.
- Zhao C, Sun G, Li S, Shi Y (2009) A feedback regulatory loop involving microRNA-9 and nuclear receptor TLX in neural stem cell fate determination. *Nat Struct Mol Biol* 16:365-371.
- Zhou QY, Quaife CJ, Palmiter RD (1995) Targeted disruption of the tyrosine hydroxylase gene reveals that catecholamines are required for mouse fetal development. *Nature* 374:640-643.

7.0 Appendix

7.1 Abbreviations

A/P	anterior-posterior
AP	alar plate
bp	base pairs
BP	basal plate
BSA	bovine serum albumine
cCasp3	cleaved caspase 3
Ci	Curie
cmp	counts per minute
cDNA	complimentary DNA
CMV	cytomegalovirus
CNS	central nervous system
di	diencephalon
dATP	2'-deoxyadenosine-5'-triphosphate
dCTP	2'-deoxycytidine-5'-triphosphate
dGTP	2'-deoxyguanine-5'-triphosphate
dNTP	2'-deoxynucleoside-5'-triphosphate
dTTP	2'-deoxythymidine-5'-triphosphate
D/V	dorso-ventral
DA	dopaminergic neuron
DIV	day in vitro
DMSO	dimethyl sulfoxide
DNA	2'-deoxyribonucleic acid
°C	degree Celsius
e.g.	for example
E	embryonic day
<i>E. coli</i>	<i>Escherichia coli</i>
EdU	5-ethynyl-2'-deoxyuridine
EDTA	ethylenediaminetetraacetate
ES	embryonic stem
Fig.	figure
FP	floor plate
g	gram
h	hours
hb	hindbrain
HEPES	N-2-hydroxyethylpiperazine-N'-2-
HRP	horseradish peroxidase
i.e.	that is (latin: id est)
<i>Isl1</i>	<i>Islet 1</i>
kb	kilobases
KCl	potassium chloride
KH ₂ PO ₄	potassium dihydrogen phosphate
l	liter
<i>Lef</i>	<i>Lymphoid enhancer binding factor</i>
<i>Lmx</i>	<i>LIM homeobox transcription factor</i>

m	meter
m	milli (10 ⁻³)
M	molar
mb	midbrain
mesDA	mesencephalic dopaminergic
mes	mesencephalon
met	metencephalon
min	minute
MgCl ₂	magnesium chloride
mRNA	messenger RNA
MH	midbrain hindbrain
MHB	mid-/hindbrain boundary
MZ	mantle zone
n	nano (10 ⁻⁹)
NaCl	sodium chloride
Na ₂ HPO ₄	sodium hydrogen phosphate
<i>Nkx</i>	<i>NK transcription factor</i>
NP-40	Nonidet-P40
<i>Nr4a2</i>	<i>Nuclear receptor sub-family4, groupA, member 2</i>
NBT	4-Nitro-blue tetrazolium chloride
NGS	next generation sequencing
NH ₄ OAc	ammonium acetate
NTP	nucleoside-5'-triphosphate
Otx2	Orthodenticle homolog 2
OE	overexpression
OM	oculomotor
<i>Phox2</i>	<i>paired-like homeobox 2</i>
<i>Pitx3</i>	<i>Pituitary homeodomain 3</i>
PBS	phosphate buffered saline
PCR	polymerase chain reaction
PFA	paraformaldehyde
PNS	peripheral nervous system
qPCR	quantitative PCR
RN	red nucleus
RNA	ribonucleic acid
RP	roof plate
RT	room temperature
RT-PCR	reverse transcriptase PCR
s	second
<i>Shh</i>	<i>Sonic hedgehog</i>
Slc	Solute carrier family
Sp	Sponge
<i>SBE1</i>	<i>Shh Brain Enhancer 1</i>
SDS	sodium dodecylsulfate
SV40	simian virus 40
SVZ	subventricular zone
tel	telencephalon
tRNA	transfer-RNA
Th	Tyrosine hydroxylase

Tris	tris(hydroxymethyl)aminomethan
TN	trochlear nucleus
μ	micro (10^{-6})
U	unit
vMH	ventral mid-, hindbrain
VZ	ventricular zone
<i>Wnt</i>	<i>Wingless-related MMTV integration site</i>
ZLI	zona limitans intrathalamica

7.2 Index of figures and tables

Figures

Fig. 1: Biogenesis of miRNA.....	12
Fig. 2: Schematic sections showing sagittal (a) and coronal (b) view of a murine embryo neural tube during midgestation, expression of the secreted factors Fgf8, Wnt1, Shh and expression domains of some ventral midbrain- hindbrain neuronal populations.....	15
Fig. 3: Schematic illustrations show (a) establishment of the mdDA progenitor domain during early stages of the mouse neural development and (b) determination of the mdDA neuron cell fate in mdDA precursors at intermediate stages of mouse neural development. Picture taken from (Prakash and Wurst, 2006).....	19
Fig. 4: Schematic coronal section of the ventrolateral midbrain at E12.5 which gives rise to OM and RN.....	22
Fig. 5: 155 candidate miRNAs predicted to target genes involved in the development of the MHB GRN, of mdDA and of other vMH neuronal populations, and in PD (courtesy of D. Trümbach).....	26
Fig. 6: 33 candidate miRNAs after logical filtering for “ON/OFF” states of miRNAs from the previous list (see Fig. 5) were predicted to target genes involved in the development of the MHB GRN, of mdDA and of other vMH neuronal populations, and in PD - there are still PD genes included in this list! (courtesy of D. Trümbach).....	27
Fig. 7: Positive and negative controls used for radioactive <i>in situ</i> hybridization detection of miRNAs on paraffin sections of whole mouse embryos.....	29
Fig. 8: Expression patterns of the four miRNAs found to be expressed in the CNS/MHR/MHB of the midgestational mouse embryo.....	31
Fig. 9: Expression patterns of <i>miR-705</i> , <i>miR-709</i> , <i>miR-712</i> and <i>miR-714</i> using LNA-ISH on sagittal brain sections of E18.5 embryos.....	34
Fig. 10: <i>miR-144</i> is specifically expressed in the liver of the midgestational mouse embryo.....	35
Fig. 11: A schematic diagram showing the luciferase sensor vector used for the <i>in vitro</i> luciferase sensor assays.....	37
Fig. 12: <i>MiR-709</i> targets the <i>Wnt1</i> 3'UTR <i>in vitro</i>	38
Fig. 13: <i>MiR-712</i> targets <i>Wnt5b</i> 3'UTR <i>in vitro</i>	40
Fig. 14: <i>MiR-714</i> targets <i>Lef1</i> 3'UTR <i>in vitro</i>	41
Fig. 15: Luciferase sensor assay revealed that miR-135b does not target <i>Otx2- and Wnt6</i> 3'UTR.....	42
Fig. 16: Both <i>miR342-5p</i> and <i>miR-221</i> target the murine <i>Wnt1</i> 3'UTR <i>in vitro</i>	44
Fig. 17: The putative conserved RNA motive.....	46
Fig. 18: Strategy to generate three different mutagenic <i>Wnt1</i> 3'UTR luciferase constructs for the putative “miRNA recognition” motif in vertebrates.....	47
Fig. 19: Relative luciferase activity of the <i>Wnt1</i> 3'UTR sensor vector (wild-type) and the three <i>Wnt1</i> 3'UTR sensor vectors in which three sequence motifs/part of the “XY” motif were mutated, after co-transfection of 30nM <i>pre-miR-221</i> or <i>pre-miR-709</i> in HEK293T cells.....	48
Fig. 20: Time-line of the 5-stage protocol for mESCs differentiation into vMH neurons and confirmation of successful differentiation into Th ⁺ neurons.....	51
Fig. 21: Enriched miRNAs in differentiated neurons using the ESC differentiation protocol by Lee et al. (2000).....	54

Fig. 22: Expression of <i>miR-125b</i> in the midgestational mouse embryo.....	55
Fig. 23: Expression of <i>miR-125b</i> in the midgestational mouse embryo.....	57
Fig. 24: Overlapping expression of <i>miR-125b</i> with <i>Sim1</i> ⁺ mes-/metencephalic BP progenitors/precursors and partial overlap of <i>miR-125b</i> expression with postmitotic <i>Phox2b</i> ⁺ OM/TN MNs in the midgestational mouse embryo.....	61
Fig. 25: Alignment of the seed sequences/bindings sites for <i>miR-125b</i> within the <i>Phox2b</i> 3'UTR (a) and <i>Sim1</i> 3'UTR (b) of five mammalian species with the <i>miR-125b</i> sequence as predicted by TargetScan 4.1.....	62
Fig. 26: Murine <i>Phox2b</i> and <i>Sim1</i> 3'UTRs are regulated by <i>miR-125b</i>	63
Fig. 27: Constitutive overexpression of <i>miR-125b</i> results in a strong downregulation of mouse <i>Phox2b</i> - and <i>Sim1</i> 3'UTR-mediated luciferase expression.....	65
Fig. 28: Viral constructs, experimental design and viral transduction efficiencies for control (empty backbone), <i>miR-125b</i> OE or sponge lentivirus of E11.5 primary vMH cell cultures.....	67
Fig. 29: <i>MiR-125b</i> regulates the numbers of <i>Phox2b</i> ⁺ cells in E11.5 primary vMH cell cultures.....	69
Fig. 30: <i>MiR-125b</i> controls the generation of <i>Isl1</i> ⁺ OM/TN neurons in E11.5 primary vMH cell cultures.....	71
Fig. 31: <i>Sim1</i> mRNA levels are not altered in E11.5 primary vMH cell cultures after <i>miR-125b</i> overexpression or knock-down.....	73
Fig. 32: <i>MiR-125b</i> appears to regulate the numbers of <i>Nkx6-1</i> ⁺ BP progenitors/precursors in E11.5 primary vMH cell cultures.....	74
Fig. 33: <i>MiR-125b</i> controls the numbers of proliferate cells (<i>EdU</i> ⁺ cells) including <i>Nkx6-1</i> ⁺ cells in E11.5 primary vMH cell cultures.....	76
Fig. 34: Reduction of <i>miR-125b</i> dosage in vMH primary cultures increases the survival of vMH cells.....	77
Fig. 35: <i>Shh-Cre-SBE1</i> transgenic construct and beta-Gal expression pattern after <i>Shh-Cre-SBE1</i> -mediated recombination of the R26R reporter in transgenic embryos/mice.....	80
Fig. 36: The offspring from <i>Shh-Cre-SBE1</i> transgenic founder male F412 shows both specific and ectopic beta-Gal expression patterns.....	82
Fig. 37: Genealogy tree showed the offsprings from three of the founders.....	83
Fig. 38: Genotyping PCR of <i>Shh-Cre-SBE1</i> transgenic mice.....	86

Tables

Table 1: A summary of the role of transcription factors in mdDA neuron development.....	19
Table 2: Candidate genes involved in the development of the MHB GRN, mdDA and other vMH neuronal populations, and in PD.....	24
Table 3: Final selection of 33 miRNAs predicted from a combination of computational algorithms with their predicted target genes.....	24
Table 4: Summary of <i>in silico</i> predicted miRNAs expression patterns during midgestational (E10.5, E12.5) of the mouse.....	30
Table 5: Selected candidate miRNAs (based on their CNS expression pattern) with their predicted target mRNAs.....	37
Table 6: Four miRNAs predicted to target <i>Wnt1</i> 3'UTR using RNA22 bioinformatics tool.....	43

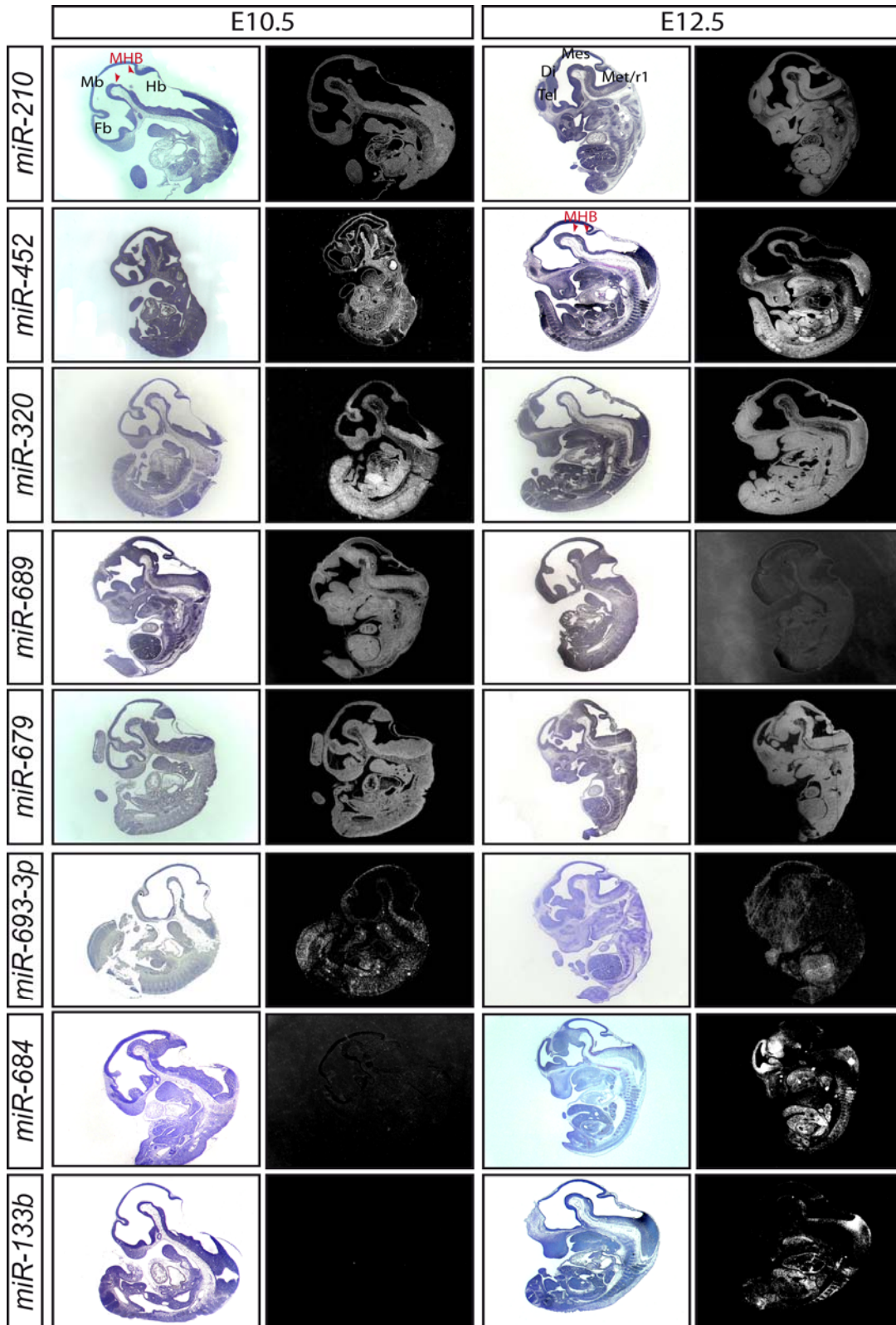
Table 7: Primer pairs and PCR conditions used to genotype <i>Shh-Cre-SBE1</i> transgenic mice.....	83
Table 8: List of equipments used.....	108
Table 9: List of consumables used.....	109
Table 10: List of chemicals used.....	111
Table 11: List of commercial kits used.....	112
Table 12: List of enzymes used.....	113
Table 13: List of antibodies used.....	113
Table 14: List of buffers and solutions used.....	114
Table 15: LNA oligo probe used to detect miRNA expression.....	116
Table 16: Riboprobes used in RNA ISH.....	117
Table 17: precursor miRNAs used in luciferase sensor assays.....	117
Table 18: Vectors used for cloning.....	118
Table 19: Primers used for mouse genotyping.....	118
Table 20: List of primer pairs used to generate candidate genes 3'UTR PCR fragment.....	119
Table 21: List of primer pairs used to generate site-directed mutagenesis on luciferase vector.....	120
Table 22: Primers used for 'motive-recognition' motive experiment.....	120
Table 23: DNA insert sequences.....	121
Table 24: Primers used to generate <i>miR-125b</i> DNA insert for lentivirus constructs...	121
Table 25: DNA insert sequences.....	121
Table 26: List of mediums for cell culture.....	122
Table 27: 3'-end labelling of LNA-modified detection probe.....	126
Table 28: Tailing of LNA modified oligo detection probe.....	127
Table 29: RNA probe labelling.....	128

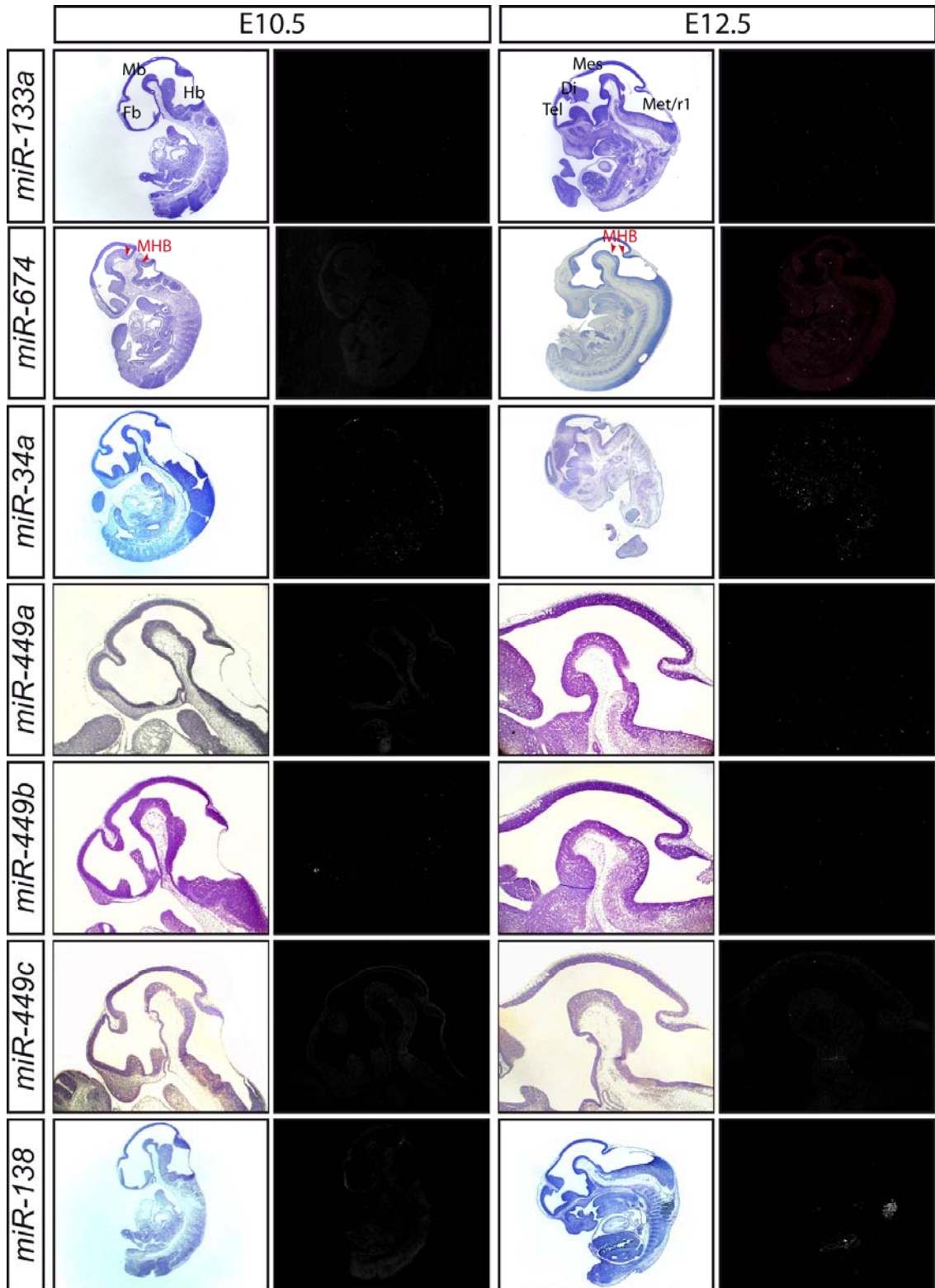
Supplementary Figures

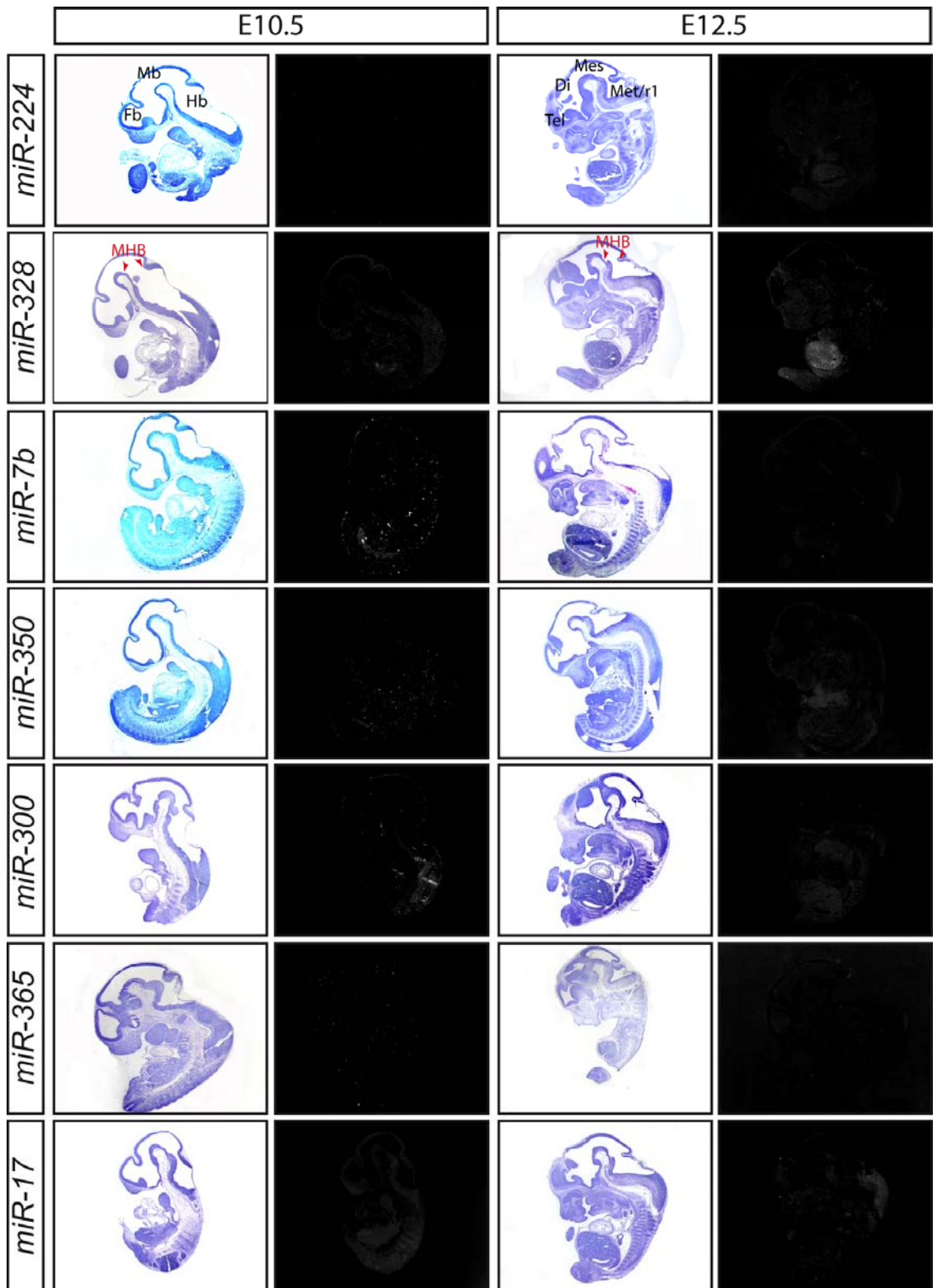
Suppl. Fig. 1: MiRNAs predicted by five combined computational algorithms expression analyses.....	150
Suppl. Fig. 2: Validation of the NGS miRNA profiling approach during mESC differentiation into vMH neurons.....	154
Suppl. Fig. 3: Sequence of the <i>Shh-Cre-SBE1</i> construct used for production of <i>Shh-Cre-SBE1</i> transgenic mice (Clone A5).....	155

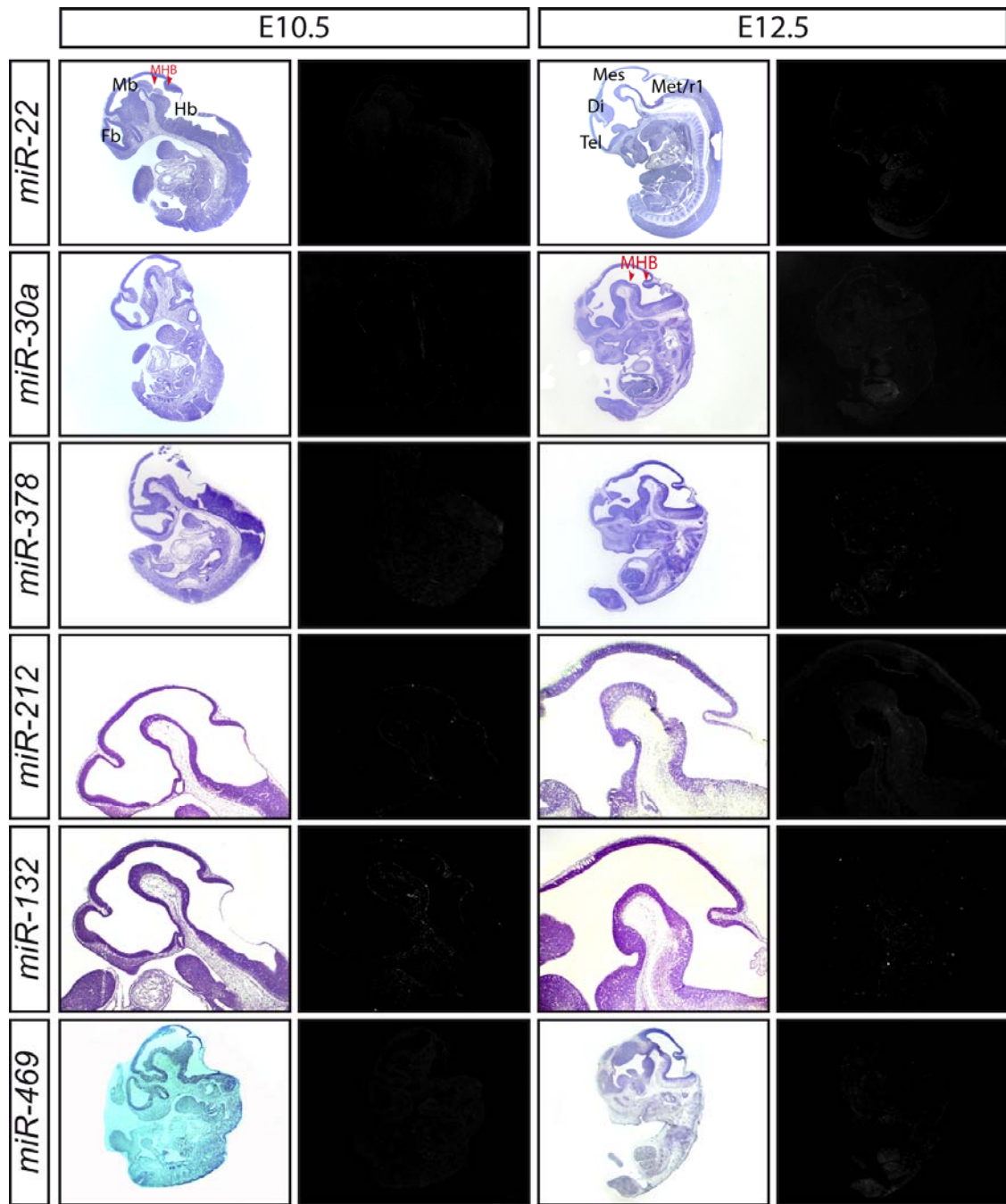
7.3 Supplementary Figures

7.3.1 MiRNAs predicted by five combined computational algorithms expression analyses.



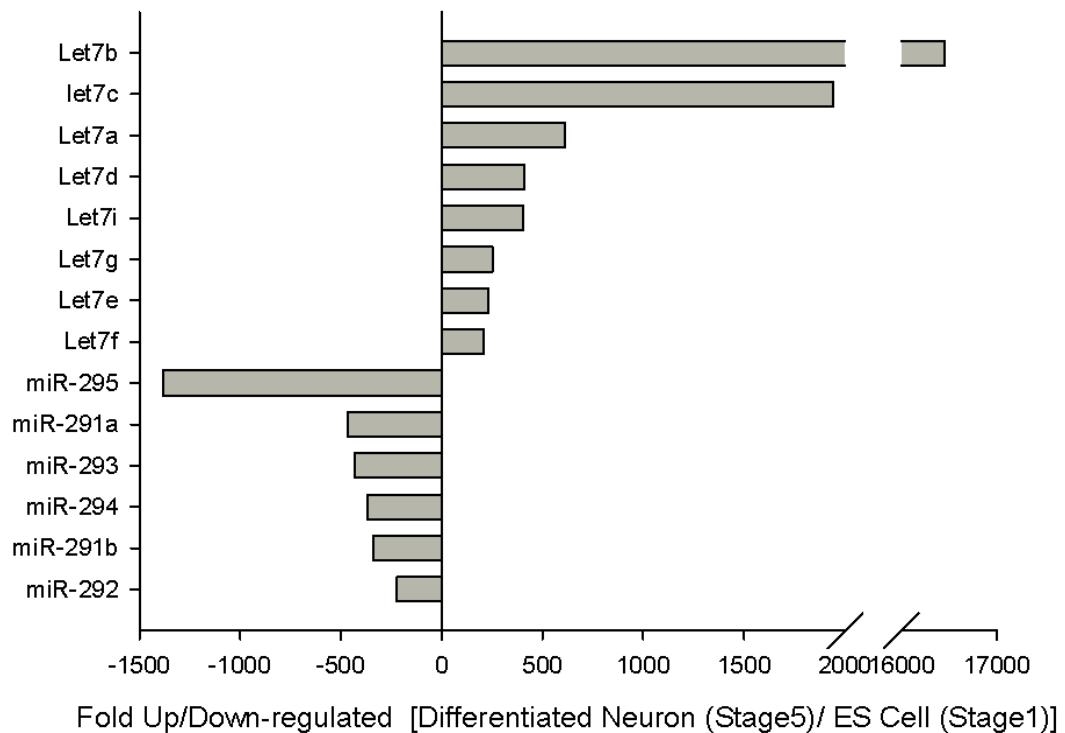






Supplementary Figure 1. MiRNAs predicted by five combined computational algorithms showed either ubiquitous expression or expression could not be determined during midgestational stages and were therefore discarded from further analysis.

7.3.2 NGS miRNA profiling of differentiating mESCs into vMH neurons - validation of the profiling approach



Supplementary Figure 2. Validation of the NGS miRNA profiling approach during mESC differentiation into vMH neurons. The mESC-specific *miR-290* family (Chen et al., 2007; Wang et al., 2008) was strongly down-regulated in differentiated neurons (final differentiation stage 5) as compared to the undifferentiated, pluripotent mESCs (stage 1), whereas the differentiated neuron-specific *let7* miRNA family (Reinhart et al., 2000; Wang et al., 2009) was highly enriched in the differentiated vMH neurons (stage 5) as compared to the pluripotent mESCs (stage 1), thus indicating a successful differentiation of mESCs into vMH neurons and validating my/our NGS miRNA profiling approach. The x-axis indicates the fold up- or downregulation (relative read numbers) of miRNAs expressed in stage 5 cells (differentiated neurons) versus miRNAs expressed in stage 1 cells (mESCs).

7.3.3 Sequence of the *Shh-Cre-SBE1* construct used for production of *Shh-Cre-SBE1* transgenic mice (Clone A5)

gtggtggcctaactacggctacactagaagaacagtatattggtatctgcgctctgctgaagccagttacctcggaaaa
agagtggtagctcttgatccggcaaaaccaccgctggtagcgggtgggttttttggttgcaagcagcagattacg
cgcaaaaaaaaggatctcaagaagatcctttgatcttaccgaagaaggccaccgctgaaggtgagccagtgag
ttgattgcagtcagttacgctggagctcgtcctgaatgatatacaagcttgaattcgttgaattccacatc
aacttaccagccctgcactttgctgggatagattggaaggggtcttccagcattgcagccttgcctactttcagtt
gccccaggcagatcaactctaccaccaagcacaccagctgcctccatgctggggtgcagcacatagaccactg
aacctatgtaccaccacattctgcagacactcttaccctgcccctcagctgggatgcatccatccacctgcagag
cttgaatgtggtgcagtcagtgagatacaataaaggacagtatcttagggcacttaaacagcaactcttaggttgt
ggccacctgtgattatcctctatctaaagatgctaaatattcaggagatgctcaggtgagctgtttcacaacccctg
gacgtctgtcctgtacactcacatctggggatggggtgtaataaggcaaacaggaggaggcagcgttgcctcaa
caattgagaggctgtttatggtcaaagcttgggggggggggagcatctggactgtccttataaaacttatgctgg
ctttaaaccaaagcatctccatttagagaaagttaagggggaagcagccctgagcacaagcaggcagtgccgggtat
ttccaataaacaggcctcctccctccaccacctttacccttagtaaaagacttcttcttcttcttcttcttctt
tctt
aataaagccacagcagccagaggggggagaaatgtagtcttctcagggttaacatcagaagacaagcttgtgagg
tggccaatcagatgcgcccctgccagctataatagtgcgaaaggcagcctgtctcacaagctctccagccttgcta
caatttaaaatcaggctcttttggcttcttaattgctgtctcgagaccaactccgatgtgttccgttaccagcagc
ggcagcctgccatcgcagcccagctcgggtggggatcggagacaagtcccctgcagcagcggcaggcaaggttata
aggaagagaaagaccagcagcgcagaggggaacgaacagcagcagcagcagcagcagcagcagcagcagcagcag
cgacacgcacaacaccgctaccgctcgcgcacagacagcgcggggacagctcacaagctcctcaggttccgctg
tactaggctcgaggtcgaccatgcccagaagaagagggtgtccaatttactgaccgtacaccaaaaatttgctg
cattaccggctcgatgcaacgagtgatgaggttcgcaagaacctgatggacatgttcagggtatcgccaggcgttttctg
agcatacctggaaaatgcttctgtcgtttgcccgtcgtgggcggcatggtgcaagtgaataaccggaaatggtttc
ccgcagaacctgaagatgttcgcgattatcttctatcttccagcgcgcggtctggcagtaaaaaactatccagcaac
atctgggcccagctaaacatgcttcatcgtcggctccgggctgccacgaccaagtgcagcaatgctgtttcactggtta
tgccggcggatccgaaaagaaaacgttgatgccggtgaacgtgcaaaaacaggctctagcgttcgaacgcaactgatctc
accaggttcgttcaactcatggaaaatagcagctcgtccaggtatcagtaatactggcattctctgggagatgcttata
acaccctgttacgtatagccgaaatggccaggatcagggttaaagatatctcacgtactgacgggtgggagagatgtaa
tccatattggcagaaagaaaacgctggttagcaccgcagggtgtagagaaggcacttagcctgggggttaactaaactgg
tcgagcagatggatttccgtctctggtgtagctgatgatccgaataactacctgttttgcccgggtcagaaaaaatggtg
ttgcccgcgccatctgccaccagccagctatcaactcgcgccctggaagggattttgaagcaactcatcgattgat
acggcgctaaagatgactctggtcagagatacctggcctggtctggacacagtgcccgtgtcggagccgcgcgagata
tggccgcgctggagtttcaataccggagatcagcaagctggtggctggaccaatgtaaatatgtcatgaactata
tccgtaacctggatagtgaaacaggggcaatggtcgcctcgtggaagatggcgattagccattaacgcgtaaatgat
tgcagatccactagttctagagctcgtgatcagcctcagctgtgcttctagttgccagccatctgttgtttgccc
tccccgctgcttcttgaccctggaaggtgccactcccactgtcctttcctaataaaaatgaggaaatgcatcgcat
tgtctgagtaggtgtcattctatctgggggggtggggggggcaggacagcaagggggaggattgggaagacaatagc
aggcatgctggggatcgggtgggctctatggctctcagggcggaaagaaccagctggggctcgagatccactagttct
agcctcgaggtcagagcggccgatcctacatcctccaaaatgagcagcggtaatccagcccggagggtctcgaaggca
gtgcagaccccggccggggaggcagctcattggcattctacacacgcgggctggggcgcgcgcttgtgtgctcaag
cggggctcgtgcgactcgacgactccggctcgcagagcccgggtcgcattccggggggctcggagtgcttccaacg
gccagcccccacacttcatgcccgggaaaacgatgagaagattaaaagccttctgtaattccagcagaaagattctt
tggcaatctctatttgccaaaagcatgatcctggagattggaatgcaagaagactaggacctccccacccctcctcc
ctggcccccctcgcctccgcccctcctcaattatgtcctccggacagtgagcctggagagctacggagggtcag
taaagcgggtagtcaaggggcttgagaaccgcgctccagcgcctcagagcaggcctggccatttaaaattcaata
cacatctcgagtaccgggggttaccaagcttccatgggcggccgcgtcgaccgatgccttgagagccttcaacca
gtcagctcctccgggtgggcggggcagatgactaggccgacgaattctctagatctcgtcaatactgacctttaa
tcatacctgacctccatagcagaaagtcaaaagcctccgaccggaggcttttgacttgatcggcacgtaagagggtcc
aactttcaccataatgaaataagatcactaccgggctgattttttgagttatcgagattttcaggagctaaaggaagct
aaaatgagccatattcaacgggaaacgctcttgctcgaggccgcgataaaattccaacatggatgctgatttatatggg
tataaatgggctcgcgataatgctgggcaatcaggtgcgacaatctatcgattgtatgggaagcccgatgcgccagag
ttgtttctgaaacatggcaaggtagcgttgccaatgatgtttacagatgagatggtcaggctaaactggctgcagggaa
ttatgcctctccgaccatcaagcattttatcgtactcctgatgatgcatggttactcaccactgcgactccgag
aaaacagcattccaggtattagaagaatatcctgattcaggtgaaaatattgttgatgagctggcaggtgttccg
cggttgcatctgattcctgtttgtaattgtccttttaacggcgatcgcgattttcgtctcgtcagggcgaatcacga
atgaataacggtttgggtgggtgcgagtgattttgatgacgagcgtaatggctggcctgttgaacaagtctggaagaa
atgcataagcttttgccattctcaccggattcagctcgtcactcatggtgatttctcacttgataacctatttttgac
gaggggaaattaataggttgtattgatgttggacgagctcgaatcgcagaccgataaccaggatcttgccatcctatgg
aactgctcggtaggttttctccttcatcagaaaacggcttttcaaaaataggtattgataatcctgatgatgaat
aaattgcagtttcaacttgatgctcagtagttttctaaattgaccaaacaggaaaaaaaccccttaacatggccgc
tttatcagaagccagacattaacgcttctggagaaactcaacgagctggacgcggatgaacaggcagacatctgtgaa
tcgcttcacgaccacgctgatgagctttaccgcagctgcctcgcgctttcgggtgatgacgggtgaaaacctctgatga
gggccc aaatgtaatcacctggctcaccttccgggtgggcctttctcgttgctggcgtttttccataggctccgccc

cctgacgagcatcacaataatcgatgctcaagtcagaggtggcgaaccgacaggactataaagataccaggcgctt
ccccctggaagctccctcgtgcgctctcctggtccgaccctgccgcttacgggatacctgtccgcctttctccctcg
ggaagcgtggcgctttctcatagctcacgctgtaggtatctcagttcgggtgtaggtcgttcgctccaagctgggctgt
gtgcacgaacccccggttcagcccagcgtgcgccttatccggtactatcgtcttgagtcgaacccggtaagacac
gacttatcgccactggcagcagccactggtaacaggattagcagagcgaggtatgtaggcgggtgctacagagttcttg
aa

Supplementary Figure 3. *Shh-Cre-SBE1* construct used for production of *Shh-Cre-SBE1* transgenic mice (Clone A5). *Shh* minimal promoter is highlighted in turquoise. Cre coding sequence highlighted in yellow. Poly(A) signal highlighted in grey. *Shh* brain enhancer 1 highlighted in red. **Shh minimal promoter** Cre CDS Poly(A) signal **SBE1**

7.4 Acknowledgment

I am truly grateful to Dr. Nilima Prakash who took me under her wings to become part of her group. Her tutelage and ideas given to me throughout the four years of my PhD time were to a large extent helpful in shaping up this thesis. Moreover, her pedagogical role and word-of-wisdom have also helped me to grow up as a better person.

I'm thankful to Prof. Dr. Wolfgang Wurst for his invaluable inputs and discussions given in my seminars. I also thank Dr. Laure Bally-Cuif and Prof. Dr. Jochen Roeper for willing to become my thesis committee members and to travel long distances to attend the meetings. Their suggestions and comments are great help in my project. I'm also thankful to Prof. Dr. Johannes Beckers for willing to become my PhD thesis defence examiner and Prof. Dr. Erwin Grill for chairing my thesis defence.

Special thanks go to Dr. Oskar Ortiz for being my greatest help in my work and cheering me up during the tough times. His selflessness and the willingness to share his knowledge on the cloning techniques, computer skills and software have made my life a lot easier. Not to forget, the mutual encouragement with Karina Kloos has helped me to work harder to reach the finishing line. Their existence in the institute has brought much laughter during my PhD life. I appreciate and thankful to Florian Giesert and Karina Kloos for translating my Abstract into Zusammenfassung.

Enormous supports from the people within the AG Wurst (Susanne Lass, Annerose Kurz-Drexler, and Dr. Jordi Guimera.) as well as other members from Nilima's group (Peng C., Götz S., Zhang J., Meier F., Fukusumi Y., Stübner S., Klafke R.) have made my work easier and smoother. A big thank you goes to them.

Much of the work in this thesis would not have been possible without the collaborations from the laboratory of Dr. Dieter Edbauer and his postdoc Dr. Julia Strathmann for being my constant lentivirus stock supplier and the laboratory of Dr. Wei Chen and his Ph.D student Na Li for helping me producing the high quality NGS data.

Outside the scientific community, my parents are undoubtedly the greatest pillars of support. Their financial support to finance my postgraduate studies has made me 10,000 miles away from home but their unconditional loves and cares have made the distance non-existence. Life in Germany would not have been as much fun if without my best buddies, Christian Becker and YingSin Phuan, and equally important others – Ling, Kie and Andy. A friend in need is a friend indeed. The footprints they left in my memory lane will be treasured.

7.5 Curriculum Vitae

PERSONAL INFORMATION

Name : Yen-Kar Ng
Date of birth : 21.04.1982
Place of birth : Taiping Malaysia
Nationality : Malaysian

EDUCATIONS AND QUALIFICATIONS

2008-to-present **PhD candidate, Institute Developmental Genetics, Helmholtz Centre Munich
Technical University Munich (TUM), Bayern, Germany**

2006-2007 **Master of Sciences (MSc) in Cancer Biology
University of Bradford, United Kingdom**
Result: Merit (equivalent to Germany system: 1.3)

2003-2006 **Bachelor of Sciences (BSc) in Biotechnology with
Management (Honours)**
National University Malaysia
Result: C.G.P.A: 3.3 (equivalent to Germany system: 1.7)

THESIS PROJECTS

Ph.D Thesis Title

Functions of microRNAs in the developing midbrain-hindbrain in the mouse.

MSc Thesis Title

Developing methods to solubilise CytochromeP450.

BSc Thesis Title

Cloning and expression of gene *ompA10* from *Burkholderia pseudomallei*.

LANGUAGES

- Native speaker in Malay and Chinese Mandarin.
- Proficient in speaking and writing in English.
- Excellent in spoken Cantonese and Hokkien (Chinese dialects).
- Basic conversation skill in German.

PUBLICATIONS

Hock S.*, **Ng Y-K.***, Wittmann D., Lutter D., Trümbach D., Wurst W., Prakash N., Theis F. Sharpening of expression domains induced by transcription and microRNA

regulation within a spatio-temporal model of mid-hindbrain boundary formation (2012). Plos Comput Biol (manuscript in revision). *Co-first author.

Peng C., Li N., Zhang J., **Ng Y.-K.**, Meier F., Chen W., Merkschlager M., Wurst W., Prakash N. (2012). A unilateral negative feedback loop between *miR-200* microRNAs and Sox2/E2F3 controls neural progenitor cell cycle exit and differentiation. J. Neurosci (Manuscript accepted)

Ng Y.-K., Li N., Strathmann J., Peng C., Zhang J., Edbauer D., Chen W., Wurst W., Prakash N. *MiR-125b* regulates oculomotor neurons development. (2012). (Manuscript in preparation)